Long Term Functional Simulation of Large Diameter Metal on Metal Hip Implants

Megan Jayne Frances Hadley

Submitted in accordance with the requirements for the degree of Doctor of Philosophy

The University of Leeds
Institute of Medical and Biological Engineering
School of Mechanical Engineering

November 2012

The candidate confirms that the work submitted is her own and that appropriate credit has been given where reference has been made to the work of others.

ACKNOWLEDGEMENTS

I would like to thank my academic supervisors, Professor John Fisher, Professor Zhongmin Jin and Dr Sophie Williams for their support, guidance, and inspiration throughout my study. Their help has been invaluable, and it has been an honour to work with them.

I would also like to thank my industrial supervisors, Professor Graham Isaac and Mrs Cath Hardaker for giving me the opportunity to pursue this research, and for making it possible to combine it with my work at DePuy. I am especially grateful to Cath for encouraging me to start in the first place, keeping me going when things got tough, and for the endless proof reading and corrections.

I wish to acknowledge the financial support provided by the Engineering and Physical Sciences Research Council (EPSRC). I also wish to thank DePuy International for their financial support, supply of test specimens and provision of laboratory equipment and facilities.

I would like to thank my colleagues at DePuy for their invaluable support throughout my project, in particular John Wye and Mahsa Shahi Avadi for their assistance in running endless simulator tests. Without them I do not think I would have found the time to fit it all in! Also thanks to Karen, Fiona, Phil and Ken for their ideas, encouragement and support throughout.

My friends and family have been my rocks throughout the last seven years, keeping me going, providing much needed distraction from work, and knowing exactly when (and when not!) to ask “how’s the thesis going?” Too many names to mention here, but especially my mum Alex, Bronwen, Owen, Carolyn, Holly, Paul, Claire and Rob. Without you all I would never have done it.

Last of all, my wonderful father, Laurence, who sadly never saw my thesis completed. He inspired me to follow him into Engineering, and encouraged and nurtured my passion for my work. This thesis is dedicated to his memory.

ABSTRACT

The artificial hip replacement or total hip arthroplasty (THA), is a widely used solution to help restore hip function following arthritic disease. Pre-clinical *in vitro* evaluation of new designs is a vital aspect of the development of joint replacements to ensure devices are safe and to better predict their performance *in vivo*.

This thesis describes the development of a number of clinically relevant stop-dwell-start protocols for *in vitro* wear simulation of total hip replacement bearings. A new wear simulator was developed and commissioned to allow application of these complex cycles, and data from the literature examined to characterise activity patterns of real THA patients.

A number of different stop-dwell-start test scenarios were investigated, examining the effect on wear of altering both the duration of dwell periods, and the number of walking cycles between dwells. Wear did not appear to increase significantly with a longer dwell period, however it was observed that bearings did not bed in under these conditions therefore overall wear volumes may be higher.

A significant increase in wear was observed when the number of cycles between dwell periods was reduced down to one or two cycles; this is believed to be due to deterioration of the lubricant film during the dwell, leading to severe lubrication conditions at start-up, and subsequent high wear of the bearing surfaces. These findings may be particularly relevant to the use of MOM devices in very infirm patients, or those in the early stages of recovery, for whom walking in a single step pattern may be more common.

These results have clinical relevance in the loads and cycle combinations used, compared with earlier studies. Both the number of walking and dwell cycles, and the dwell period load are based on data from real hip patients in the literature, showing that activity bursts are generally short and change frequently, and the load during a pause is low compared with peak loads during walking.

It is believed this use of more clinically relevant activity simulations for pre-clinical *in vitro* testing of hip replacement bearings is vital for improved understanding of bearing tribology and more accurate prediction of implant performance *in vivo.*

TABLE OF CONTENTS

List of Tables

List of Figures

NOMENCLATURE

MOM	metal on metal
COM	ceramic on metal
MOP	metal on polyethylene
COP	ceramic on polyethylene
THA	total hip arthroplasty
SDS	stop-dwell-start
λ	lambda ratio
$h_{\min}$	predicted minimum film thickness
R_a	composite surface roughness
R	effective radius
η	lubricant viscosity
u	entraining velocity
E'	Young's modulus
w	Load

CHAPTER 1: INTRODUCTION

The artificial hip replacement was initially conceived in the late nineteenth century as a solution to help restore joint function following arthritic disease (Gluck, 1891), and is now an increasingly common solution for patients with degenerative joint problems, with over 80,000 THA operations performed in England and Wales alone in 2010 (National Joint Registry for England and Wales, 2011).

The main aim of this treatment is to substitute the femoral head and acetabular socket for a ball and socket of metal, plastic or ceramic, replacing the diseased bone and cartilage. The Charnley hip, the first widely used product, developed in the 1960s utilising a steel femoral head and an ultra high molecular weight polyethylene acetabular component, proved to be highly successful and this hip is still regarded as a gold standard today (Charnley, 1961; Devitt et al., 1997). In the past fifty years many technological advances have taken place, producing significantly improved hip replacements with a variety of materials and designs, all providing previously handicapped patients with up to 20 years of additional joint function and improved quality of life (Howie et al., 2005).

Metal-on-polyethylene (MOP) bearings based on the original Charnley design have been in successful widespread use ever since, although some have been associated with osteolysis, an immune reaction to the wear debris, causing loosening and failure of the THA. Metal-on-metal (MOM) bearings were initially developed in the 1960s but early designs experienced mixed degrees of success, with some devices performing well, but others exhibiting high wear rates and equatorial binding (McKee et al., 1966). More recently, these designs have been modified and have now been successfully used clinically for over ten years. Further developments of the MOM concept, including large diameter and resurfacing solutions have come onto the market in recent years, and have shown some good results, however many concerns remain as to the immunological reactivity of the metal wear products. Material developments in the form of ceramic-on-ceramic (COC) and ceramic-on-metal (COM) bearings have also been introduced to address some of these issues (Dowson, 2001).

As hip design technology has improved, so too have the techniques for pre-clinical evaluation of designs, including computational simulation, material testing and joint

function simulation. These all contribute to thorough examination of a new product prior to clinical trials, thus reducing the potential risk faced by a patient being treated with a newly developed and unproven device. Regulatory bodies such as the Medical and Healthcare Products Regulatory Agency (MHRA) in the UK, and the Food and Drug Administration (FDA) in the USA, set stringent requirements for orthopaedics companies to demonstrate the performance of a device before it is given approval for general use, leading to an ever increasing need for pre-clinical evaluation to provide more accurate and realistic predictions of product performance to meet these regulations.

This study focuses in particular on joint function simulation for pre-clinical testing, where the ball and socket are subjected to typical loads and motions to which they would be exposed *in vivo* (Barbour et al., 1999). The simulations can potentially recreate up to the full life of the implant, approximately 20-25 years in the body and throughout this, components are periodically examined to evaluate the degree of wear and change in geometry. Currently most wear simulation recreates only walking loads and motions, and this has been shown in many studies to be a highly accurate method for comparing different types of implants and predicting their performance once in a patient (Firkins et al., 2001; Dowson et al., 2004a). However, recent focus on this area has shown that there is often a discrepancy between the wear rates of MOM implants tested in a simulator, which are frequently lower than actual wear rates once implanted in a patient.

The wear of MOM bearings measured in a wear simulator is bi-phasic, with an initial high wear rate lasting approximately one million cycles or steps, followed by a lower steady state wear rate (Hu et al. 2004). It is believed that during the period of higher wear, the geometries of the head and cup wear to conform to each other, at which point the wear rate lowers. Higher wear rates in patients are thought to be due to the variation in activities of patients, from running and stair climbing to standing still and sitting down, compared with the continuous walking used in simulator testing. Changing activity in simulator testing has been shown in some preliminary studies to increase wear rates (Bowsher et al. 2006; Bowsher et al. 2006b). It is thought this may be due to a disruption of the conforming profile of the bearing pair and extension of the bedding in period, thus increasing overall wear (Jalali-Vahid et al., 2004). It is believed that MOM bearings may be more susceptible to this change than MOP bearings. As arthroplasty is being increasingly used to treat younger and more active patients than the

typical elderly sedentary patient, there is a need for pre-clinical testing to take account of the change in environmental conditions for implants, and be able to reproduce more accurately the wear rates observed in these patients.

This investigation will review the current techniques for wear simulation of hip replacements, and highlight potential areas where improvements in replication of *in vivo* wear may be possible. Published data defining patient joint kinematics will be used to develop new simulator inputs representing typical patient activities and the effect of these profiles on implant tribology will be examined using friction and wear simulation. The eventual aim of this study is to develop a protocol for wear simulation which more accurately reproduces the *in vivo* conditions in the hip joint, and allows improved prediction of the performance of THA.

1.1 Background

1.1.1 Anatomy of the Hip Joint

The hip is an enarthrodial joint between the pelvis and head of the femur (Gray, 1918). It is one of the largest joints in the body, and one of the most stable, afforded by the ball-and-socket type enclosure of the rounded head of the femur by the concave acetabulum of the pelvis. The hip is capable of withstanding forces as great as two to three times body weight during walking, up to five times body weight during stair ascent (Bergmann et al., 1995; Heller et al., 2001), yet provides a wide range of motion in flexion-extension, abduction-adduction and rotation, contributing to effective locomotion.

The opening of the acetabulum on either side of the pelvis faces anteriorly and laterally at an angle of 40º from the front plane of the body, and downwards at 60º from the horizontal. A ring of fibrous tissue lies around the opening of the acetabulum, known as the acetabular labrum, which adds depth to the socket, and enhances the high static stability of the joint. When unloaded, the acetabulum is slightly smaller than the femoral head, but elastically deforms to accommodate the femur when loaded, creating a congruous joint interface (Nordin et al., 2001).

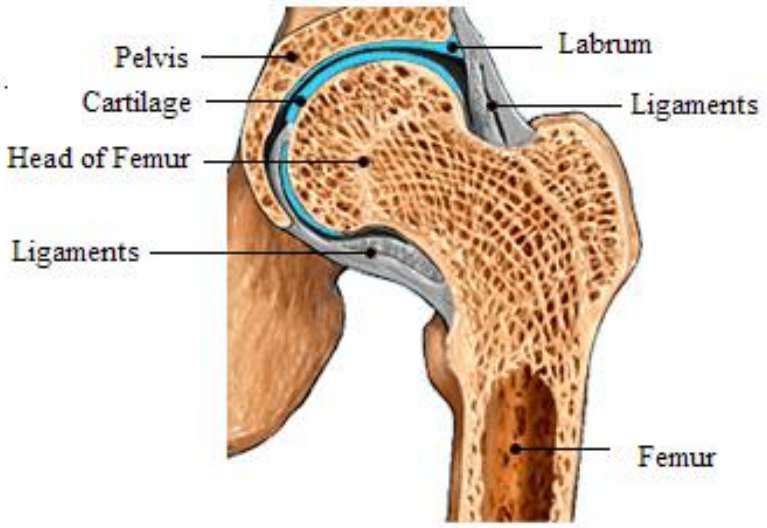

Figure 1: Anatomy of the hip, adapted from (Connecticut, 2006)

The bony structures of the hip are surrounded by a membranous synovial sac which encloses the lubricating synovial fluid of the joint, and strong ligaments which assist in

stability and prevent dislocation of the joint. Five major ligament groups connect the pelvis and femur, extending from the base of the spine and the rim of the acetabulum to various locations on the femoral neck and greater trochanter, further encapsulating the joint. These provide much of the weight-bearing support of the body during relaxed standing. An additional ligament lies within the joint, between the inferior acetabulum and a small depression, or fovea, in the centre of the femoral head. It does not contribute significantly to support of the joint, but does contain an artery providing nutrition to the femoral head (Seeley et al., 2000).

The load bearing surfaces of the acetabulum and the femoral head are covered in a layer of hyaline cartilage – a dense, connective tissue allowing load distribution over a wide area, thus reducing stresses in the joint. The cartilage consists of condrocyte cells supported within a rigid matrix constructed of collagen fibres and various organic molecules, which absorb water, providing the cartilage with time dependent poro-elastic properties, allowing the tissue to resume its original form after loading. It offers extremely low friction, with coefficients as low as 0.005 (Dowson et al., 1981), providing very low resistance to joint movement, and contains no nerve endings, therefore no pain is felt when the joint is loaded during movement. The cartilage also contains no blood vessels, which leads to a very slow healing rate after injury (Gray, 1918).

1.1.2 Total Hip Replacement

Trauma or disease in the natural hip can result in severe pain and loss of function for the patient. The most common disease treated with THA is osteoarthritis, when the articular cartilage breaks down, leading to bone on bone contact and severe pain and immobility. In the case of trauma, fracture of the femoral neck in particular, is one of the most common fractures in the elderly population (Nordin and Frankel, 2001) and is frequently treated with total joint arthroplasty.

The total hip replacement has four main functions:

- *Patient pain relief* – in the instance of disease, when the cartilage which contains no nerve endings deteriorates, the bone underneath which does contain nerves becomes the load bearing surface, resulting in pain for the patient. In trauma cases, the pain is more likely to be caused by fractured bone and the accompanying loss of structural support.

- *Restoration of joint function* – post surgery, the patient must ideally be able to ambulate as naturally as possible, both for comfort, and to reduce the risk of potential problems brought about at a later date by poor gait.

- *Durability* – implantation of a THA requires major surgery, in particular when a failed joint must be replaced with a new, or revision device. It is desirable to ensure implants last as long as possible *in vivo*, which can be achieved through reduction in wear, and design of implants to withstand the mechanical forces in the joint.

- *Reliability* - implants should where possible, be insensitive to minor surgical alterations such as misalignment, and to variations in size within tolerance. Implant performance should also not be adversely affected by differing patient gaits.

The conventional total hip replacement consists of a metal shaft located in the femur with a proximal head which sits in a cup in the acetabular socket of the pelvis, mimicking the natural anatomy of the hip. The components are either cemented in position or pressed into an interference fit in the bone, which then grows into a rough surface on the implant to secure it. The femoral head may be manufactured from a

ceramic, such as alumina or zirconia, or from metal, typically cobalt chrome molybdenum. The acetabular cup may be ceramic, metal or polyethylene. Both head and cup, particularly in metal and ceramic components are manufactured with a high surface finish and tolerances to optimise bearing function, and can range in size from 22mm to 44mm diameter. Significant cost differences exist between bearing types, with polyethylene bearings generally being less expensive than all metal and all ceramic bearings (DePuy International, 2007).

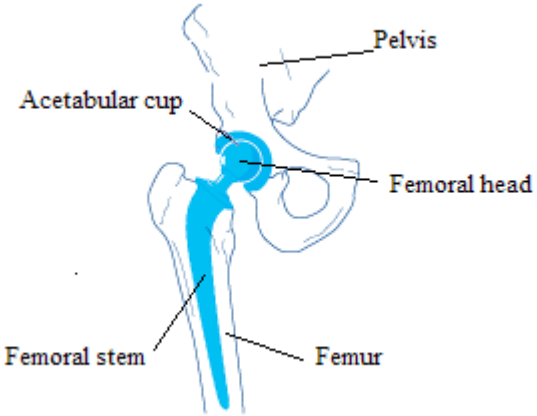

Figure 2: Conventional total hip replacement

More recently, surface replacement, or resurfacing, of the hip has been developed as a conservative alternative, consisting of a similar acetabular cup to the conventional THR, and a hollow femoral component which sits over the existing bony femoral head, with larger bearing diameters from 40mm to over 60mm. This study however, focuses mainly on conventional hip replacement.

Of particular importance in the design of THA implants is the need to reduce wear of the bearing in use. Although it is highly unlikely that a hip will 'wear out', the sub micrometre sized wear particles and ions released throughout the life of the implant can cause an immune response in the body. Osteolysis, or particle disease, is thought to be one of the primary causes of failure of joint replacements. It occurs when the wear debris from the joint is phagocytosed by macrophages (white blood cells), activating an immune response whereby osteoclasts, which are cells responsible for the resorption of old bone, are over-stimulated, resulting in reduction of bone stock (Ingham et al., 2000). The degree of osteolysis has been linked to material, size and volume of wear particles (Tipper et al., 2001).

The materials used in hip bearings have been shown in wear simulator testing to wear differently under the same environmental conditions, especially in terms of material wear rate, and the size of the resultant wear particles. Typically polyethylene cups with metal (MOP) or ceramic (COP) heads yield the greatest volume of wear particles, while metal-on-metal (MOM) and ceramic-on-ceramic (COC) bearings produce wear volumes one and two orders of magnitude less respectively. The typical wear volumes and debris sizes measured *in vitro* for the different bearing material combinations are compared in **Error! Reference source not found.**.

Table 1: *In vitro* wear results of different bearing materials

Bearing material	Typical steady state wear volume / million cycles	Wear debris size
Metal on polyethylene	35±11mm^3 (Barbour et al., 1999) 40.8mm^3 (Smith et al., 1999)	300±200nm (Tipper et al., 2005)
Ceramic (zirconia) on polyethylene	31±4.0mm^3 (Tipper et al., 2001) 30±5mm^3 (Barbour et al., 1999) 33.3mm3 (Smith et al., 1999)	No data
Metal on metal	1.23±0.5mm^3 (Tipper et al., 2001) 0.11mm^3 (Chan et al., 1996)	30±2.25nm (Tipper et al., 2005) 46nm (Catelas et al., 2003)
Ceramic on ceramic	0.05±0.02mm^3(Tipper et al., 2001) 0.004mm^3 (Clarke et al., 2000)	9±0.5nm (Tipper et al., 2005)

Osteolysis has been observed to occur most often in joints containing a polyethylene component, however it is not known whether this is due to the material, or the larger size of polyethylene particles initiating the response (Campbell et al. 2002). It has been observed that the size of particles generated in polyethylene bearings are in the size range known to generate a response in macrophages, whereas metal and ceramic particles are generally below this range (Ingham et al. 2000). Polyethylene bearing components have also been linked to a slightly higher risk of subsequent implant loosening than all metal bearings (Naudie et al., 2004). Hard on hard bearings produce a lower wear volume of particles than hard on soft bearings, however the smaller size of particle produced is believed to lead to significantly greater numbers of particles being released into the body, and concerns exist as to their reactivity and potential systemic toxicity, due to both increased quantities and a different size range (Ingham and Fisher, 2000; Tipper et al., 2005).

Despite the significant advantages MOM and COC bearings currently appear to offer over MOP and COP bearings in terms of wear and osteolytic potential, some concerns still exist around these materials. Ceramic components have been frequently observed to fracture *in vivo,* particularly after patient trauma such as a fall, and due to the brittle

properties of the ceramic, the component fails catastrophically, requiring revision surgery (Suzuki et al., 2003; Park et al., 2006).

The greatest concerns around MOM bearings are currently focused on the effect of metal ions released into the body from wear debris and corrosion product. Measured ion levels in patients with MOM hips have been shown to be significantly higher than those with MOP or COP implants and pre-surgery patients (Saikko et al., 1998; Savarino et al., 2002; Rasquinha et al., 2006). Nickel, cobalt and molybdenum ions, when released into body tissue, are swiftly transported to the blood and excreted in urine, however chromium has been shown to build up in body tissues (Merritt and Brown, 1996). An increased release of metal ions into the blood has been associated with increased activity and exercise, which may be due to higher wear occurring under these conditions (Khan et al., 2006).

The systemic reactions believed to be associated with ion release include increased lymphocyte activity (Hallab et al., 2004), cell necrosis and apoptosis (Huk et al., 2004), chromosome alteration (Ladon et al., 2004), pseudotumour (Matthies et al., 2012) and possibly carcinogenic effects, although this has not yet been conclusively proven (Signorello et al., 2001). The level of ion release into the body which can be tolerated before adverse reactions occur is not currently fully understood (MacDonald, 2004), but as longer term clinical results with these implants become available this relationship can be investigated further.

1.1.3 Biomechanics of the Hip

Nearly forty muscles act on the hip joint to effect movement, which is grouped into three major directions. Flexion and extension involves the motion of the thigh forwards and backwards in the sagital plane, while abduction and adduction consist of movements in the coronal plane forcing the thigh away from the centre line of body and back towards the body respectively. Finally medial and lateral rotation, also commonly referred to as internal and external rotation, involve rotation of the thigh about its long axis in towards the centre of the body or away respectively (Figure 3). Table 2 shows the range of motion possible in each of these directions.

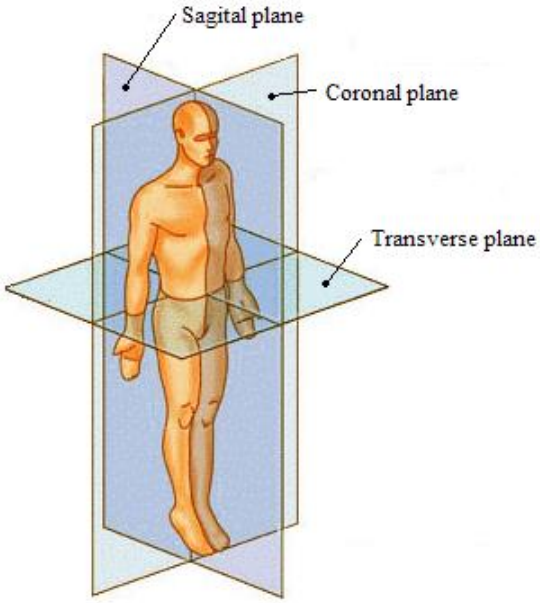

Figure 3: Anatomical planes of the body

Table 2: Range of motion of the hip (Nordin and Frankel, 2001).

Direction of motion	*Range of motion*
Flexion - Extension	140° forwards - 15° backwards
Abduction - Adduction	30° lateral - 25° medial
External - Internal Rotation	90° external - 70° internal (applies when hip is flexed, this range is reduced during extension)

During various types of movement, contact forces within the hip joint can extend to many multiples of body weight, and the resultant force vectors move over a wide area of the hip surface as motion takes place. The kinematics of the most common activities have been studied widely, and are reviewed here with a view to using the data to develop new testing protocols. This data is derived from published reports of loading and motion measured in gait studies. Where possible, measurements covering a number of different activities have been obtained from the same researchers to reduce the

variation introduced by differing experimental techniques, although these results have also been compared to other studies for verification. The broadest range of activity studies have been carried out at Charité - Universitätsmedizin Berlin (Bergmann et al., 2001); this study primarily references the data from that group, alongside others.

When evaluating the loading within the joint, one of two main techniques is generally utilised: either calculation and modelling using values from force plates on the ground and derivation of muscle actions across the joint, or *in vivo* measurement using instrumented implants. The former technique is more susceptible to variation depending on the exact model developed, but offers the benefit of being easy to perform on a wide range of subjects. The latter can be more accurate in the actual measurements taken, however sample size is limited, and information on the gait during these measurements is not always generated (Paul, 2002). Comparisons of these techniques show generally good agreement is achieved between the two, with reported discrepancies ranging from 10-23% peak load values, which is a similar range to the cycle-to-cycle variation for a single patient (Brand et al., 1994; Stansfield et al., 2002).

Where joint contact loads are reported in three axes, this is generally based on a coordinate system fixed to the femoral head (Figure 4).

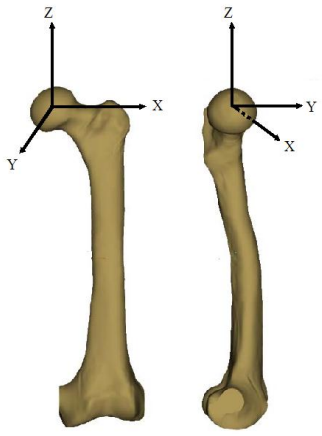

Figure 4: Three dimensional coordinate system of the left femoral head shown on anterior (left) and medial (right) views

1.1.3.1 Walking

Loads in the hip during walking are generally accepted to occur in a twin-peak profile, with the major motion in the sagital plane (Paul, 1966).

The values presented in Figure 5 are drawn directly from a published study (Bergmann et al., 2001), where load was measured by means of an instrumented implant, and motion analysed using a laboratory fixed camera system monitoring markers placed on the body.

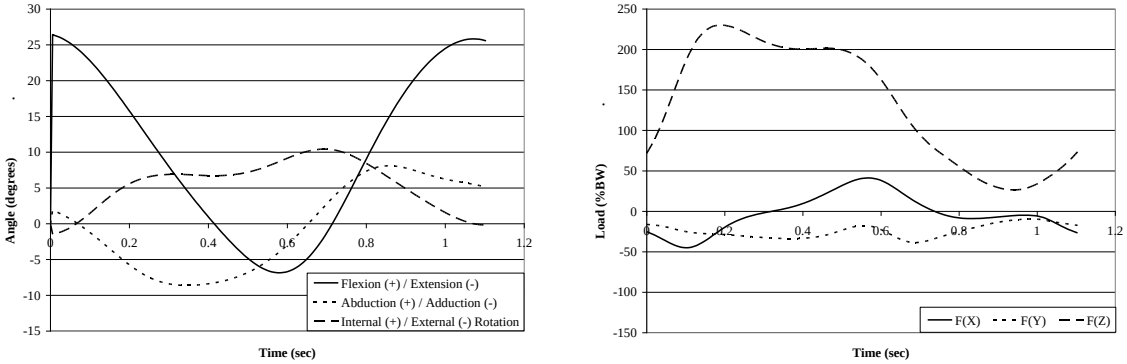

Figure 5 Motion and loading values in three axes for walking at a normal speed (Bergmann et al., 2001)

Results were averaged from four patients with unilateral total hip replacements, at least 11 months post surgery. The major motion is flexion / extension of approximately 34˚, with a twin peak loading profile in the vertical axis and a peak load of 2.3BW. Other studies have found similar results for peak hip contact force using both calculated and measured results using instrumented implants (Table 3).

Table 3: Hip joint peak contact forces during walking. Velocity of walking presented where published.

Study	*Peak Vertical Load (F(Z)) During Walking*
(Stansfield et al., 2003)	3 BW (calculated & measured)
(Brand et al., 1994)	2.5-3.5 BW (calculated and measured)
(Crowninshield et al., 1978)	3.5-5 BW (calculated)
(Paul, 1967)	3.88 BW (calculated)
(Paul, 1976)	2.5-3.5 BW (calculated)
(Van den Bogert et al., 1999)	2.5 BW @ 1.5ms^{-1} (calculated)
(Bergmann et al., 1993)	2.8 BW @ 0.3ms^{-1} (measured)

The kinematics of the hip during walking have been demonstrated to change significantly with both age and walking velocity. A study evaluating gait using body mounted markers, and calculating hip contact forces using measurements from force plates showed that an increase of velocity from 0.3ms^{-1} (0.6mph) to 1.2ms^{-1} (2.7mph) raised average hip peak contact force from approximately 3.5BW to 4BW for patients aged 60-80 years, and to 5BW for patients aged 20-30 years. Similar relationships were demonstrated for peak hip resultant force and moment transmitted from the femur to the pelvis. Range of hip flexion increased from 20˚ at 0.3ms^{-1} for both age groups, to 30˚ and 40˚ at 1.2ms^{-1} for the older and younger patient groups respectively (Crowninshield et al., 1978).

Similar studies also reported increases of hip contact force from 4.9BW to 7.6BW with walking velocity increase from 1.5ms^{-1} to 2ms^{-1} for worst case patients (Paul, 1976), and from 2.8BW to 4.8BW for a velocity increase of 0.27ms^{-1} to 1.35ms^{-1}(Bergmann et al., 1993). Hip flexion was also reported to increase from 42˚ to 48˚ for a velocity change from 1.5ms^{-1} to 2ms^{-1}(Paul, 1976).

The international standard defining the requirements for total hip replacements recommends loads to be applied to the hip during pre-clinical testing of 3kN, which equates to 3.6BW for a typical 85kg patient (International Standards Organisation, 2002). This does however allow replication of worst case scenarios, such as those encountered in younger patients or at higher velocities.

1.1.3.2 Running

As normal walking velocity, typically 1.1ms^{-1} (2.5mph), increases through fast walking to jogging at a rate of up to 2-3ms^{-1} (4.5 – 6.7mph), the force and motion characteristics remain similar, however certain aspects become more pronounced. The twin peak loading of walking, where the two peaks are of similar force, tends to a single peak load dominated by the forces following heel strike, occurring at approximately the same time during the cycle as the first load peak in walking (Figure 6).

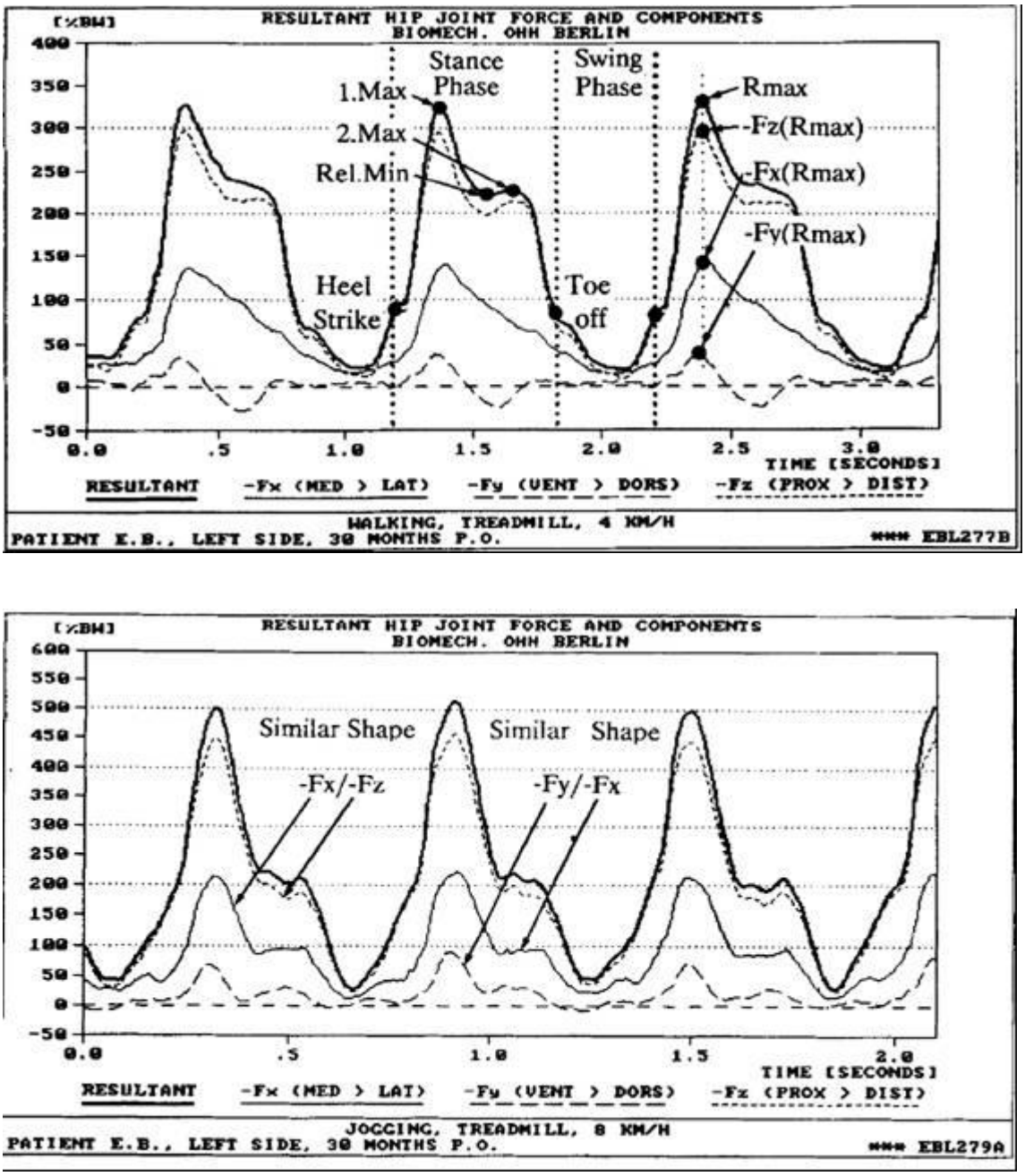

Figure 6 Loading in the hip during walking at 4km/h (2.5mph) (above) and jogging at 8km/h (5mph) (below) (Taken from Bergmann et al. 2003)

Peak contact forces have been measured at 2.2ms^{-1} using an instrumented implant (Bergmann et al., 1993) and at 3.5ms^{-1} using force plate analysis (Van den Bogert et al., 1999). Both studies reported very similar peak loads of 5.0 - 5.2BW. In contrast to slower walking velocities, the forces during running in all three axes follow very similar profiles, with the highest loads in FZ, and FX and FY approximately 50% and 70% lower respectively (Bergmann et al., 1993).

1.1.3.3 Stair Ascent and Descent

Maximum joint force in the hip is reported by (Bergmann et al., 2001) as 2.5BW for stair ascent, and 2.6BW for descent. Forces were recorded using an instrumented implant. The load profiles are similar to walking, with a twin peak phase between heel strike and toe off, followed by a swing phase at lower load. The motion is significantly different to walking however, with high flexion occurring during climbing as the leg is lifted up to the next step. During stair descent the loading follows a similar profile but in reverse, however motion is much lower as the majority of movement occurs in the knee.

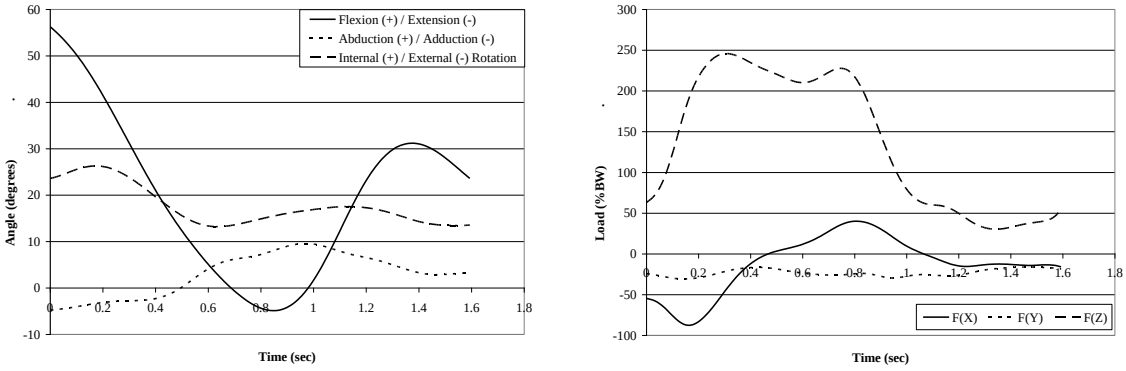

Figure 7: Motion and loading values in three axes for stair ascent (Bergmann et al., 2001)

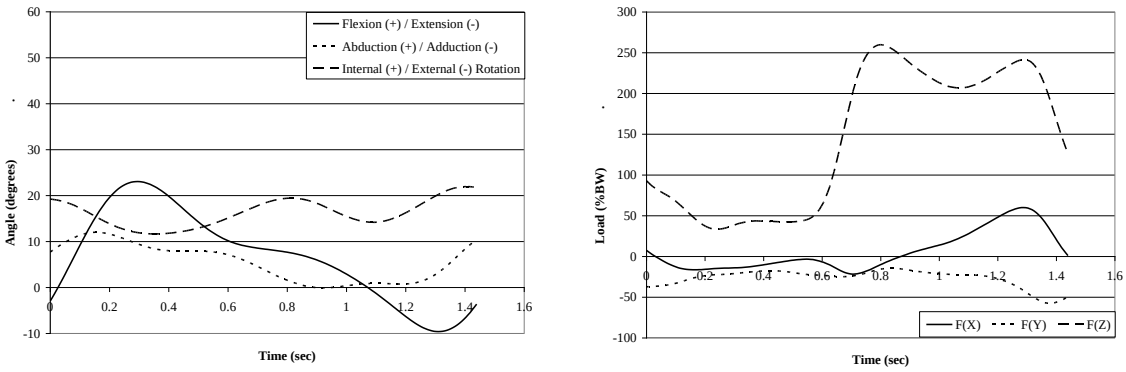

Figure 8: Motion and loading values in three axes for stair descent (Bergmann et al., 2001)

These results are in good agreement with another study which reports peak loads during stair ascent as 2.6BW, again measured using an instrumented implant (Davy et al., 1988). In contrast, maximum loads of 7.2 BW during ascent and 7.1 BW during descent have been reported (Paul, 1976), which are calculated values from force plate measurements. No literature could be found comparing the relative accuracy of instruments versus calculated methods of measuring load during activities other than walking, however it may be that modelling of the more complex activity is more prone to error, hence the large discrepancy.

1.1.3.4 Standing

Bi-lateral stance, or standing on both legs, results in a peak hip contact force of 0.8-1.0BW, measured using instrumented implants (Davy et al., 1988; Bergmann et al., 2001). No literature could be found evaluating the frequency and nature of different types of two legged stance however, such as where body weight is shifted onto one leg and the pelvis dropped on the opposite side. Such positions may significantly alter the magnitude and direction of loads in the joint.

The change in loading of the joint in bi-lateral stance in the early post-operative period from three to 31 days after surgery has also been reported (Davy et al., 1988). The peak hip contact force was only 0.5BW at three days when the patient used a walking frame for support, and 0.7BW at 6 days when a stick was used. Full loading was reached at approximately 16 days post surgery.

1.1.3.5 Sitting

Peak loads in the hip, measured in an instrumented implant, during sitting down into a chair and standing up again are reported as 1.55BW and 1.73 BW respectively (Bergmann et al., 2001) (Figure 9). Similar values of 1.4BW and 1.5BW for getting into and out of bed have also been reported, which involve a similar movement to sitting into a chair (Davy et al., 1988).

In both sitting and standing up, the majority of motion occurs in the sagital plane, with a peak occurring approximately halfway through the cycle corresponding with the subject bending the trunk forwards to aid balance while changing position. The flexion of the trunk also corresponds with load peaks in all three load axes. A positive force is recorded in the vertical (z) axis, while F(x) and F(y) are both negative, indicating high forces in the medial and posterior directions.

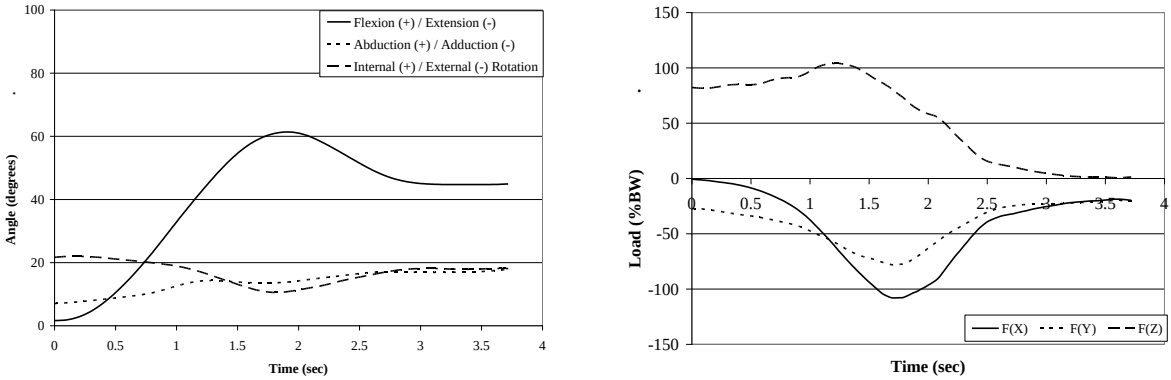

Figure 9: Motion and loading values in three axes for sitting down (Bergmann et al., 2001)

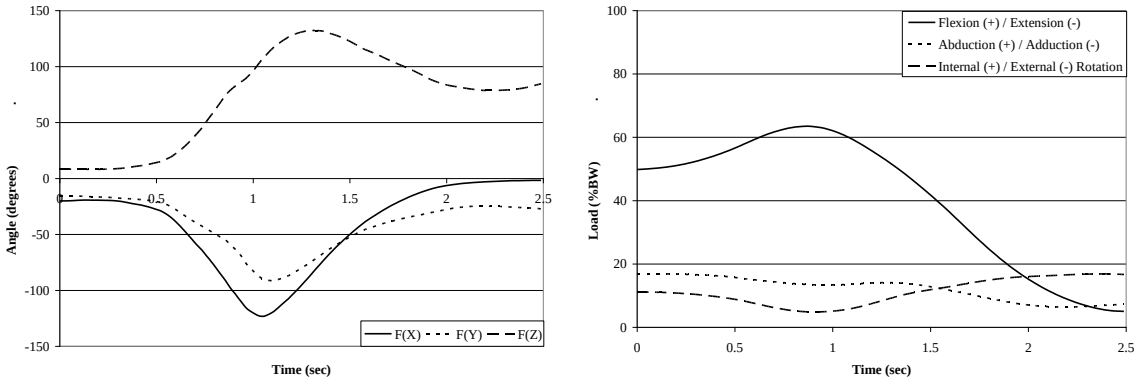

Figure 10: Motion and loading values in three axes for standing up (Bergmann et al., 2001)

1.1.3.6 Stumbling

The kinematics of stumbling is not widely reported in the literature, possibly due to the varying nature and dependence upon environmental conditions of this type of activity. A study on one patient with an instrumented implant was reported, and measured a peak hip joint loading of 8.7BW (Bergmann et al., 1993). The initial stumble caused a peak load of approximately 4BW, but was followed by three rapid steps with increasing peak load as the patient tried to restore balance before resuming normal walking patterns (Figure 11). Stumbling is normally an accidental occurrence, therefore reproduction in the laboratory may not accurately represent normal conditions, and there may be a significant level of variability in the kinematics depending on the cause of the stumble.

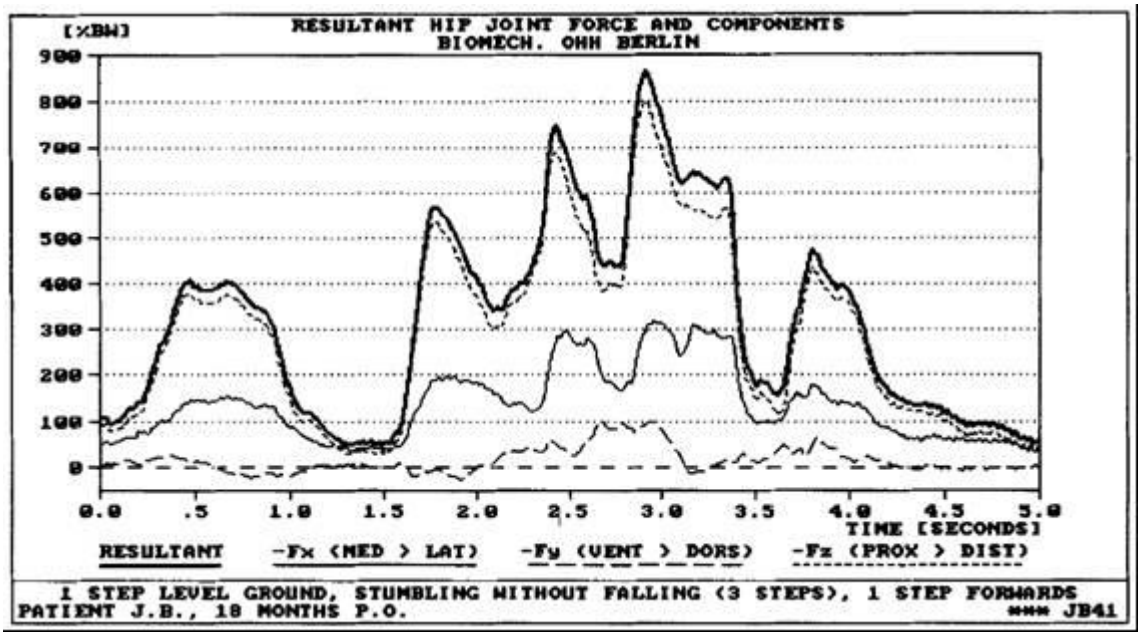

Figure 11 Loading in the hip during stumbling (Taken from Bergmann et al. 1993)

1.1.4 Activity Levels of THA Patients

Total activity levels of patients have been studied by a number of groups (Schmalzried et al., 1998; Zahiri et al., 1998; Shepherd et al., 2000; Smith et al., 2002; Silva et al., 2005). These studies measured the number of ambulation cycles per year on patients with hip replacements, evaluating the differences caused by gender and age (a young patient is considered by all of these authors to be less than 60 years). One cycle of walking consists of both the ground contact phase and the swing phase for one leg, during which time the opposite leg is in contact with the ground. Therefore each cycle is effectively two steps, one on the right leg and one on the left.

Zahiri and Schmalzried both recorded a mean of approximately 900,000 cycles per year; those under 60 years generally walked 20% more steps per year than those older than 60, and males similarly walked 20% more than females. These were all measured using a pedometer.

Shepherd and Silva both took simultaneous measurements with a pedometer and a step activity monitor (SAM) which is a small accelerometer attached to the ankle. They found significant differences between results for the two devices, with a mean annual cycle count for the pedometer and SAM of 1.25 million cycles (mc) and 1.96mc respectively. Validation trials measured error of the pedometer at 6.1%, but only 0.5% for the SAM, suggesting pedometer studies are significantly underestimating true patient activity levels.

A further study (Smith et al., 2002) measured patients with healthy, intact hips, and considered demographic factors affecting activity levels. Activity was very strongly linked to occupation across a wide range of professions including active groups such as postmen and nurses through to sedentary groups such as office workers and retired persons. This study also generated activity levels for a much wider age range (20 - 90 years), and when considered with the range of occupations, provides a good approximation of activity levels for the whole population. A strong correlation between age and activity level was established (Equation 1) from which a mean value for steps/year for the 20 – 60 years age group from Smith et al can be calculated as 2,233,983 steps. This matches approximately the age range over which Schmalzried, Zahiri and Shepherd obtained their data for young patients, and falls within the range of the studies on THA patients.

Number of steps per year = 365 (10,823 – (85.5 x age in years))

Equation 1

The mean number of steps per year for a patient below 60 years of age averaged from the four studies described above is approximately 2 million cycles. This increased cycle count should be taken into account when developing simulator protocols representing younger patients.

Studies into the distribution of different activities used by a typical patient highlight that 50-75% of patient waking time is not spent in ambulatory activity, but in static positions such as standing, sitting and lying (Morlock et al., 2000, 2001).

Daily typical activities of adults with total hip arthroplasty have been evaluated (Morlock et al., 2001). The most commonly occurring activity types and the relative proportions of each during a typical day are summarised in Table 4. These measurements were typically taken over a period of 9.5 hours. The data is given both in terms of actual number of steps per day, and also in terms of number of sequences. A sequence is the number of individual periods of time during which that activity was used, for example a period of walking continuously for one minute preceded and followed by standing still is considered as one sequence of walking. This allows for better comparison between static and dynamic activities.

Table 4: Typical activity distribution throughout the waking day for a THR patient (Morlock et al., 2001)

Activity	Mean steps / day	Mean sequences / day	Total time / day (min)
Walking	6324	286	59.8
Stair climbing	278	33	2.5
Sitting	-	63	261.8
Lying	-	2	33.3
Standing	-	611	141.2

The duration of pauses during activity, and the position during pause was also studied by Morlock et al. and is summarised in Table 5 and Table 6 (Morlock et al., 2000).

Table 5: Typical pause duration and position throughout the waking day for a THR patient (Morlock et al., 2000)

Duration of resting periods	**Frequency of resting periods (No. / h)**
2s – 5s	99.4 ± 43.1
5s – 10s	35.6 ± 14.2
10s – 30s	25.6 ± 13.7
30s – 60s	6.4 ± 3.6
60s – 180s	3.6 ± 2.4
Average duration of resting periods (s)	11.2 ± 3.0

Table 6: Typical pause position throughout the waking day for a THR patient (Morlock et al., 2000)

Resting position	**Time in position (%)**
Standing	37.0 ± 21.8
Laying	8.7 ± 18.0
Sitting	54.3 ± 23.7

The lubrication conditions within a hip joint can be significantly affected by the relative motion of the head and cup, and periods when the patient is not active may have a significant effect on bearing wear. These static periods should therefore be considered when planning pre-clinical testing.

This data is derived from patients with an average age of 63 years and may not be truly representative of younger patients, however this type of data for patients younger than 60 years could not be found in the literature.

1.1.5 Demographics of THA Patients

Over 800,000 total hip replacements are performed worldwide annually (Crowninshield, 2006), with 83,000 in 2010 in England alone. The majority of cases (93%) are required to relieve the symptoms of osteoarthritis, with the remainder for indications including avascular necrosis, fractured neck of femur and congenital dislocation (National Joint Registry for England and Wales, 2011). Typically a hip replacement is expected to last 10 to 15 years in a patient before complications or device failure require revision of the implant. Each revision of an implant requires a progressively more invasive approach and complicated procedure, therefore traditionally THA was offered to elderly patients who would be less likely to require multiple revisions. Recent developments in implant design have reduced the rates of wear and increased the expected lifetime *in vivo*, therefore younger patients can be treated using these new devices. With this change in patient however, a change in the conditions to which an implant is exposed occurs, with younger patients being more active, thus requiring implants to last longer to reduce the need for revision.

Overall average age for a primary hip is 67 years, however numbers of younger patients, typically aged less than 55 years, have been increasing. From 1994 to 2003 the number of male THA patients aged 85 or over rose by 53%, whereas for those aged 45-54 years this increase was 81%. Slightly smaller increases were seen for equivalent female patients of 13% and 37% respectively (The Swedish National Hip Joint Arthroplasty Register, 2004). Since 2003 levels in the UK appear to be more stable, with a consistent 12-13% of patients under age 55 every year up to 2010. In 2010 31% of patients were over 75, and the largest group was between the ages of 65 and 74 with 35% of patients (National Joint Registry for England and Wales, 2011).

Increasing life expectancy is posing a challenge for orthopaedic surgery, with an average 65 year old now living 26% longer than in 1960 (Crowninshield et al., 2006). Over the same period of time, the obesity rates for the general population have increased by over 15%, and an associated increased incidence of arthritis has been shown. Activity levels are increasing within the older population, and younger patients who receive implants are generally even more active than older age groups. Improved healthcare information services, in particular the internet, have also led to better educated patients who consequently develop higher expectations of implants (Crowninshield, 2006). All of these factors contribute to increased performance

requirements for THA devices, in terms of longevity and load bearing ability, therefore increasingly severe pre-clinical testing is needed to evaluate new devices.

At the commencement of this study in 2005, metal-on-metal implants were widely used and considered a low wearing, high performance solution for patients. This led to the decision to focus this study on all metal arthroplasties. More recently widespread concerns have been raised about MOM bearings with high reported revision rates and poor patient outcomes, leading to a significant reduction in the numbers of these devices currently being implanted. These concerns are discussed in more depth later in this chapter.

1.2 Metal on Metal THA

1.2.1 Historical Development of MOM THA

Metal on metal (MOM) bearings for THA were originally developed in the 1950s and 60s, however many early designs were unsuccessful, with high wear rates and binding of the bearing reported in many patients (McKee, 1982). Around the same time the Charnley low friction MOP arthroplasty was launched, which proved highly successful, and remains a gold standard today (Charnley, 1961, 1982). MOM dropped out of favour for a number of years, only to return into common use in the late 1990s (Amstutz and Grigoris, 1996).

The first successful full metal on metal total hip replacement to be developed was the McKee-Farrar hip at Norwich Hospitals in the early 1950s. McKee combined a small diameter femoral head designed by Thompson, with an acetabular cup which was cemented in situ using polymethymethacrylate; a technique pioneered by Charnley. They discovered that cobalt chrome alloys performed significantly better in wear than stainless steels, and that the surface finish of the material was critical to success. Good early results were reported with survivorship of over 90% at four years post implantation (McKee et al., 1966). Over the following ten years over 800 of these devices were implanted, and by the 1980s many survived. A review of these devices showed nearly 50% demonstrated good or excellent performance as measured using the Harris Hip Score and nearly 80% caused the patient little or no pain (Harris, 1969; August et al., 1986).

A number of studies retrospectively examined the performance of the McKee-Farrar hip to determine the reasons for some surviving much longer than others (McKellop et al., 1996; Howie et al., 2005). Certain design parameters, including increased femoral head diameter and lower bearing clearance were correlated with low bearing wear compared with MOP implants, however very low clearance was shown to lead to equatorial binding of devices and subsequent loosening of the acetabular cup (August et al., 1986).

From the late 1980s onwards, 2nd generation metal-on-metal bearings were introduced, including such designs as the Metasul (Zimmer GmbH) with hugely successful clinical results (Delaunay, 2004; Long, 2005). Resurfacing type designs, which had previously

been unsuccessfully trialled in various materials, were revisited in a MOM bearing combination and were also shown to perform well (McMinn et al., 2011).

More recently, a number of publications have highlighted potential flaws with the MOM concept, particularly in resurfacing implants, and described severe patient reactions to the wear debris from these devices and subsequent revisions observed with a higher frequency then with other implant materials. Surgeons have reported revision rates of up to 49% (Langton et al., 2011). Patients have presented with severe pain, restricted activity, and clunking or squeaking coming from the hip region (Browne et al., 2010). Metal hypersensitivity has been identified as a key cause of these problems, whereby wear products from the device, including metal particles and ions, induce an immune reaction, resulting in aseptic loosening of implants. Many patients with metal sensitivity exhibit massive soft tissue necrosis around the joint, metallosis or metal staining of the tissues, large cystic fluid filled masses associated with pseudotumour and ALVAL (aseptic lymphocytic vasculitis-associated lesions). Concerns have also been raised, although not proven, over carcinogenicity of metal ions (Dumbleton and Manley, 2005; Mäkelä et al., 2012). Other potential causes of failure suggested in the literature include infection and implant mal-positioning (D Shetty and N Villar, 2006; Browne et al., 2010; Fabi et al., 2012). The British Medicines and Healthcare Products Regulatory Agency (MHRA) and the US Food and Drug Administration (FDA) have both issued guidance on monitoring of patients with MOM devices with blood ion level assessment and imaging using MRI or ultrasound to identify problems early on (Food and Drug Administration (FDA), 2012; Medicines and Healthcare Products Regulatory Agency (MHRA), 2012). Significant work remains however to fully understand the problems with these implants. Several metal-on-metal implants have now been withdrawn from the market.

1.2.2 Tribology of MOM THA

The lubrication within a MOM bearing is a significant factor affecting the wear behaviour of the joint. The nature of the lubrication in a bearing can be classified into one of three categories: boundary, fluid film, or mixed which is a transition phase between the two. In the boundary regime, although the lubricant may coat the surface, the asperities, or peaks which are a feature of the surface of the material, remain in contact with each other, and friction behaviour of the bearing is similar to that of a dry bearing (Dowson and Jin, 2006). Fluid film lubrication occurs when the bearing surfaces are fully separated by a layer of lubricant, and there is no asperity contact.

The lubrication regime within the joint is largely determined by the material and lubricant properties, bearing geometry, entraining velocity, and joint loading. Composite surface roughness of the opposing parts also plays a significant part in determining the regime. The effect of this is defined by the lambda ratio, between the predicted minimum lubricant film thickness, and the composite R_a measurement of the surface roughness (Equation 2). It is generally accepted that a lambda ratio of less than one equates to boundary lubrication, while a value of greater than three indicates a fluid film regime. An approximation for film thickness in a ball-on-plane bearing is shown in (Equation 3) (Hamrock and Dowson, 1978), and this has been shown to agree well with predicted film behaviour in a conforming ball-in-socket model (Jagatia and Jin, 2001).

$$\lambda = \frac{h_{\min}}{R_a}$$

Equation 2

$$\frac{h_{\min}}{R} = 2.80\left(\frac{\eta u}{E'R}\right)^{0.65}\left(\frac{w}{E'R^2}\right)^{-0.21}$$

Equation 3

λ	lambda ratio	R_a	composite surface roughness
$h_{\min}$	predicted minimum film thickness	w	load
η	lubricant viscosity	E'	Young's modulus
u	entraining velocity	R	effective radius

In MOM hip bearings, the lubrication regime can be determined through friction testing, and by plotting the relationship between the coefficient of friction and the Sommerfeld number, which forms the Stribeck curve (Figure 12). The Sommerfeld number is a function of a number of environmental parameters. The change between different lubrication regimes is not generally distinct, but a gradual change from one dominating mechanism to another. Mixed lubrication for example, is more severe towards the boundary region of the Stribeck curve, than it is towards the fluid film region.

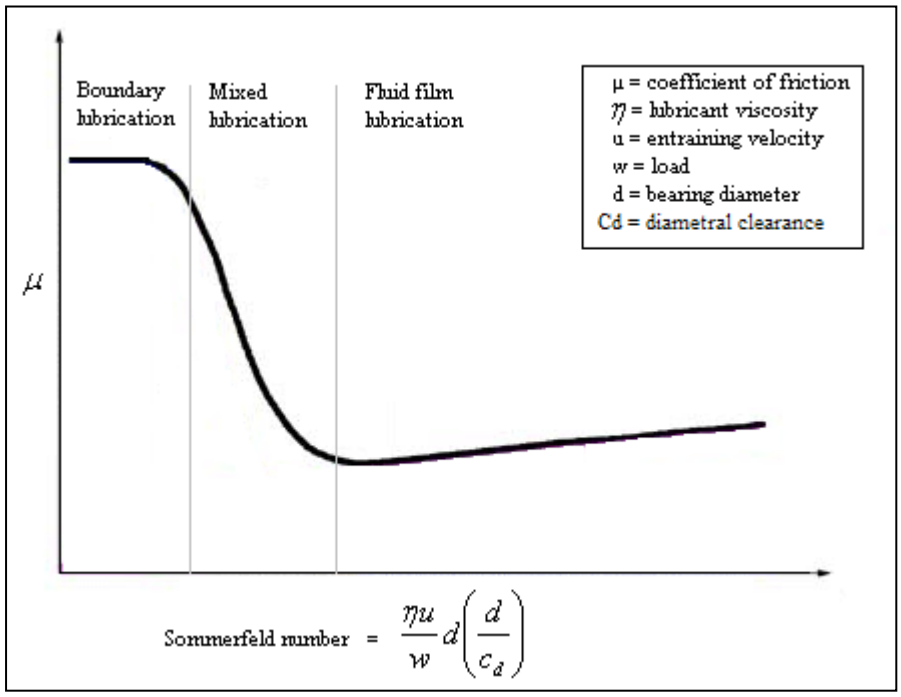

Figure 12: Stribeck curve illustrating relationship between friction coefficient and Sommerfeld number (Smith et al., 2001b)

Despite the apparent dependence of the lubrication regime on the load and entraining velocity, in natural joints a fluid film is maintained throughout the walking cycle. This is thought to be caused by entraining behaviour drawing lubricant into the bearing during the swing phase of the motion cycle, and squeeze film action maintaining it during the stance phase (Jin et al., 1997; Medley et al., 2001). In contrast, MOP bearings generally operate in the boundary / severe mixed lubrication regime, due to the relatively high surface roughness of polyethylene compared with harder bearing materials (Hall and Unsworth, 1994). COP bearings however, tend to operate mostly in the mixed regime (Dowson, 2001).

1.3 Wear of MOM THA

1.3.1 Wear Mechanisms

Wear rate of metal-on-metal joints *in vitro* has been shown to be split into two distinct phases: bedding in, where an increased rate is observed for the first one or two million cycles, and steady state wear, where the rate decreases rapidly after the initial phase, to a stable, relatively low level of wear (Anissian et al., 1999; Tipper et al., 2001; Dowson et al., 2004a). This is due in part to a change in contact area between the bearing components. The parts wear predominantly in a concentrated area on the pole of the head and the superolateral region of the cup, leading to flattened zones and to greater conformity in the bearing. As this wear takes place the contact stresses in these regions reduce, leading to improved conditions for lubrication. Eventually an optimal contact area is achieved, where reduced stresses lead to significant improvement in lubrication and reduction in wear to steady state levels (Hu et al., 2004).

A number of wear mechanisms have been identified in MOM bearings, including abrasion, where asperities or loose particles gouge the opposing material; surface fatigue, where indentation of the surfaces causes material loss; and tribochemical reactions (Wimmer et al., 2001). The latter cause the formation of carbon rich layers on the surface of the bearing faces, which are believed to be formed by proteins decomposing in the high temperatures occurring during motion. These protein layers may act as a solid lubricant, reducing wear. The layers have been observed on specimens tested *in vitro*, as well as on explanted prostheses (Wimmer et al., 2003). No evidence of adhesive wear was observed in these studies, as would usually be expected of MOM bearings, which was attributed to the lubricating effect of the solid carbon layers. Recently, it has been suggested that surface fatigue of the bearing interfaces causes localised hardening of the surface. This occurs through simultaneous mechanisms of rolling clusters of atoms at the material surface, and shearing of grains at stacking faults, which lead to recrystallisation of the material, a reduction in grain size and increase in hardness. This is believed to be a cyclic process, and contributes to local high wear resistance (Bűscher et al., 2005). A significant proportion of material loss in reciprocating bearings has also been attributed to corrosion, in addition to mechanical wear (Yan et al., 2006).

1.3.2 Factors Affecting Wear

The geometry of a MOM hip bearing is known to have one of the most significant effects on tribological behaviour and hence the wear properties of the joint. Size of the bearing used is decided by the surgeon based on a number of parameters including patient age, anatomy and activity level. An increase in bearing diameter is associated with an improvement in the lubrication regime for MOM from boundary for 16mm and 22mm sizes, to mixed for 28mm and larger (Goldsmith et al., 2001; Dowson et al., 2004a) This corresponds with a reduction in wear with increasing diameter for those sizes operating in mixed lubrication, but a decrease in wear with diameter reduction for the sizes operating with boundary lubrication (Jacobs et al., 1998; Goldsmith et al., 2000). *In vitro* wear results for MOM bearings have been reported for 22mm and 36mm bearings as 6.3mm^3/million cycles (mc) against 0.07mm^3/mc respectively (Smith et al., 2001a). Increased diameter leads to a reduction in wear due to an improvement in tribological conditions; as diameter increases, entraining velocity increases, and the lubricant film thickens, allowing more separation of the surfaces and less asperity contact.

It has also been shown that increased head diameter increases joint range of motion and stability, which reduces the rate of dislocation in patients. Dislocation can substantially increase bearing wear *in vivo* due to damage caused to the surfaces (Cuckler et al., 2004; Burroughs et al., 2005). Increased bearing size has also been associated with an increase in cobalt and chromium ion levels in the blood for patients who have a current, well functioning implant (Clarke et al., 2003). This contradicts the previous studies showing a decrease in wear with larger diameters, however the study also suggests the ions may be a product of corrosion, which would be a separate mechanism to wear.

Clearance between the opposing bearing parts can typically range from 80µm to 350µm depending on bearing diameter and design. A high clearance for all bearing sizes has been shown to increase wear, however very low clearances such as 20µm cause an increase in wear, possibly due to equatorial binding, or deflection of the cup causing local negative clearances (Chan et al., 1999; Rieker et al., 2004). A study examining the effect of reduction in diametrical clearance from 100µm to 65µm resulted in mean wear reduction from 0.67mm^3/mc to 0.11mm^3/mc for 28mm diameter bearings (Chan et al., 1999). Similarly a different study showed that for 36mm implants, wear during the bedding in period was shown to reduce from 3.51mm^3/mc to 2.32mm^3/mc for a

clearance reduction from 143µm to 105µm (Dowson et al., 2004b). Low clearance may allow the reduction in wear through an increase in the contact area between components, thereby reducing contact stresses, or by increasing the squeeze film component of lubrication, increasing separation of the opposing surfaces.

Within cobalt chrome MOM bearings the alloy selection has been shown to also significantly affect wear. Reduced wear is seen in high carbon content (0.2%) alloys when compared with low carbon (0.07%) alloys, and lower carbon content resulted in larger wear particle sizes (Tipper et al., 1999). Similar findings were reported in other studies (Medley et al., 1996; Dowson et al., 2004a), with a significant increase in wear observed for low carbon alloys. The effect of using cast or wrought material however, was insignificant on wear.

1.4 Pre-Clinical Testing of Hip Replacements

Pre-clinical evaluation of a THA is both a requirement of regulatory bodies, and necessary for the manufacturer to ensure safety and efficacy of their device. Wear testing of the materials and bearing interface is one of the most important aspects of this evaluation, due to the effects poor wear properties can have on overall survivorship of the implant and more significantly, the health and well-being of the patient.

1.4.1 Material Characterisation

Functional hip wear simulation is a relatively recent development in the area of wear measurement, with most early simulation machines having been designed in the 1990s. Prior to this, assessment of material wear properties was conducted on simple wear measurement equipment such as the pin-on-disc machine.

A number of pin-on-disc or pin-on-plate devices have been described in the literature (Saikko and Ahlroos, 1999; Saikko, 2005) in which a pin of one sample material is moved against a plate or disc of the matching sample material whilst under pre-load. Different movement types can be incorporated, such as linear sliding or figure-of-eight type motion, and multiple stations can be tested simultaneously. The samples can also be immersed in a bath of lubricant if required. Periodically throughout the test the material samples are removed and gravimetrically assessed to measure material loss due to wear. A slightly different pin-on-ball technique has also been described (Wimmer et al., 2001), loading concave faced pins against a femoral head in an oscillating motion designed to loosely replicate the flexion occurring in the hip during walking.

These techniques allow simple comparison between materials selected for THA designs in a relatively short time, with typical testing durations of hours and days rather than the months necessary for a full wear simulator study. The major drawback of this type of testing however is that results are not clinically relevant. In recent years, the focus has shifted from researching wear properties of material selection and manufacturing effect, to factors directly associated with the conforming ball-in-socket bearing, such as geometry changes, for which a functional wear simulator is necessary.

1.4.2 Wear Simulation

Hip wear simulators allow more clinically relevant measurement of the wear occurring within a bearing by applying realistic loads and motions to a femoral head and matching acetabular cup for millions of cycles, replicating *in vivo* use of the joint. Simulators have allowed significant development in the area of hip design, by facilitating evaluation of tiny changes in bearing design and the associated effect on wear, which was not possible using previous techniques. In addition to the ethical benefits of *in vitro* testing, simulator testing offers advantages over clinical measurements of joint performance, in allowing standardisation of applied loads and motions, and removal of patient specific variables such as activity levels and gait variation (Barbour et al., 1999).

A typical simulator can test between 6-12 stations simultaneously, depending on the design selected, and samples are immersed in a bath of lubricant. Motion can be usually controlled in the flexion / extension direction, in addition to internal / external rotation and / or abduction / adduction. Load is typically only applied in the vertical axis, due to the complexity of introducing a full set of three load controlled axes, although some six-axis simulators are available. The head and cup can be removed periodically throughout the test for gravimetric and dimensional analysis to measure wear. Current simulator test techniques generally use an estimate of one million cycles to be equivalent to one year's *in vivo* use. A standardised simulator test has been defined (International Standards Organisation, 2002), to allow different research centres to draw accurate comparisons between different studies.

Several different designs of hip simulator are currently used in research, incorporating slightly different kinematics, or featuring different numbers of controllable axes for loading and motion. A number of studies have examined the effect of modifying the kinematics in hip simulator wear testing from loads and motions close to those recorded *in vivo*, to a simplified single or twin axis motion with a less complex loading pattern, allowing for more cost effective machines.

Comparisons between the wear generated in different simulator types have been reported in the literature. The wear on wrought 28mm MOM articulations has been measured (Firkins, Tipper, Ingham, et al., 2001), comparing the effects on wear of a three axis simulator, incorporating flexion / extension, internal / external rotation and load, and a four axis simulator, adding in adduction / abduction. The four axis simulator

resulted in significantly lower wear than the three axis simulator, which is suggested to be caused by greater eccentricity in the motion cycles in the three axis machine, leading to less efficient bearing lubrication. The authors also suggest that some gaits or activities other than ISO 14242 defined walking may have a greater level of eccentricity, which could lead to higher wear rates, more in line with those found *in vivo*.

Different motion protocols have also been compared (Smith and Unsworth, 2000), measuring the effect of reducing two axes of motion (F/E and I/E rotation to a single axis (F/E only), and found the later significantly reduced wear in ceramic / UHMWPE pairings. The effects on MOM pairings were not studied. They did however, find that simplified loading, where the twin peak loading defined in ISO 14242 was replaced by a flat plateau at peak load, did not significantly alter wear volume in both metal and ceramic heads paired with UHMWPE cups.

Wear simulation offers a very clinically relevant method for evaluating the expected *in vivo* behaviour of joints, although the type of simulator used and the inputs set must be considered when comparing different studies to get an accurate assessment.

1.4.2.1 Historical Development of Hip Wear Simulators

The first simulators were intoduced in the 1960s and consisted of simple single station, cam operated pendulum type machines developed at the Royal National Orthopaedic Hospital Stanmore, and at the University of Leeds (Clarke, 1981; Dowson and Jobbins, 1988). Developments were made by many centres over the following decades. The University of Leeds introduced electro-hydraulic servo-controls to their simulators in the 1970s, leading onto a full six axis multiple station machine in the 1980s (Dowson and Jobbins, 1988). Sulzer Medical in Switzerland introduced their first single station simulator in 1972 with a single load and motion axis, similar to the twin station machine developed at Masachusetts Institute of Technology, Boston, with both applying physiological flexion / extension motion and dynamic loading with a Paul type curve (Clarke, 1981).

The Matco simulator developed at Los Angeles Orthopaedic Hospital was one of the earliest multiple station simulators with a capacity for ten stations, significantly reducing test times and improving statistical significance of data. The Matco applied load via hydraulic actuators and two axes of motion (Clarke, 1981).

Different types of simulator began to emerge in the 1990s; the anatomical wear simulator is in common use today and applies physiological motions in two or three axes to a bearing couple positioned as they would be *in vivo.* Examples include the AMTI (Advanced Mechanical Technology Inc., MA, USA) and ProSim (Simulation Solutions, Manchester, UK) simulators (Bragdon et al., 1996; Goldsmith and Dowson, 1999). This type of simulator is defined in ISO 14242:1 (International Standards Organisation, 2002).

In contrast an orbital type of simulator has also emerged, where the bearing is inverted and motion is applied in a single orbital arc, rather than individual axes of motion. The kinematics are less anatomical than an ISO 14242:1 simulator, however good parity with clinical wear has been demonstrated. The MTS (Mejia and Brierley, 1994), HUT (Helsinki University of Technology) (Saikko et al., 1992; Saikko, 1996) and Shore Western (Clarke et al., 1997) are all examples of the orbital bearing machine (OBM) and the general concept is described in detail in ISO 14242:3 (International Standards Organisation, 2009)

1.4.3 Computational Modelling

More recently computational modelling has added a further dimension to pre-clinical evaluation of implants. Predictions of the tribological conditions within the hip have been modelled and compared to experimental results from friction testing with good agreement (Brockett et al., 2006). Wear behaviour of polyethylene components in total knee arthroplasty using finite element adaptive remeshing techniques has also been modelled, again with good equivalence to experimental data (Knight et al., 2007).

These techniques allow very swift prediction of bearing behaviour, with substantially reduced equipment requirements compared to *in vitro* testing, however many computational techniques still require further development to give results with the same accuracy and validity as physical tests. Wear simulation still has a significant part to play in pre-clinical evaluation.

1.4.4 Comparison between *in vitro* and *in vivo* wear rates

A number of comparisons have been made between the samples from *in vitro* wear testing and explanted devices, particularly in terms of the wear volumes measured and

the nature of the debris generated, with a view to evaluating the accuracy of *in vitro* testing as a mimic for *in vivo* conditions.

Wear particles from an orbital type simulator have been compared with those extracted from periprosthetic tissue, and good agreement found for both particle size and shape (Catelas et al., 2004). Another study compared a number of different simulators and showed all to produce significantly lower wear rates in MOP bearings than *in vivo* (Barbour et al., 1999), even those utilising a motion pattern very similar to physiological motion. In MOM bearings, higher rates have also been reported for *in vivo* studies, compared with *in vitro* simulation (Medley et al., 1996, 2002; Firkins et al., 2001; Catelas et al., 2002, 2004). A number of studies have suggested this may be due to the continuous nature of the simulator testing, which differs significantly from the constantly varying movement patterns of typical patients (Medley et al., 2002). This is thought to be due to the changing activity *in vivo* causing breakdown of the lubricating fluid film between the components of the implant leading to an increase in wear. The comparatively continuous motion employed in walking simulation leads to a more optimal lubrication regime in the bearing, resulting in lower wear rates.

Measurement of *in vivo* wear rates in MOM bearings are difficult due to the minute geometrical changes involved, however some studies have attempted to measure this (Reinisch et al., 2003; Rieker et al., 2004), and presented linear wear of 28mm metal on metal bearings of 7.6µm and 6.2µm respectively. A relationship between linear and volumetric wear, established from measurements of explanted and *in vitro* tested samples was proposed and is shown in Equation 4.

$$V = 0.0283L^{1.69}$$

Equation 4

where V equates to volumetric wear in mm^3 and L represents linear wear in µm (Medley et al., 2002). Using this equation, the linear wear measurements presented above equate to $0.87mm^3$ and $0.62mm^3$ respectively in volumetric wear. However, the study by Reinisch measured volumetric wear of the same samples with a co-ordinate measuring machine and presented rates of $2.02mm^3$/year which differs significantly from the value generated by the equation (Sieber et al., 1999).

The majority of results for *in vivo* wear rates are derived from explanted failed prostheses, which can give a 30-60% higher rate of wear than typically found in a well

functioning replacement joint, possibly due to higher wear occurring prior to or as a result of joint failure. Well functioning retrievals, usually obtained post mortem, are rarely reported in the literature. Clinical measurements of satisfactorily functioning joints are possible for MOP bearings where linear wear can be measured by means of x-ray or similar, but not for MOM articulations. Because of these issues, caution must be exercised when comparing reported *in vivo* wear rates with results from simulator testing.

1.5 Current wear simulation practices

1.5.1 Walking simulation

The majority of studies currently undertaken for wear simulation adhere as far as possible to the method for an anatomical simulator specified in ISO 14242 Part 1 (International Standards Organisation, 2002). This specifies motion in three axes with flexion / extension of +25º to -17º, internal / external rotation of +2º to -10º, and abduction / adduction of +7º to -4º. All motions are applied in an approximately sinusoidal waveform. Load is applied along the main axis of the femoral head in a twin peak 'Paul' type profile (Paul, 1967). Implants are generally positioned anatomically with the cup superior to the head. The cup rim is oriented at 35º from the horizontal, with load applied vertically. The joint reaction force *in vivo* occurs at 10º from the vertical, and normal recommended positioning for a cup in the acetabulum is 45º, therefore positioning the cup at 35º *in vitro* allows use of a vertical applied load in the simulator (Williams et al., 2008). New born calf serum is used as a lubricant (Wang et al., 2004) and has been shown at 25% dilution to have an equivalent protein content (aproximately 17g/L) and offer similar lubrication to natural synovial fluid.

Steady state wear rates for MOM bearings in simulators have been reported for 28mm diameter 80µm clearance low carbon wrought bearings as 0.25mm^3/mc (Scholes et al., 2001). Wear rates for similar 36mm bearings have been reported between 0.0325mm^3/mc and 1.6225mm^3/mc once in steady state wear (Goldsmith et al., 2000).

1.5.2 Motion interruption

The typical motion of patients, as discussed previously, is not continuous in nature like current simulator testing, but frequently changes activity and involves regular periods of no motion. A number of wear studies have attempted to mimic this by introducing pauses into tests and evaluating the subsequent change in tribological behaviour (Bergmann, 2002; Medley et al., 2002).

Frictional studies of stopping during walking simulation have been shown to demonstrate an increase in friction after stopping periods, with the magnitude of friction positively correlated with the duration of pause (Nassutt et al., 2003; Wimmer et al., 2006). An increase of 191% in friction was reported after a pause of 60 seconds.

The increase was attributed to interlocking of the carbon layers which are found on the surface of the bearing as previously described.

Wear rate and friction have been evaluated simultaneously in a pin-on-ball rig (Wimmer et al., 2001), and it was shown that an increase in the duration of a pause between two periods of continuous simulated walking motion caused a corresponding rise in frictional torque at the point when motion restarted. For a duration of zero seconds – effectively occurring at the change in direction of swing – torque averaged 3.06Nm, compared with 7.96Nm for a rest period of 60 seconds. This increase in torque however, was shown to cause no significant increase in wear in testing over two million cycles, incorporating 30 second periods of continuous walking cycles, followed by 15 second pauses. Load during the pauses is not recorded. Due to the absence of an increase in wear, the authors dismiss the possibility of adhesion or cold welding as causes of the increased torque, and suggest that mechanical carbide interaction or tribochemical reactions are responsible.

These results stand in contrast with those found when using a similar stop-dwell-start protocol on a physiological joint simulator, which reported a two-fold increase in wear (Chan et al., 1999). This increase was attributed to breakdown of the elastohydrodynamic film in the joint, caused by full body weight loading during the dwell periods. The differences between these studies could be due to the different equipment used, as the tribological conditions between a ball and pin will be substantially different to those between a head and cup.

Stop-dwell-start protocols have also been used by other groups (Medley et al., 2002), on the basis that they represent a more realistic representation of *in vivo* conditions in MOM prostheses than incidences such as microseparation, which is not as commonly observed as in ceramic and hard on soft bearings (Dennis et al., 2001). Ten minute periods of continuous walking cycles were applied to 28mm MOM bearings of both cast and wrought cobalt chrome alloys, followed by one minute's rest at 3.3kN load. The volumetric wear results were higher than those in a conventional simulator cycle, and were found to be more in line with explant wear rates for both first and second generation MOM prostheses. However studies of *in vivo* joint force during a two legged stance, which would be typical during a pause in motion, report *in vivo* hip joint load as one body weight, or 0.7 – 1.0kN (Davy et al., 1988), which is significantly lower than

the 3.3kN used by Medley. This high stance load could be artificially inflating the wear rates, and it may be that the stop-dwell-start protocol is not as realistic as suggested.

A further study using stop-dwell-start protocols on 28mm wrought CoCrMo bearings with a dwell period load of 1350N showed no significant change in wear rate compared with normal walking (Liao et al., 2004). This protocol did however differ slightly from the previous study in that the ratio of motion to pause time was 5:1 as opposed to 10:1. Other activity representations in conjunction with stop-dwell-start protocols may also be needed to bring simulator test results closer to *in vivo* wear estimations.

1.5.3 Microseparation

Microseparation is a phenomenon believed to occur *in vivo* either during the swing phase of gait, where the head drops out of the cup slightly due to joint laxity, or at the point of maximal flexion or extension due to impingement between the femoral implant and acetabular cup. In either case, microseparation can contribute to increased wear, causing significantly deeper wear scars than those seen during sliding wear (Williams et al., 2005). Microseparation has been shown to occur *in vivo* in MOP joints, but in MOM joints no definitive measurements of microseparation were made (Dennis et al., 2001).

Microseparation has been recreated in simulator testing of MOM articulations, and resulted in an increase of wear volume in both the bedding in and steady state wear phases of 28mm wrought bearings (Williams et al., 2004), when compared with testing according to ISO 14242, from 0.58mm^3/mc to 1.58mm^3/mc in steady state wear. The same study revealed reducing the swing phase load from this ISO recommended 280N to 100N during gait simulation reduced mean steady state wear volume to 0.06mm^3/mc, highlighting the sensitivity of MOM bearings to small changes in loading conditions. The typical load during the swing phase has been shown to be approximately 0.3BW, or 225N for an average 75kg patient (Bergmann et al., 2001).

In COC bearings, microseparation leads to a visible ‘stripe’ of wear on the head, and damage on the rim of the cup (Stewart et al., 2003). It is thought that the actual impact damage caused by microseparation in MOM bearings however, is less significant due to a local recrystallisation, phase transformation and chemical reaction similar to that occurring in the main wear region, which has been identified in the area of microseparation damage, and which leads to increased localised hardness and resistance to damage (Fischer and Wimmer, 2006).

1.5.4 Accelerated gait

Although increased gait velocity is not reported as frequently occurring in current THA patients, a number of studies have attempted to incorporate it into simulator testing with a view to anticipating the wear effects for younger, more active patients who are becoming more frequent recipients of THA.

Fast jogging has been simulated on 40mm cast metal-on-metal resurfacing components, incorporating an increased cycle frequency of 1.75Hz, and an increased peak load of 4500N and found to increase wear rate by five to twelve times the rate during normal walking cycles at 1Hz with a peak load of 2450N (Bowsher, Nevelos, et al., 2006). This was associated with an increase in wear particle size, change in particle morphology , and a twenty-fold increase in the surface area of these particles, which may lead to an increased systemic reaction to the debris (Bowsher, Hussain, et al., 2006). This study also found that a change in the angle at which the acetabular cup was positioned caused volumetric wear to increase by 60% when the cup angle was altered from horizontal to 35º.

Stumbling has also been incorporated into simulator testing and evaluated using MOP bearings (Bowsher and Shelton, 2001). The stumble profile consisted of a highly loaded twin peak input, with a peak load of 5kN. This caused no significant increase in polyethylene wear rate when applied at an equivalent rate to 53 times per week. No studies could be found in the literature reporting the effects of stumbling on MOM bearings, but based on previous examples of the susceptibility of MOM to changes in load profile, this effect could be significant. Occurrence of stumbling is not reported in the studies of patient activity patterns however, and due to its accidental and unpredictable nature, both in terms of occurrence and gait, may not be relevant for consideration in pre-clinical evaluation.

1.6 Summary of Literature Review

Metal on metal bearings offer an improved solution for total hip replacement over conventional metal or ceramic on polyethylene implants, however concerns still exist as to the toxicity of the wear particles released into the body, and the failure of these implants associated with high wear, leading to a systemic immune response and severe pain for the patient. Development of these bearings therefore needs to focus on reduction of wear, however evaluation of this is only possible with a robust method of testing which accurately reproduces the conditions to which an implant may be exposed *in vivo*. This need is emphasised when considering the increasing use of THA to treat young and active patients. Currently, total hip replacement wear simulators are used to apply continuously oscillating physiological loads and motions to an implant femoral head and acetabular cup pairing whilst in a bath of lubricant. This generates a typical walking cycle to recreate *in vivo* conditions and provide a prediction of expected wear rates and behaviour of the implant in the body.

The wear rates generated by current simulator testing are approximately of the same order of magnitude as those found *in vivo*, but the wear values are often significantly lower in *in vitro* testing. The wear debris produced in these studies is often dissimilar to physiologically produced debris, and the physical appearance of simulator tested bearings is very different to those explanted from patients. These discrepancies have been attributed in part to the differing activity levels to which implants are exposed *in vi*vo, compared with the continuous nature of simulator testing, which will lead to different tribological behaviour in each condition, and accordingly affect wear. The kinematics of the hip during a variety of typical daily activities, including standing still, sitting down and stair climbing, have been shown to vary significantly.

A number of studies have introduced activities into simulator testing, and all demonstrated an increase in wear rates to varying degrees, however not all achieved clinically relevant rates. Currently, no studies have been published incorporating a clinically relevant range of activities into a simulator programme. MOM bearings are evidently very susceptible to changes in load and motion inputs in pre-clinical wear simulation, and this approach may go some way to bridging the gap between current *in vitro* and *in vivo* behaviour of bearings.

1.7 Introduction to the Present Study

1.7.1 Rationale

Current standards for this hip wear simulation comprise a continuously repeated cycle representative of walking, however the wear rates generated by this type of testing are frequently significantly lower than *in vivo* results. A number of studies have suggested this may be due to the continuous nature of the simulator testing, which differs significantly from the constantly varying movement patterns of typical patients. This is thought to be due to the changing activity *in vivo* causing breakdown of the lubricating fluid film between the components of the implant leading to an increase in wear. The comparatively continuous motion employed in walking simulation leads to a more optimal lubrication regime in the bearing, resulting in lower wear rates.

It is hypothesised that a simulator cycle which incorporates the different activities into a simulation programme will give wear more clinically representative wear rates than are currently generated by simulator testing. Previous studies in this area have generally demonstrated increased wear rates, however, these studies only considered the effect of individual activities, which still differs significantly from the variety of movement types utilised by a person during a typical day. One possible outcome of this type of testing is that the bedding in period of wear may be disrupted due to the sub-optimal lubrication regime caused by the different activity profiles, leading to higher overall wear. This more aggressive style of wear simulation may provide the added benefit of improved ability to differentiate between the wear properties of very similar bearing designs, and to predict more accurately the effect of small alterations to such parameters as bearing clearance, roughness, diameter or sphericity.

1.7.2 Aims

Wear simulation provides a useful tool for the evaluation of newly developed implants, however discrepancies between *in vitro* wear rates and behaviour *in vivo* have been found, attributed to a number of possible factors, including the continuous cyclic nature of current simulation practices when compared with constantly changing activity patterns for typical patients, and the differing kinematics of motion. This is compounded by the need to consider both younger patients, and the older patients who are physiologically younger and lead a more active lifestyle, and take account of the increased levels of activity typical of such patients.

A need is apparent for a range of simulator profiles which replicate differing patient activities of daily living. The eventual aim of this study is to develop and evaluate a wear simulator protocol which is more representative of the conditions to which total hip replacement implants are exposed *in vivo,* and provides more clinically relevant results than current practices. There are many activities to consider, and to cover all thoroughly is beyond the time constraints of this study. Therefore this work will focus in particular on the most common activity: motion interruption. This has been studied previously, as discussed, however many of the previously studies used arbitrary parameters, and yielded wide ranging results. The aim of this study is to develop a clinically relevant technique, using parameters measured from real patients, to allow a better understanding of the true effects of motion interruption on the wear of hip replacememts.

1.7.3 Objectives

- Identify activity patterns and kinematics for typical patients with a focus on the loading in the joint during interrupted motion, and the frequency of occurrence.
- Define wear simulator input parameters from this patient data.
- Collaborate with external suppliers to develop a simulator capable of running these parameters and validate and commission the simulator.
- Investigate the effect of individual characteristics of interrupted motion; two variables are of interest, the duration of a pause during walking, and the frequency of occurrence, i.e. the number of steps taken between pauses.

CHAPTER 2: METHODS AND MATERIALS

2.1 Hip Wear Simulation

2.1.1 Development of the Deep Flexion Hip Wear Simulator

The main aim of this study was to develop and evaluate new protocols for wear simulation of total hip replacement bearings. This required a wear simulation machine which was capable of applying greater and more varied load and motion inputs than previously used, and able to apply a number of varied inputs in sequence to better reproduce varied patient activity. At the commencement of this work no equipment was commercially available which met these requirements, therefore a collaboration was established with Simulation Solutions (Manchester, UK) to develop a new simulator. This was specified following the literature review and definition of new testing parameters at the start of this study. Simulation Solutions developed and built the ProSim Deep Flexion Hip Wear Simulator based on an original design described in the literature (Goldsmith and Dowson, 1999) (Figure 13). The new simulator is a ten station, three axis simulator, holding the bearing components in an anatomical position. The capabilities of the existing simulator and the new design are outlined in Table 7.

Figure 13: ProSim Deep Flexion Hip Wear Simulator

Table 7: Comparison between old and new designs of hip simulator

	Existing ProSim Hip Wear Simulator	**New ProSim Deep Flexion Hip Wear Simulator**
Load	Peak load 4kN	Peak load 6kN New types of pistons and valves were fitted to facilitate the higher loads and response times required
	Two rotating load cells (one per bank) Open loop control	10 fixed load cells (one per station) Closed loop feedback control
Motion (Flex/ext)	± 30º	± 60º To accommodate this the stations were spaced further apart on the machine to prevent impingement at high flexion angles.
Motion (IER)	± 10º	± 30º
Positioning calibration cycle	Positioning calibration cycle occurs at profile change - the existing machine must run a single cycle of motion over the full range of flexion each time the profile changes in order to re-calibrate its position, however this interrupts lubrication in the bearing, and may affect the wear measured on the test.	Encoding motor type adopted to eliminate need for postioning calibration cycle.
Profiles	Maximum of four profiles in sequence	Maximum of 20 profiles in sequence
Frequency	1Hz	0.29 – 1.5Hz
Microseparation	Not possible	Possible up to 2mm

2.1.2 Components and Fixturing

All testing in this study was performed on 36mm diameter CoCrMo wrought metal-on-metal total hip replacements from DePuy (UK). The Articuleze femoral head was used, in conjunction with a Pinnacle acetabular shell and Ultamet liner (Figure 14). The batch cards of all components were checked, and confirmed that all parts were within drawing specification during manufacturing checks.

Table 8: Components used in all testing

Component	Part ID	Lot	Drawing Number
Articul/eze® Cobalt Chrome 36mm Ultamet® Head +1.5	136551000	2696779	DWG-136551000
Pinnacle™ Ultamet® Cobalt Chrome Neutral Liner 36mm x 52mm	121887352	2703388	DWG-121887352
Pinnacle™ 100 Titanium Porocoat® Acetabular Shell 52mm	121701052	245390	DWG-121701052

The femoral head has a female taper allowing connection to a femoral stem. The liner has an external male taper which locks inside the acetabular shell. This, in turn, is secured into the pelvis with a press-fit in the acetabulum, and over time is secured by bony tissue growing into the porous backing surface.

Figure 14: Articuleze femoral head, Ultamet liner and Pinnacle acetabular shell (DePuy Synthes, 2012)

The femoral heads were mounted on spigots which in turn were bolted onto a lower plate which is screwed into the simulator station (Figure 15). A laser marked line was used on the head and spigot as an alignment guide to ensure repeatable positioning of the components throughout the test.

Figure 15: Femoral head fixture

The acetabular shell was cemented in a pot using polymethylmethacrylate (PMMA) bone cement at an angle of 35º from horizontal , which is equivalent to an angle of 45º *in vivo* (Figure 16). The joint reaction force *in vivo* occurs at 10º from the vertical, and typical recommended positioning for a cup in the acetabulum is 45º, therefore positioning the cup at 35º *in vitro* allows use of a vertical applied load in the simulator (Williams et al., 2008). The PMMA was sealed with a thin bead of clear silicone sealant to prevent cement particles coming loose and contaminating the lubricant.

Figure 16: Acetabular cup and liner fixture

The relative positions of the head and liner with the fixtures was tightly controlled to ±0.5mm to ensure the centre of rotation of the bearing coincided with the axes of motion of the hip simulator. The position of components was measured using a Vernier height gauge and callipers for accuracy. A gimbal beneath each femoral head allows for any slight misalignment of components within these tolerances. This control over positioning ensures consistent loading and motion to each station.

Each sample was fixed in the same station of the test throughout the wear simulation to eliminate variability. The fixtures and spigots were labeled for each station, and the same fixtures used on each station throughout the study. A silicone gaiter secured with jubilee clips was used to contain the bearing in lubricant (Figure 17).

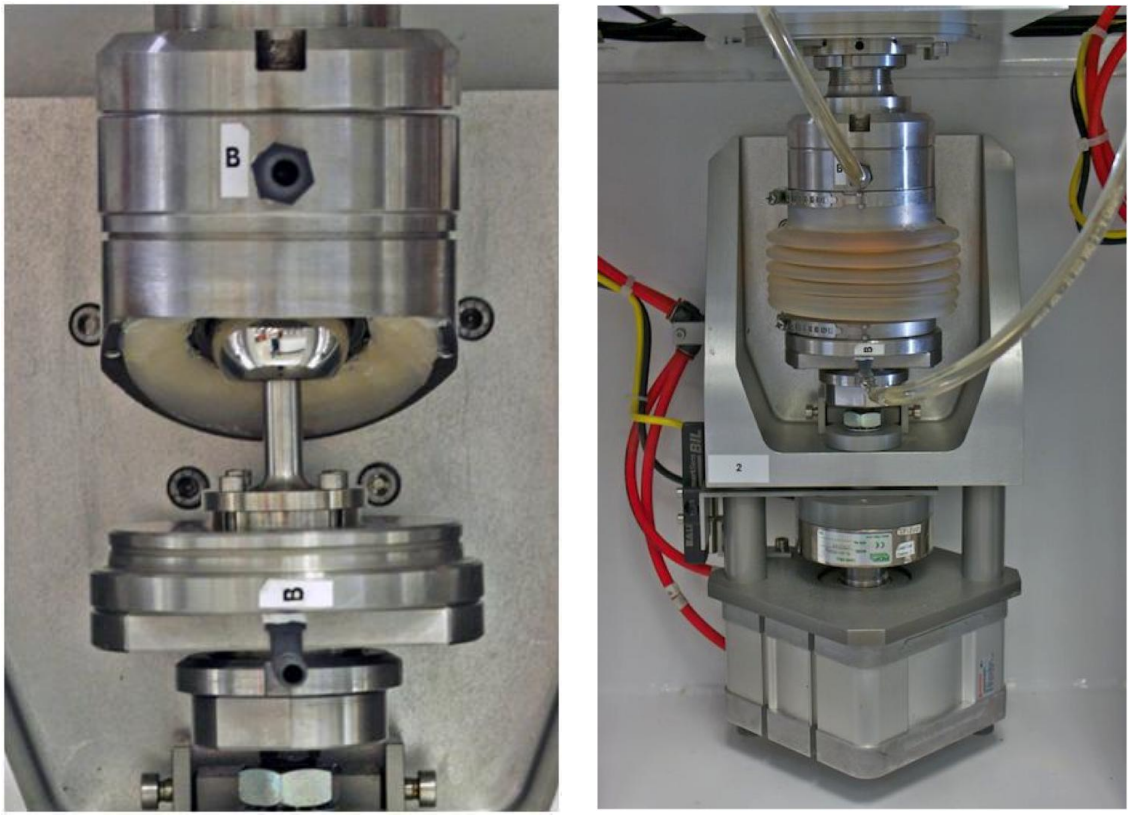

Figure 17: Individual station of simulator, showing bearing components in situ (left), and with gaiter and lubricant (right)

2.1.3 Simulator Loading and Kinematics

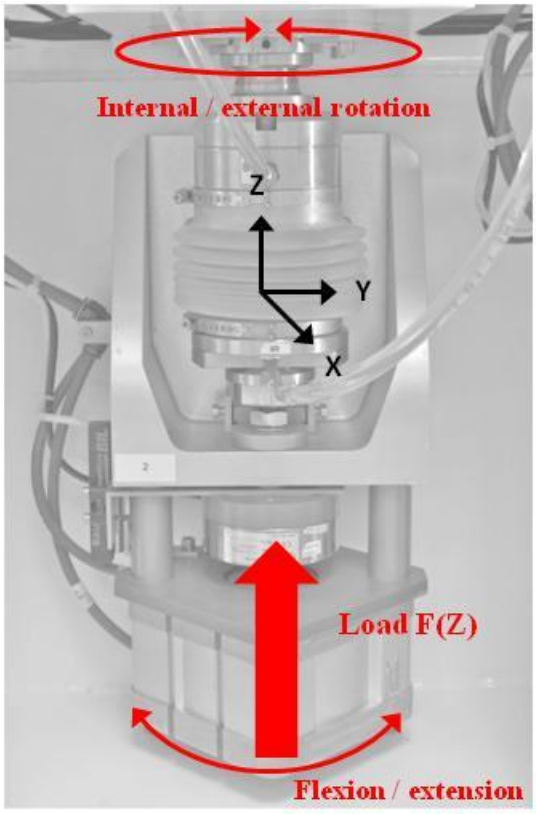

Figure 18: Load and motion inputs for a standard walking cycle as applied in the simulator

The simulator applies load in one axis (F(Z)) and rotation about two axes: flexion / extension about x and internal / external rotation about z (Figure 18). Load was applied vertically through the femoral head by means of a piston in the housing beneath each station. The simulator is set up with ten stations in two banks of five. Each station has load pneumatically controlled via an individual valve. Load was monitored throughout the test via load cells beneath each station, and a continuous feedback loop was utilised from these load cells to the pneumatic input controls to control loads.

Flexion / extension (F/E) and internal / external rotation (I/ER) were controlled by link arms attached to the back of each station and a central motor, again ensuring that every station operated under the same conditions, and eliminating inter-station variability.

For each of the wear simulation tests run in this study, the simulator inputs were based on a standard walking cycle adapted from ISO 14242:2 (2002) described in Chapter 1. The protocol used in this study deviates from the ISO slightly with the removal of rotation about the y axis (abduction / adduction) (Barbour et al., 1999). The range over which F/E and I/ER motion is applied was adjusted slightly to compensate. This allows

the building of a less complex machine, as described by (Goldsmith and Dowson, 1999), however as discussed previously in Chapter 1 this has been shown to generate clinically relevant wear rates for MOM bearings (Firkins et al., 2001).

The standard walking cycle used applied load in a twin peak 'Paul' type waveform with a peak load of 3kN and swing phase load of 300N. Flexion / extension motion was applied from +30º to -15º, and internal / external rotation of ±10º (Figure 19).

Tests were all run at a frequency of 1Hz.

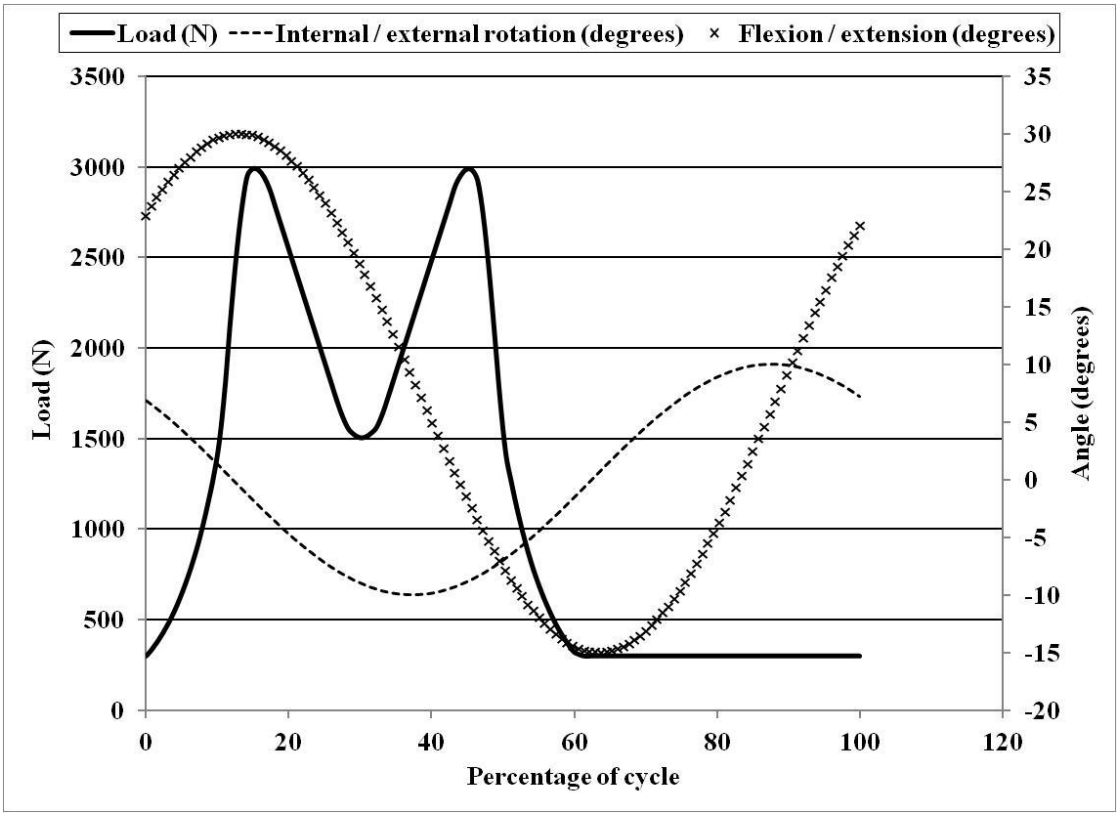

Figure 19: Load and motion inputs for a standard walking cycle in the simulator (Barbour et al., 1999)

2.1.4 Simulator multi-profile tests

A number of different variations of simulator input profiles were used for the various aspects of this study. For the commissioning and validation test described in Chapter 3 a standard continuous walking cycle was used as described in 2.1.3. For the stop-start tests discussed in Chapters 4 and 5 a combination of different profiles were added.

The standard walking cycle is shown in Figure 19. The dwell cycle, representing the 'stop' phase of the test is similarly illustrated in Figure 20. During trials of the test it

was found that transition cycles were necessary to prevent the simulator from crashing during the profile change, therefore 'stopping' and 'starting' cycles were developed to smooth the profile change. These are illustrated in Figure 21 and Figure 22 respectively. These cycles were defined following trials which showed that these offered the smoothest response in the wear simulator.

'Soft' stop start features were also utilised on the simulator at each profile change; this slows the simulator down slightly before a profile change, and introduces a one second pause at each change. Without these measures it was found that the system controllers were incapable of maintaining load and motion inputs at speed without tripping.

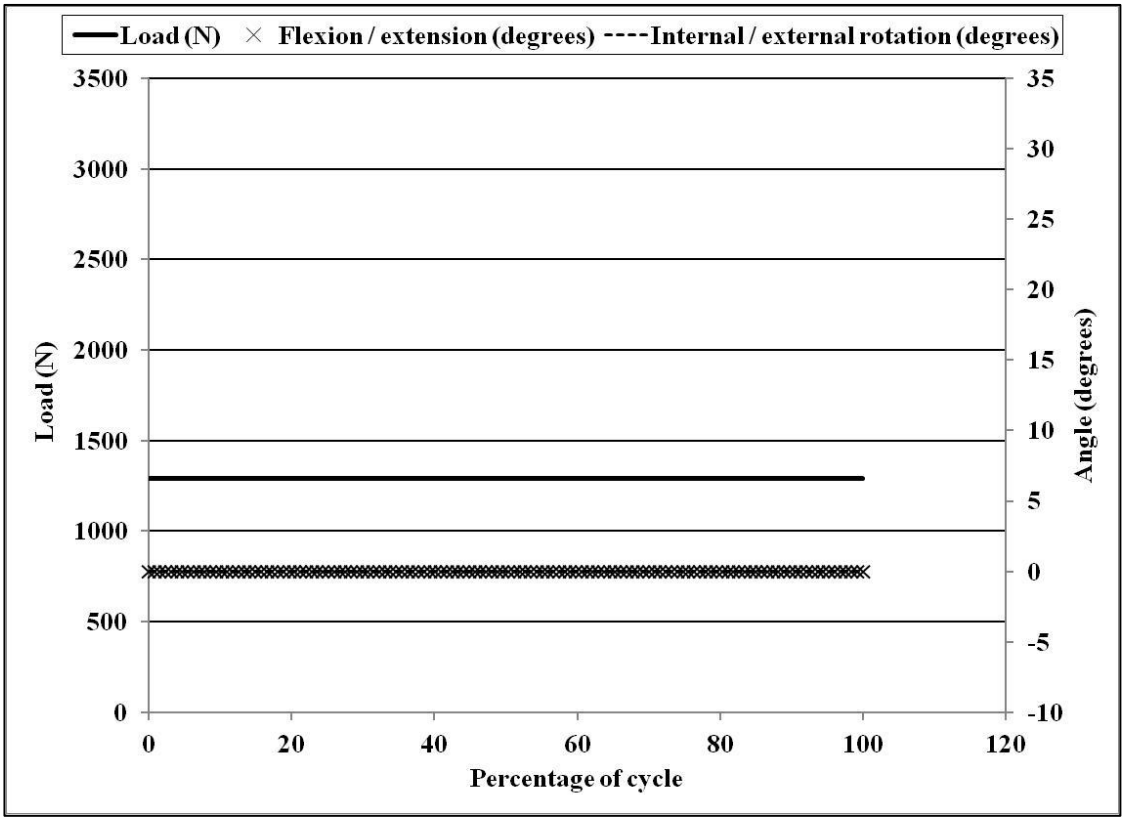

Figure 20: Load and motion inputs for a dwell cycle in the simulator

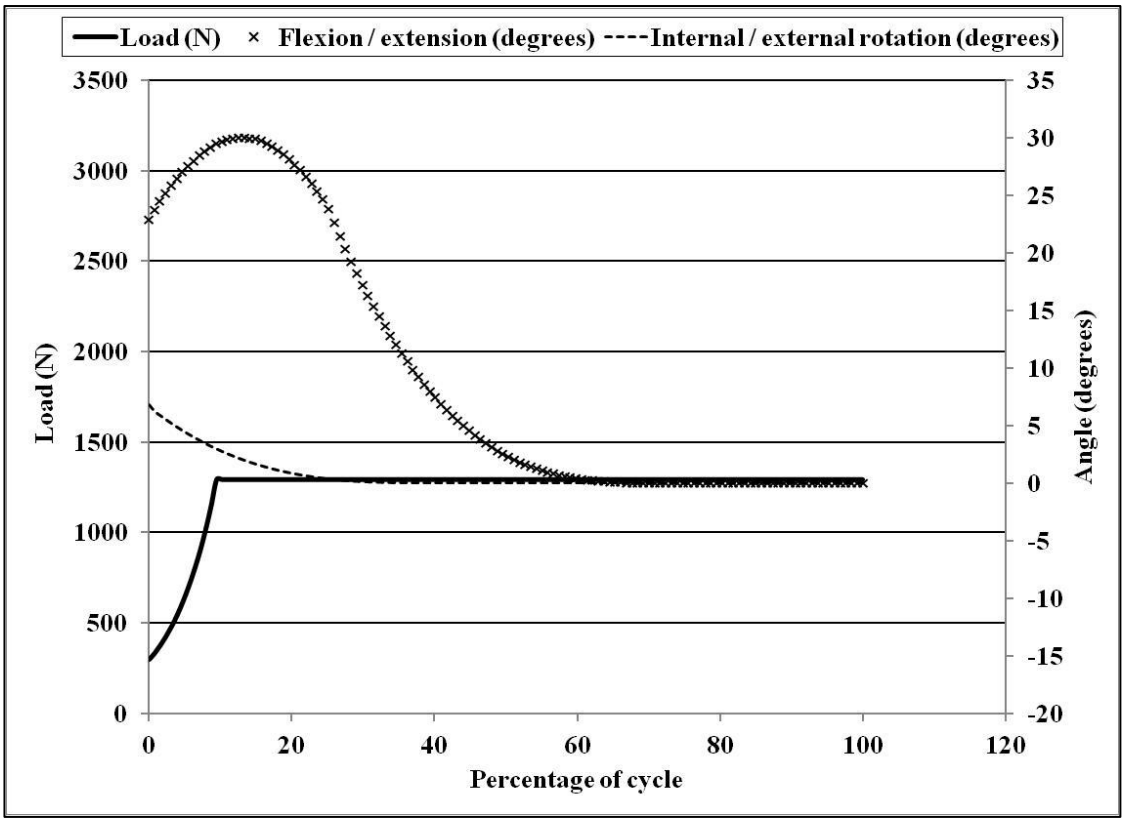

Figure 21: Load and motion inputs for a stopping transition cycle in the simulator

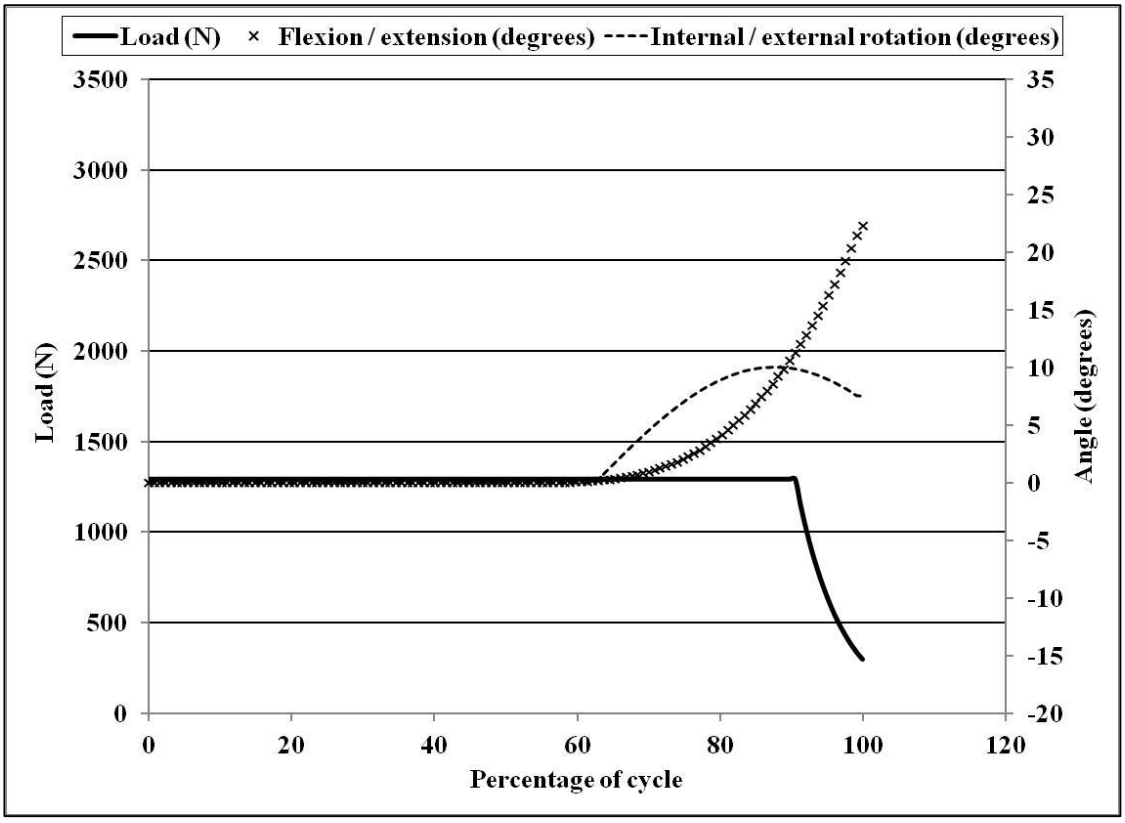

Figure 22: Load and motion inputs for a starting transition cycle in the simulator

These four cycles were programmed together in different combinations depending on the current test, and a continuous cycle of this program run. Figure 23 shows an example of this.

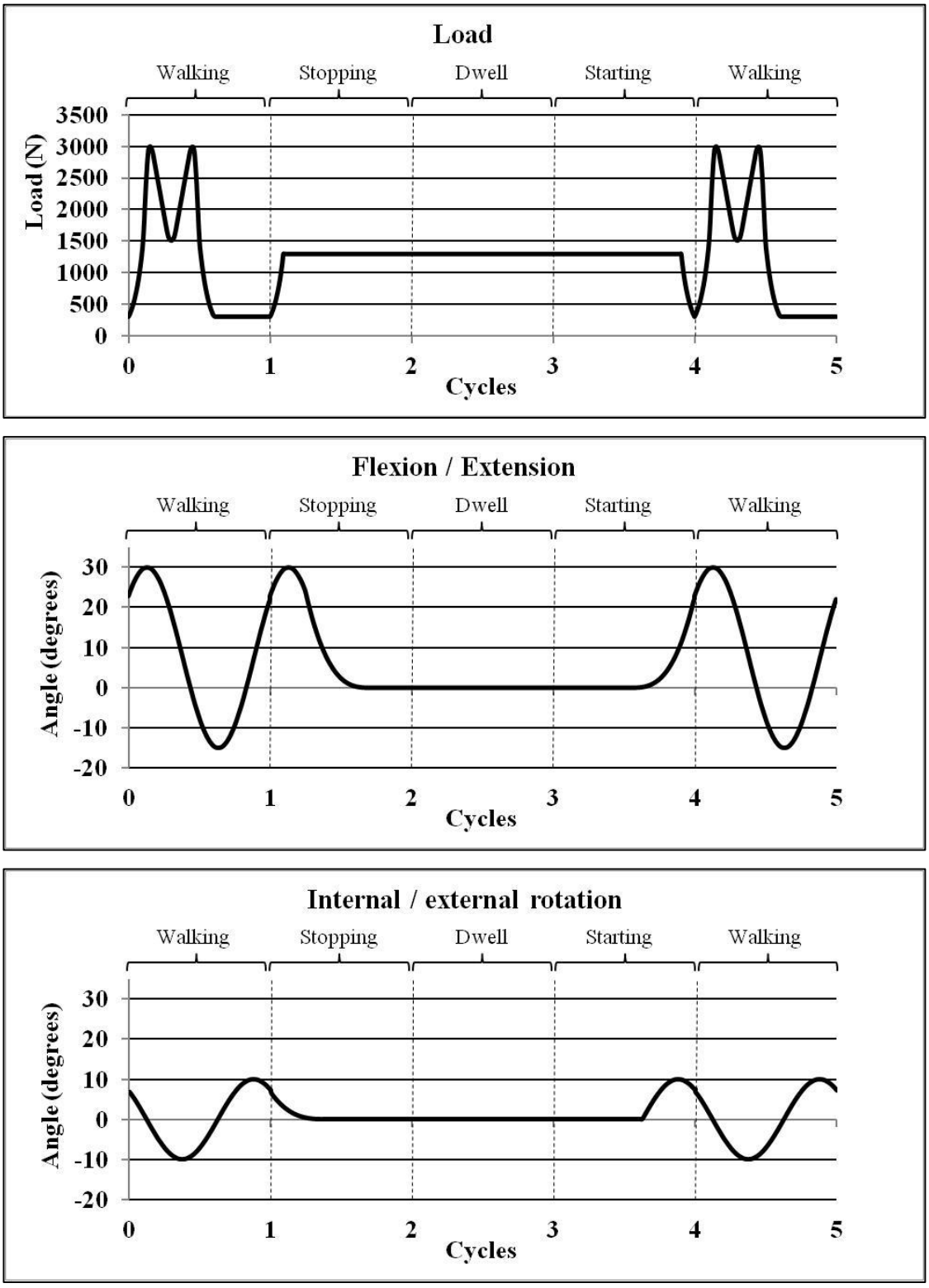

Figure 23: Load and motion inputs for five cycles of an SDS test

When counting cycles on multi profile stop start tests, only cycles where the walking cycle was running were counted for the purposes of calculating wear rates, on the assumption that no wear would occur during the dwell period. If the dwell cycles were also included this would incorrectly deflate the final calculated wear per cycle.

2.1.5 Lubrication

All tests were conducted in 25% (v/v) newborn bovine serum with a minimum of 17g/L protein (SeraLabs, UK) with 0.1% (w/v) sodium azide and 0.02% (w/v) ethylenediaminetetraacetic acid (EDTA) added to retard bacterial and excessive protein growth. Serum was changed every 330,000 to 500,000 cycles (equating to approximately 3-4 days) throughout the test, depending on the measurement intervals used. The serum change interval used is detailed with the individual method section of each test, however internal studies have shown that variation of the serum change interval over this range does not have any significant effect on the wear measured in a test.

2.1.6 Test Method Validation

This study was the first time this new simulator had been used, therefore a validation and commissioning study was run initially to determine whether accurate and repeatable results were being produced. This validation study was also run to provide control data for this study, and the results are detailed in Chapter 3.

2.2 Gravimetric Wear Analysis

To assess wear of the hip bearings, gravimetric assessment was performed prior to and at regular intervals throughout the test. The frequency of intervals varied depending on the duration of the test but for a typical standard walking test this was set at 0.5 million cycles (mc). For the more complex tests later in the study this was reduced to 0.1mc, further details of this are given in the relevant method sections for each test.

2.2.1 Cleaning

Due to the accuracy required during gravimetric analysis all components were thoroughly cleaned prior to each measurement point. Upon removal from the simulator bulk serum debris and protein were removed under a running stream of deionised water, and the samples wiped down with a lint free cloth and acetone to remove all visible

contamination. Samples were then placed in deionised water in an ultrasonic bath for ten minutes, followed by 30 minutes ultrasonication in a 5% detergent in deionised water solution. A further two ten minute ultrasonic baths in deionised water were then used to remove all trace of detergent. Samples were rinsed again under deionised water and wiped with acetone before being left to dry (International Standards Organisation, 2000).

2.2.2 Weighing

Prior to weighing samples were left to dry in the weigh room for at least 24 hours. The weigh room is a controlled temperature and humidity environment with room conditions controlled at 20±2ºC and 45±5%$_{RH}$. A Sartorius MC210s balance was used; accurate to $1x10^{-5}$g.

Samples were weighed three times and an average taken. If the three measurements were found to deviate by more than 0.1mg then measurement was repeated.

Mass changes for each stage of a test were calculated and converted into volumetric units using a density of CoCrMo of 8.28g/cm^3 (F1537-08 (ASTM, 2011), (MatWeb, 2011)).

2.3 Geometrical Analysis

2.3.1 Co-ordinate Measuring Machine

Prior to testing, all parts were geometrically characterised using a co-ordinate measuring machine to quantify form and diametral clearance (Ernsberger, 2008).

A Zeiss Prismo 5 NavMass SAC co-ordinate measuring machine was used, with a 2mm probing tip (Carl Zeiss Ltd., Rugby, UK). Calypso software was used for programming and analysis. Components were securely fixtured on the machine bed, with the femoral heads placed on a spigot and the acetabular liners clamped in a pot (Figure 24). Five scans were taken of each component: around the equator, and four equally spaced across the pole (Figure 25, Figure 26). The Calypso software was used to capture approximately 18,000 points per scan, and measurements were accurate to 0.7μm.

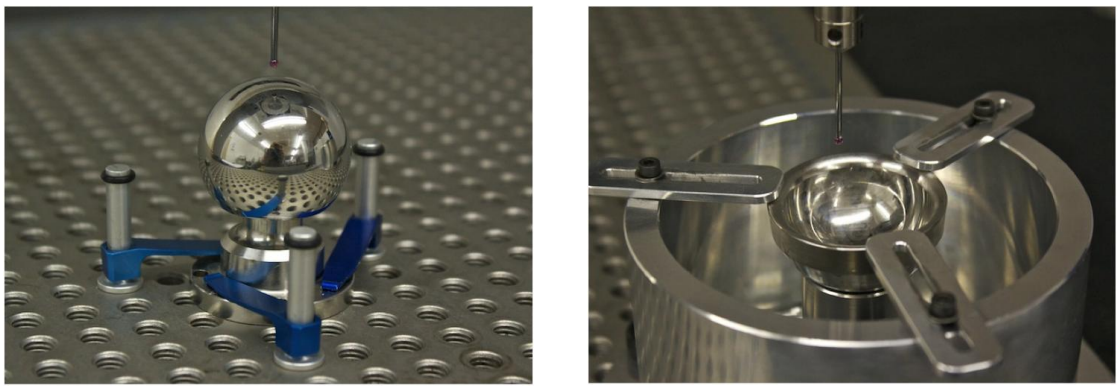

Figure 24: Zeiss Calypso CMM Head measurement

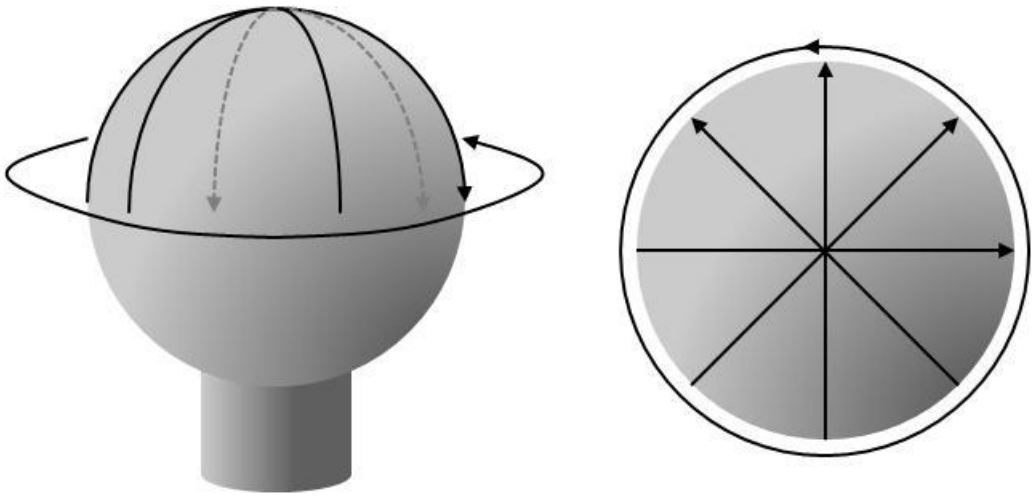

Figure 25: Graphical illustration of measurement scans on head

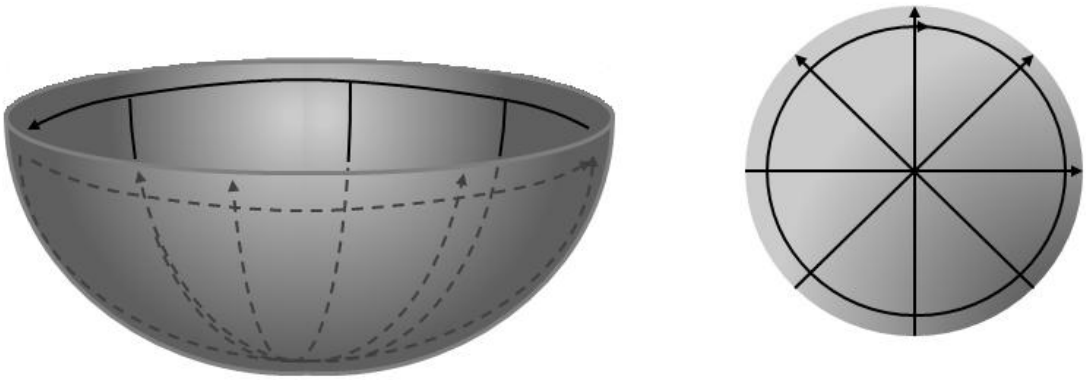

Figure 26: Graphical illustration of measurement scans on cup

The polar and equatorial dimensions of the head were also calculated from these measurements. This determines the geometry of the component over a specified region of the bearing surface. The polar region extends ±45º from the head pole, and covers the area where wear normally occurs in a standard simulator test. The equatorial region exends from 45º below the pole, to the equator, and represents the unworn region.

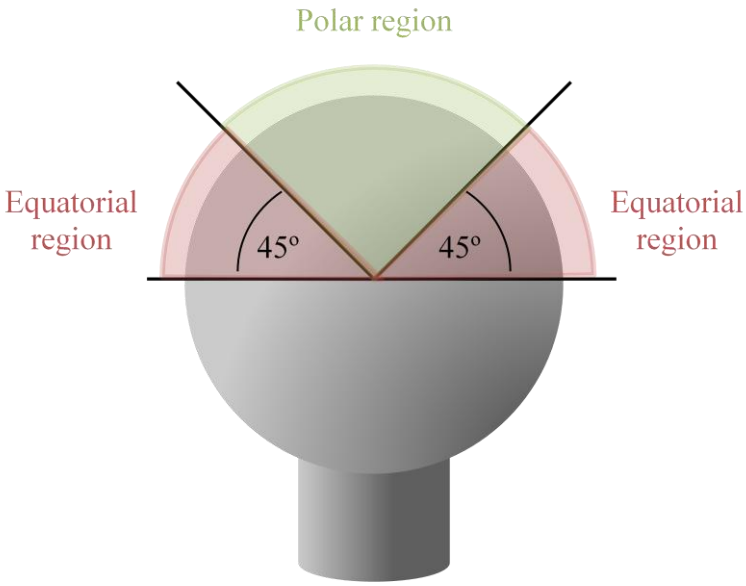

Figure 27: Graphical illustration of measurement scans on cup

2.4 Surface Roughness Analysis

Surface roughness of all parts was measured before and after testing, using a Taylor Hobson CCI3300 white light interferometer (Taylor Hobson, Leicester, UK). Measurements were taken using a 20x lens, and scans taken over a $1mm^2$ area.

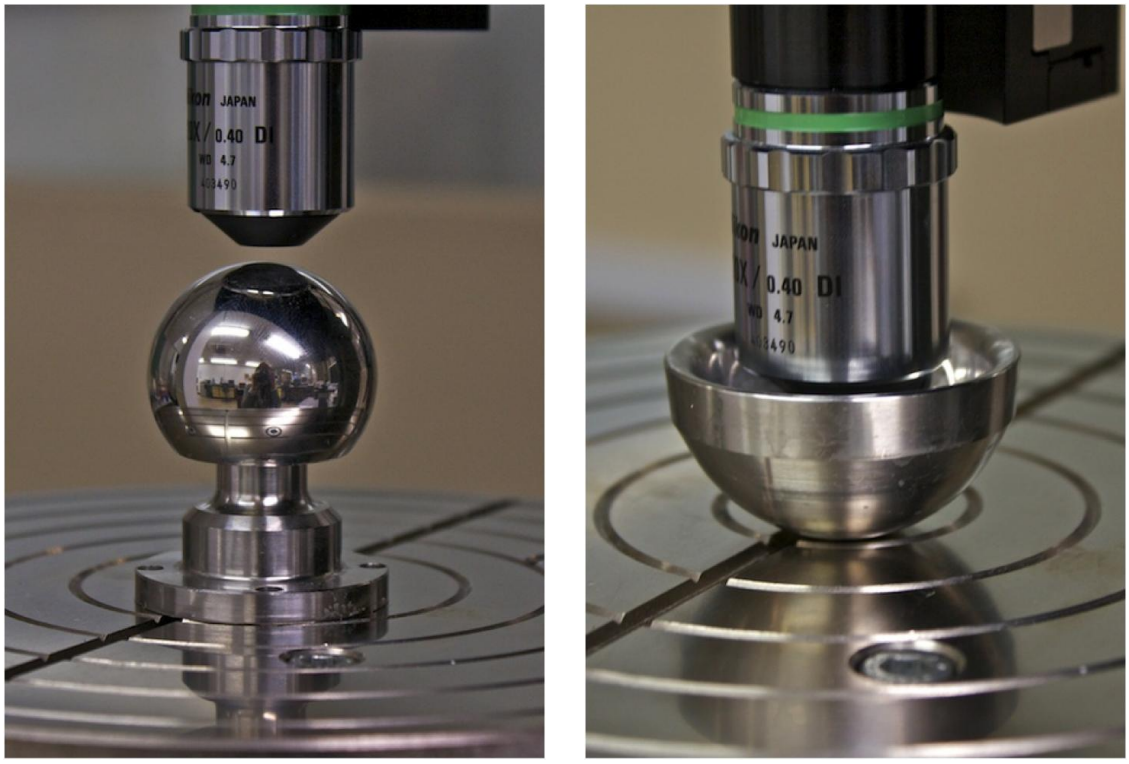

Figure 28: Talysurf measurement set-up for femoral head and acetabular liner

The CCI generates areal roughness parameters which are a 3D representation of the surface. The parameters selected for analysis were S_q (Root mean square deviation (µm)) and S_z (Maximum height of surface (µm)).

Each sample was measured before and after testing. A scan was taken at the pole and at four points 30º from the pole (Figure 29). Each scan was repeated four times and an average taken to eliminate potential noise from light and vibration. No filters were used in data analysis. The lens was focused on the surface and the scanning range set to ensure the scan covered the entire height of the surface. Measurements pre and post test were compared.

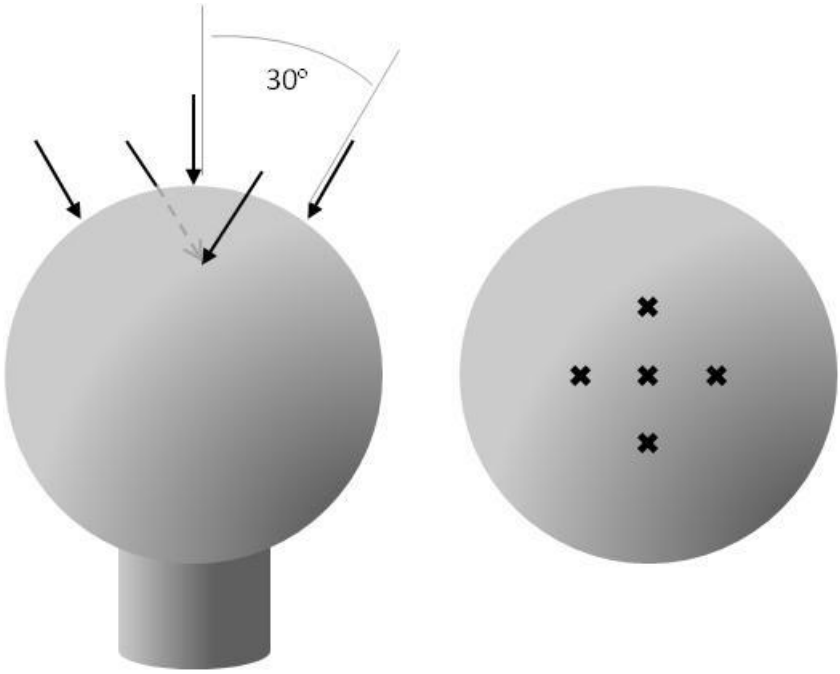

Figure 29: Talysurf measurement schematic for femoral head

2.5 Summary of Methods

This chapter has described the major methods used in this thesis:

- Standard condition hip wear simulation using a walking cycle, which is utilised in Chapter 3.
- Stop-dwell-start (SDS) condition hip wear simulation, which is utilised in Chapters 4 & 5.
- Wear analysis of hip wear simulator test components using gravimetric techniques, and geometrical analysis using CMM and Redlux optical scanning, which are all utilised in Chapters 3, 4 & 5.

CHAPTER 3. WEAR OF 36MM METAL-ON-METAL TOTAL HIP REPLACEMENTS UNDER STANDARD WALKING CONDITIONS

3.1 Introduction

This chapter describes the studies of the wear of 36mm metal on metal (MOM) hip replacements under a standard walking profile on the Deep Flexion Hip Wear Simulator. Substantial published data already exists on this device tested under these conditions as described in Chapter 1. This study was conducted to validate the new simulator against existing results and provide control data for later studies under different conditions on currently manufactured devices.

3.2 Methods and Materials

Ten 36mm Pinnacle MOM total hip replacements from DePuy International (UK) were used for this study (DePuy International, Product code 136553000, DWG-136553000 (Internal confidential drawing)). Each individual component was assigned a unique reference number for identification in the format yy_xxxx, where yy represents the year of initial sourcing of the parts, and xxxx is a unique identifier assigned consecutively.

3.2.1 Hip Simulator

The samples were prepared and mounted as described in Chapter 2 and subjected to a standard walking wear test adapted from ISO 14242-1:2002 (International Standards Organisation, 2002). Load was applied to the components in a twin peak Paul-type waveform with a peak load of 3kN and swing phase load of 300N. Flexion / extension and internal / external rotation were applied in a sinusoidal waveform over +30º/-15º and ±10º respectively, as described in Chapter 2. This cycle was applied continuously at a frequency of 1Hz.

3.2.2 Geometric analysis

All samples were measured using CMM prior to testing to define sample diameter and bearing clearance. The Zeiss CMM was used for these measurements as described in Chapter 2.

3.2.3 Gravimetric Analysis

All samples were weighed following cleaning using the techniques described in Chapter 2 every 500,000 cycles throughout the test.

3.2.4 Surface analysis

Surface roughness measurements of the samples were taken before and after testing, and at 500,000 cycle intervals during the test, following the procedure described in Chapter 2.

3.3 Results

3.3.1 Geometric analysis

The ten 36mm MOM acetabular components were found to have a mean diameter of 36.083±0.001mm (±95% confidence interval) with a mean form of 0.004±0.001mm (Table 9). The femoral heads had a mean diameter of 35.999±0.002mm with a mean sphericity of 0.008±0.001mm (Table 10).

Table 9: CMM results for acetabular components prior to testing

Station	Sample No.	Diameter (mm)	Form (mm)
1	08_1460	36.080	0.009
2	08_1427	36.082	0.003
3	08_1455	36.082	0.003
4	08_1441	36.083	0.002
5	08_1449	36.083	0.006
6	08_1434	36.083	0.004
7	08_1453	36.084	0.003
8	08_1467	36.084	0.003
9	08_1426	36.084	0.004
10	08_1425	36.084	0.002
Average		**36.083**	**0.004**
95% Confidence		**0.001**	**0.001**

Heads and cup pairs were matched to give a low variation in diametrical clearance between the ten stations.

The CMM measurements highlighted a small difference between the global, polar and equatorial geometries for femoral heads. The mean diameters were global: 35.999±0.002mm, polar: 36.015±0.001mm and equatorial: 35.998±0.003mm, while form was measured as global: 0.008±0.001mm, polar: 0.003±0.001mm and equatorial: 0.006±0.001mm respectively. This represents a significant difference between the polar region and the rest of the head, and indicated that the polar region is very slightly flattened in form relative to the equatorial region. This difference will have the effect of decreasing clearance in the polar region. A reduced clearance in the polar region has been shown to cause lower bearing wear (Ernsberger, 2008).

Table 10: CMM results for femoral components prior to testing

Station	Sample No.	Global Diameter (mm)	Global Sphericity (mm)	Polar Diameter (mm)	Polar Sphericity (mm)	Equatorial Diameter (mm)	Equatorial Sphericity (mm)
1	08 1475	36.001	0.008	36.012	0.006	36.000	0.005
2	08 1476	35.999	0.008	36.012	0.004	35.998	0.007
3	08 1487	35.996	0.010	36.017	0.004	35.994	0.007
4	08 1489	36.000	0.008	36.014	0.003	35.998	0.007
5	08 1510	36.006	0.007	36.018	0.001	36.004	0.004
6	08 1495	36.002	0.007	36.018	0.002	36.001	0.007
7	08 1518	36.004	0.006	36.016	0.001	36.002	0.003
8	08 1479	35.992	0.011	36.016	0.003	35.990	0.007
9	08 1515	36.003	0.008	36.019	0.002	36.001	0.007
10	08 1494	35.993	0.012	36.018	0.004	35.991	0.008
Average		35.999	0.008	36.015	0.003	35.998	0.006
95% Confidence		0.002	0.001	0.001	0.001	0.003	0.001

The wear region on a simulator tested femoral head oriented vertically, and tested under standard walking conditions lies around the femoral pole (Hardaker et al., 2006), therefore polar geometry was used for pairing the samples for testing. Clearances were calculated for the samples with a mean polar clearance of 68.073±0.465μm (Table 11).

Table 11: Calculated clearance between head and cup for global, polar and equatorial geometries prior to testing

Station	Global clearance (μm)	Polar clearance (μm)	Equatorial clearance (μm)
1	78.704	68.333	79.997
2	82.413	69.835	83.973
3	82.291	68.246	83.941
4	82.549	68.416	84.303
5	87.027	68.083	88.960
6	88.305	67.550	90.720
7	79.843	67.470	81.106
8	91.566	67.809	93.665
9	81.826	67.923	83.264
10	80.067	67.061	80.926
Average	83.459	68.073	85.086
95% Confidence	2.573	0.465	2.817

3.3.2 Gravimetric Analysis

The total mean wear for these samples under standard walking conditions was 0.19±0.16mm^3 after 2 million cycles (Figure 30, Figure 31). Wear appeared to be bi-phasic in nature, with a slightly increased bedding in wear rate between 0 and 1 million cycles (mc) compared with the steady state rate between 1 and 2mc. The bedding in wear rate was 0.16±0.15mm^3/mc, compared with 0.04±0.02mm^3/mc during steady state wear (Figure 32). This was not statistically significant (P=0.07, Paired T-test).

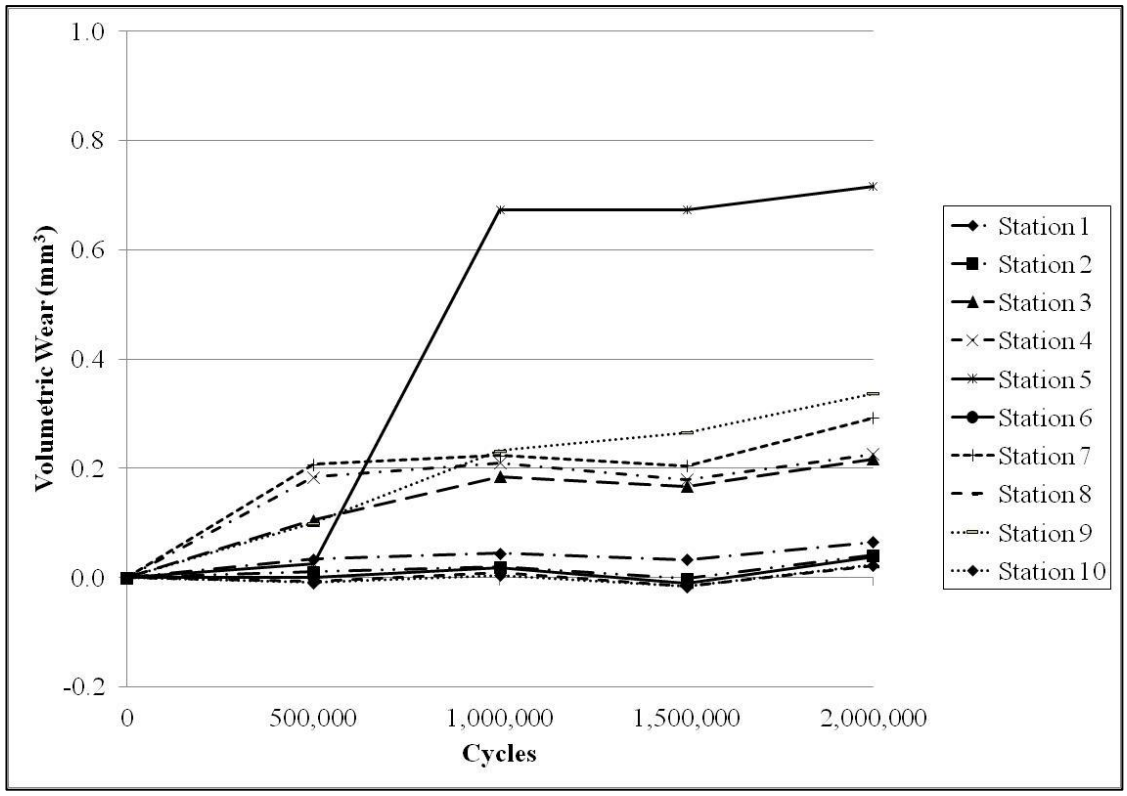

Figure 30: Cumulative individual volumetric wear of 36mm MOM under standard walking conditions

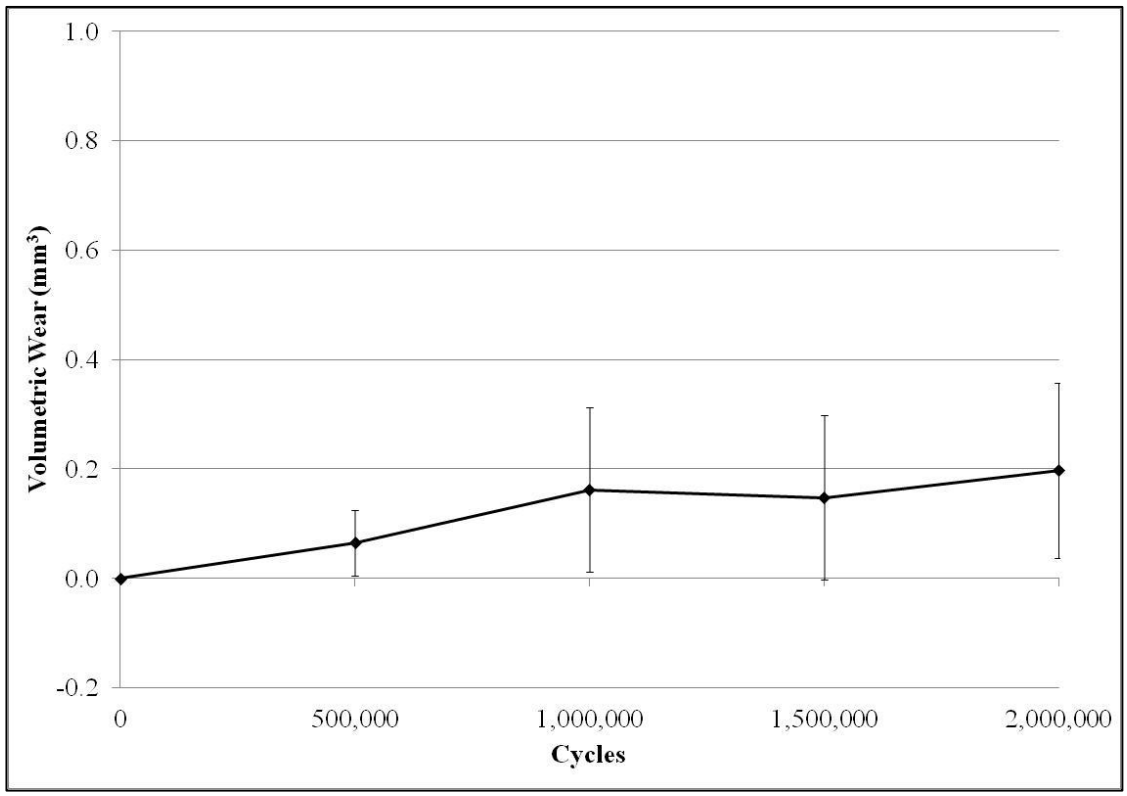

Figure 31: Mean cumulative volumetric wear of 36mm MOM under standard walking conditions (n=10, ±95% confidence intervals)

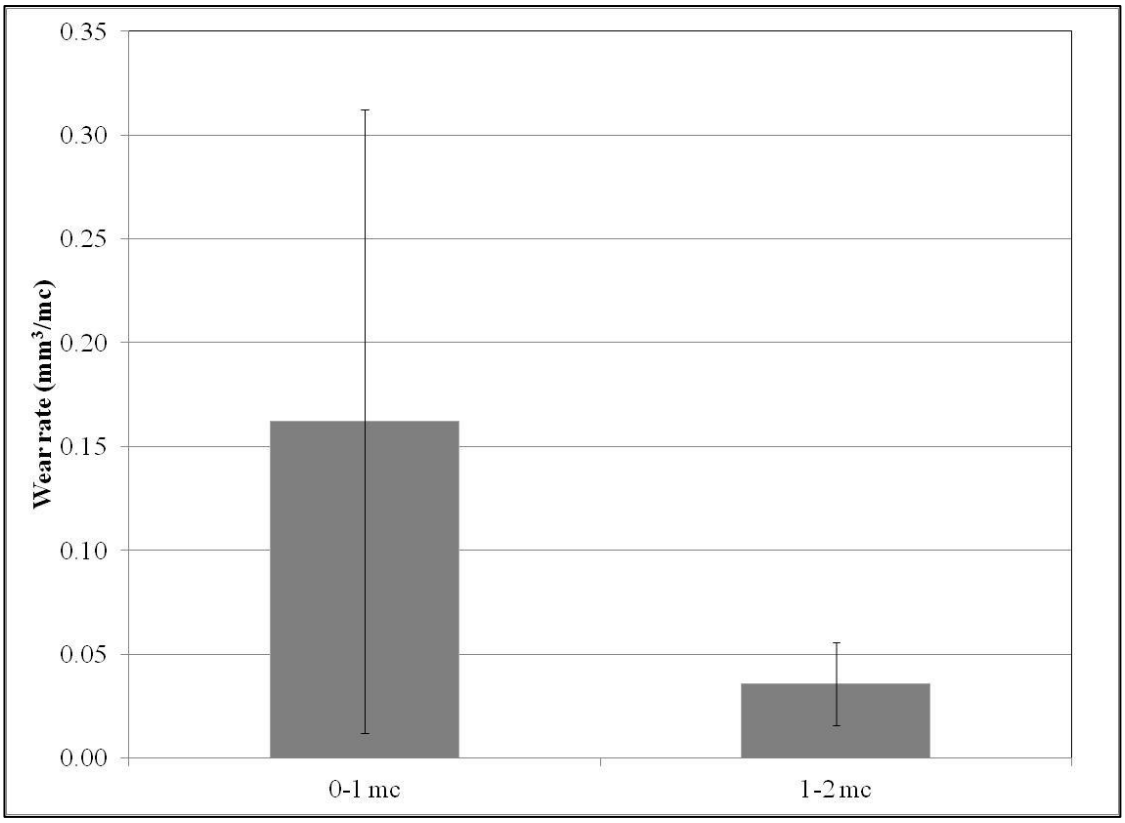

Figure 32: Mean bedding in (0-1mc) and steady state (1-2mc) volumetric wear rates of 36mm MOM under standard walking conditions (n=10, ±95% confidence intervals)

One station from this test, Station 5, exhibited higher wear than the other samples in the study (Figure 30). The significance of this was examined using the Grubbs' Test, and this sample was found to be a significant outlier at the 5% significance level (T_n = 2.38, Table value = 2.29).

The data from Station 5 was examined in further depth to try to determine the cause of the higher wear. The components were examined and no unusual damage on the samples could be observed. No technical issues were encountered with fixturing or during cleaning and weighing of these parts, which may have caused damage. The individual wear measurements of the femoral head and acetabular liner were examined separately to determine if the effect was due to one component or both (Figure 33).

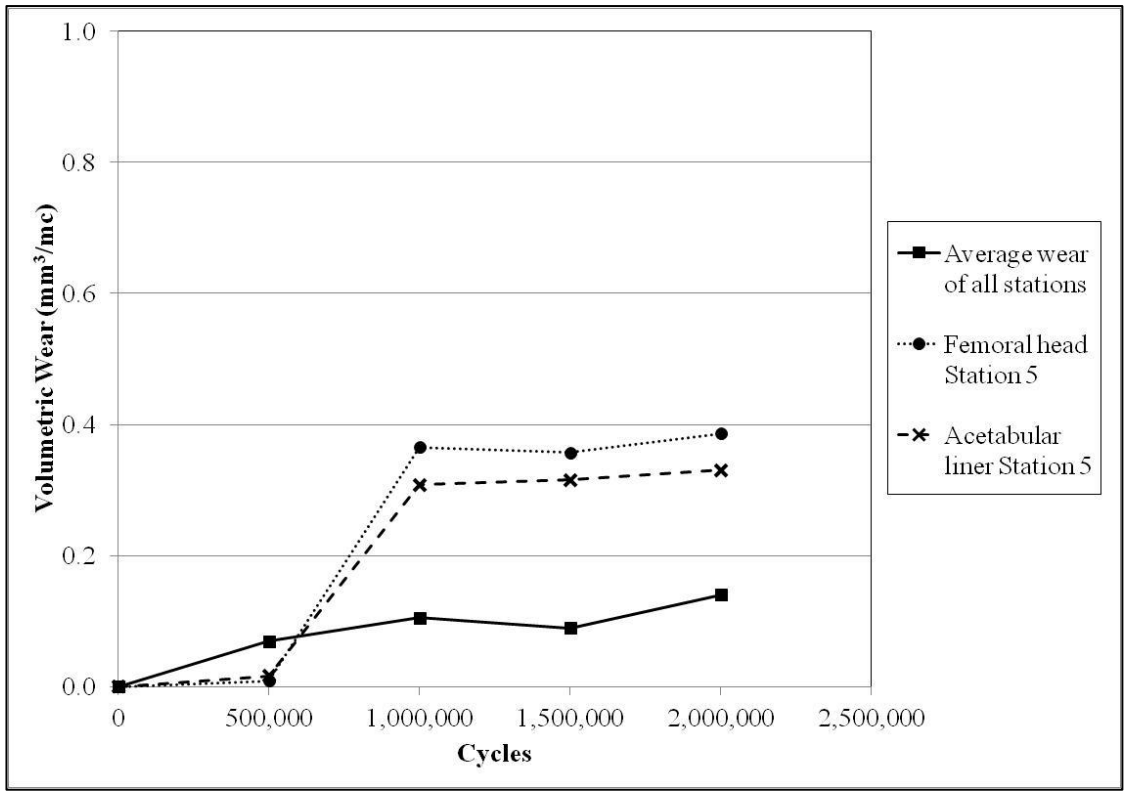

Figure 33: Individual wear of head and cup from Station 5 compared with mean wear of all stations, 36mm MOM under standard walking conditions

The femoral head and acetabular liner exhibited wear at similar rates throughout the test (Figure 33), indicating a possible issue with the test or machine, rather than the individual components. Wear rate was only elevated between 0.5mc and 1mc; during the remainder of the test wear rates appear similar to the other samples in the set.

The data logs for load output from the wear simulator were examined for unusual test conditions which may have caused the high wear. The motion axes on the simulator were linked mechanically, therefore it is known that all samples underwent identical motion throughout the test. Load plots from the high wearing station and two other 'normal' stations were compared during the high wearing period, and before and after this period. A number of cycles throughout each stage of the test are presented in a series of graphs in Appendix 1. For any given test the load cycles were plotted on top of each other to allow easy identification of anomalous cycles.

Analysis of the load outputs from the simulator (Appendix 1) clearly show a discrepancy between the outlier station (Station 5) and the two other randomly selected stations (Stations 1 & 7) between 500,000 and 1 million cycles. This correlates with the period when high wear was observed on Station 5. Substantial noise was observed on

the load outputs for Station 5, and the cycle deviated significantly from the input. This error was identified at the time, and the machine was examined for faults. A malfunctioning pneumatic valve was found to be the cause, this was replaced at the 1mc interval, and load outputs were subsequently examined and found to be normal.

Following identification of the outlying station and its cause, it was considered reasonable to exclude this station from summary statistics of the data set. Data is presented in the following graphs with and without the outlier for comparison (Figure 34, Figure 35).

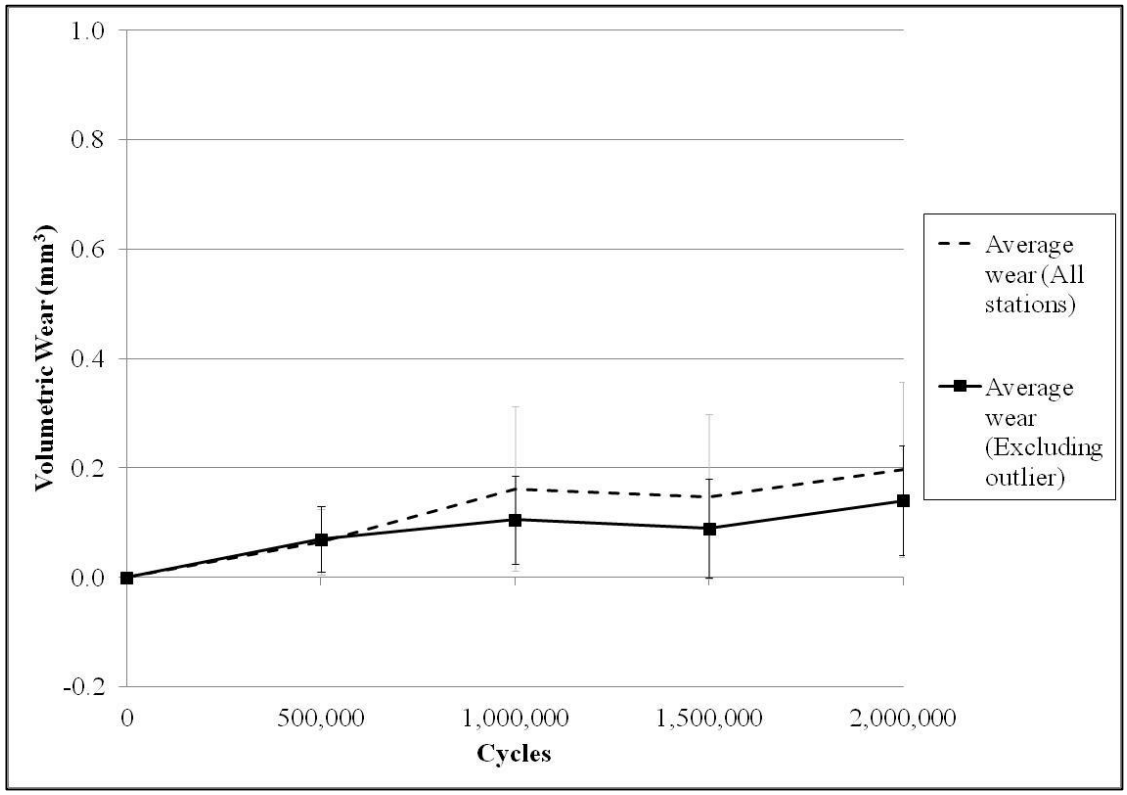

Figure 34: Mean cumulative volumetric wear for 36mm MOM under standard walking simulation before and after exclusion of an outlier (n=10, ±95% confidence limits)

Mean cumulative wear for the walking simulation test is presented in Figure 34. The wear appears to remain bi-phasic, with an increased rate of wear between 0mc and 1mc, and a lower wear rate thereafter. The mean wear rate during the inital, 'bedding in' phase was $0.11\pm0.08 mm^3$/mc, and during the second 'steady state' phase was $0.03\pm0.02 mm^3$/mc (Figure 35). This represents a statistically significant difference (P=0.038, Paired T-test).

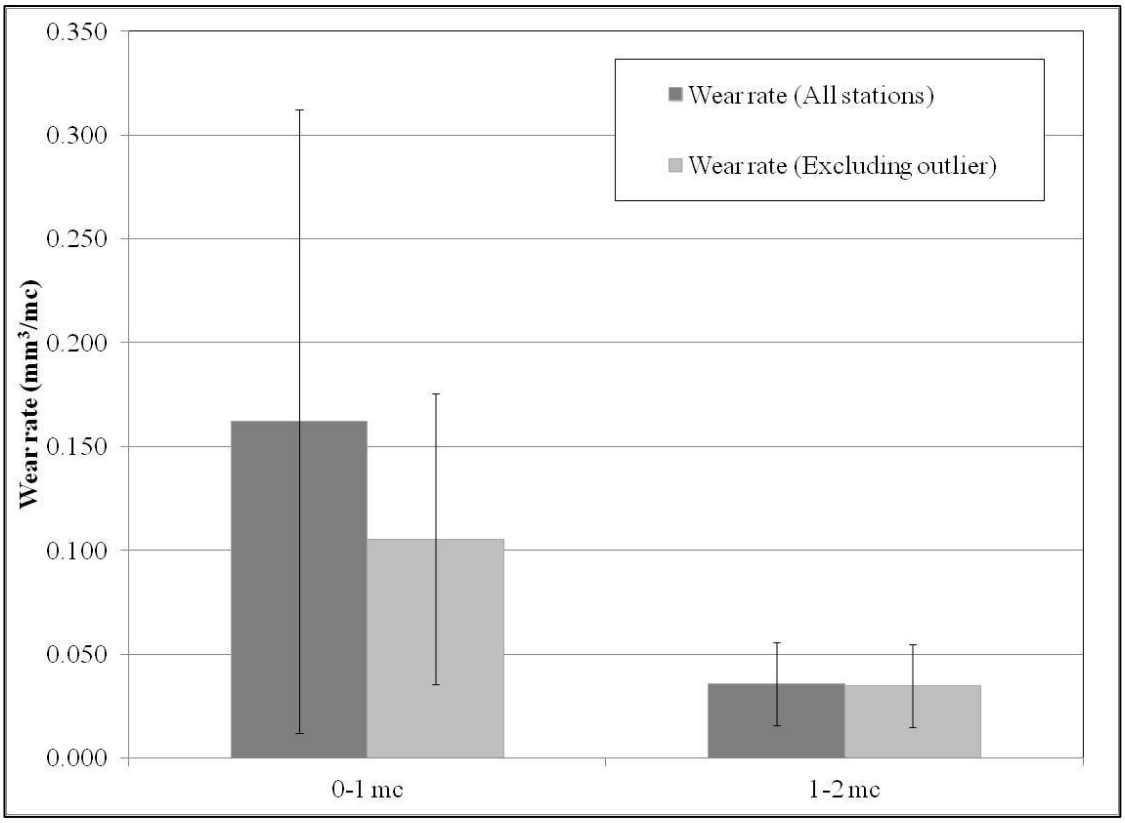

Figure 35: Mean bedding in and steady state volumetric wear rates of 36mm MOM under standard walking conditions before and after exclusion of an outlier (n=10, ±95% confidence intervals)

3.3.3 Surface analysis

The samples in this test exhibited scratching to varying degrees after 2mc of wear simulation. This ranged from a distinct wear scar with scratching in a focused region to a largely undamaged surface with a few isolated fine scratches. The degree of visible scratching appears to correlate generally with the gravimetrically measured wear. Two examples are shown here. The samples from the high wearing Station 5 (Figure 36, Figure 37) exhibit a very distinct wear scar consisting of a densely scratched region which appears slightly cloudy in appearance compared with the surrounding unworn surface. The wear scars appear on the head at the pole, and on the cup in a lateralised position. In contrast, the samples from the relatively low wearing Station 9 are also shown (Figure 38, Figure 39). The scratches appear in a similar region of the components, however they are isolated and appear in low density, and it is difficult to delineate the wear region from the surrounding unworn areas. The majority of samples from this test appeared most similar to Station 9, with a few exhibiting surface damage more closely comparable with Station 5.

Figure 36: Station 5 Femoral head

Figure 37: Station 5 Acetabular cup

Figure 38: Station 9 Femoral head

Figure 39: Station 9 Acetabular cup

Figure 36 to Figure 39: Examples of differing degrees of surface scratching on high (7 & 8) and low (9 & 10) wearing stations. All photographs taken following 2mc of standard walking simulation.

Surface roughness analysis was completed on all samples every 0.5mc throughout the test, to correlate with the gravimetric measurement intervals. Femoral heads were measured at the pole, and at four locations 30 degrees from the pole, as described in Chapter 2. Acetabular cups were measured only at the pole.

The mean Sq (root mean square areal roughness) for femoral heads and acetabular liners is presented in Figure 40. Surface roughness was generally observed to increase with the number of wear cycles for femoral heads in the first half of the test, with a significant increase from 7.4±2.5nm at 0mc up to 30.1±7.9nm at 1mc (P=0.000, Paired T-test). At 2mc, roughness was 21.8±3.2nm; there was no significant difference from the measurements at 1mc (P=0.337, Paired T-test). In contrast no statistically significant change was observed for acetabular cups.

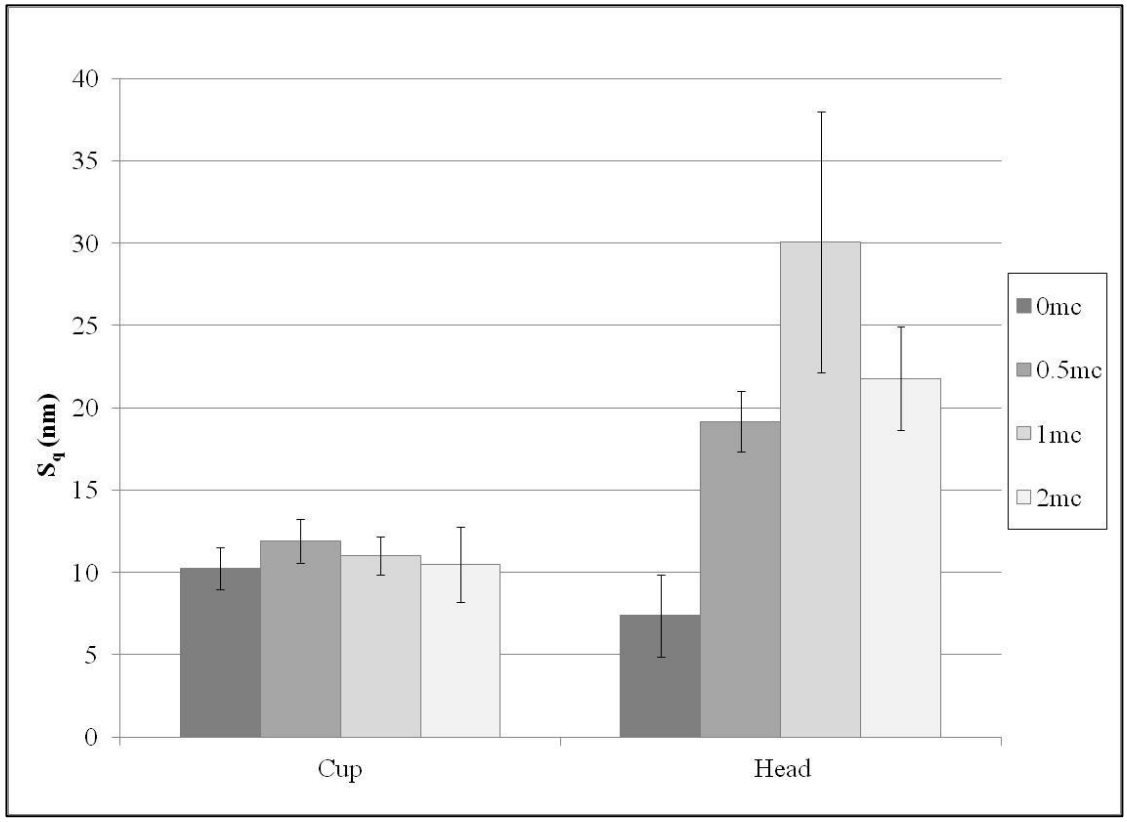

Figure 40: Surface roughness (Sq) of femoral heads in the polar region and at 30º from pole, and acetabular liners in the polar region, during 2mc of standard walking simulation (n=10, ±95% confidence intervals)

Following examination of this data post-testing, it was hypothesised that the measurement of the cup was possibly not optimal, as visual examination of the parts indicated the wear scar on the cups was lateralised from the pole. At this stage only four cups from this test available for further measurement; all others had been subsequently used on other tests. These remaining four cups were remeasured for surface roughness at 35 degrees from the pole to focus the measurement in the worn region. These results are presented in Figure 41, where the same data as Figure 40 is shown alongside the new cup measurements for reference. When roughness measurement is focused on the wear scar region of the cup a similar roughness is seen to the heads with a mean S_q of 28.8±45.1nm.

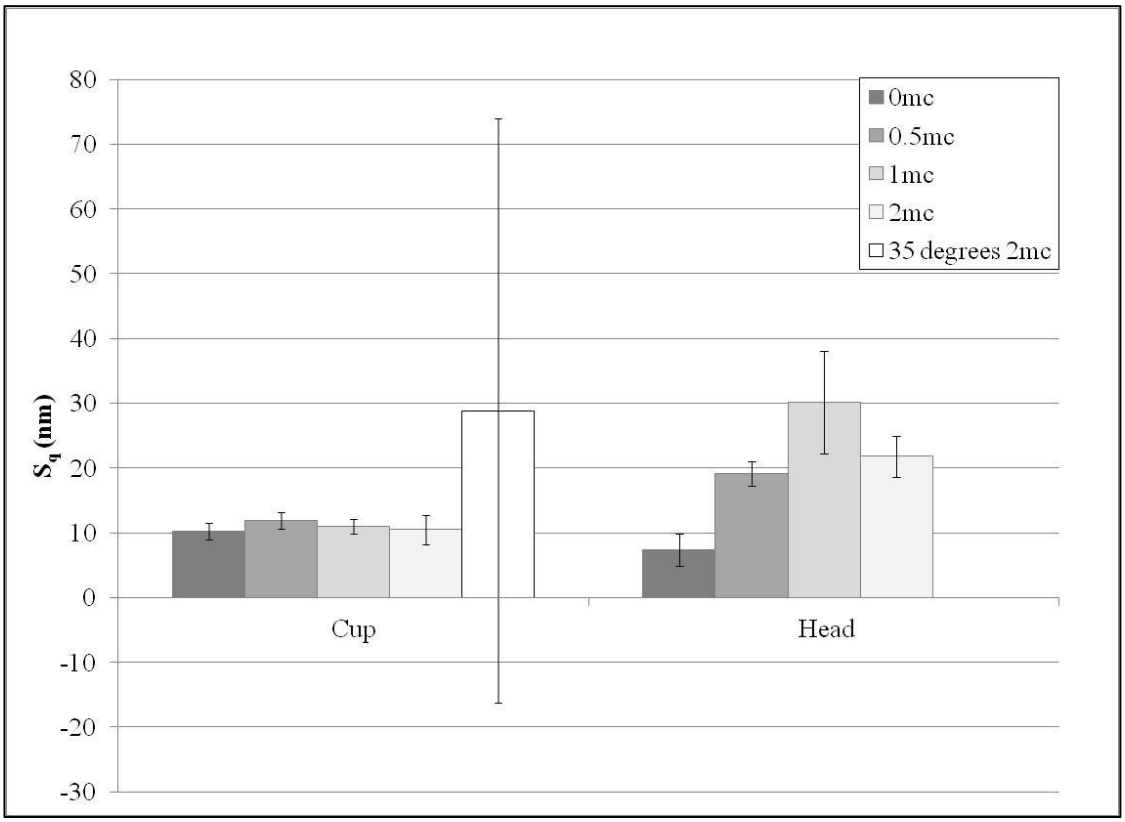

Figure 41: Surface roughness (Sq) of femoral heads in the polar region and at 30º from pole, and acetabular liners in the polar region, compared with acetabular liners at 35º from pole, during 2mc of standard walking simulation (n=10, ±95% confidence intervals)

The surface roughness of the femoral heads at the pole and at 30 degrees was compared. These results are presented in Figure 42. There was a trend for the surface roughness to be slightly higher at the pole but this was not statistically significant.

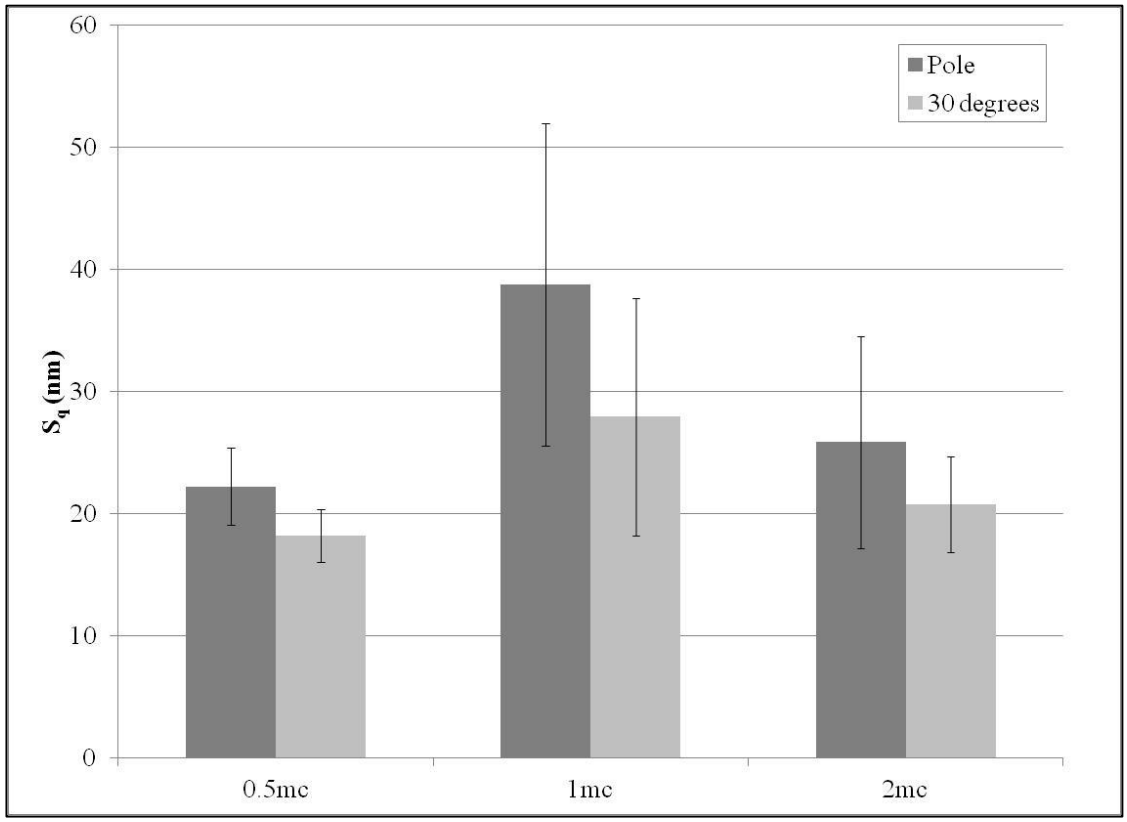

Figure 42: Root mean square surface roughness (S_q) of femoral heads during standard walking wear test comparing measurements at pole and 30 degrees from pole (n=10, ± 95% confidence intervals)

3.4 Discussion

The wear of 36mm metal-on-metal total hip replacements was evaluated using a standard walking simulation adapted from ISO 14242-1. This testing allowed both commissioning of the newly developed wear simulator, and confirmation that the simulator was delivering *in vitro* wear rates comparable with existing data in the same implant. Testing was performed on commercially available hip replacements from DePuy International Ltd.

All samples were geometrically characterised prior to testing. Mean sample diameter for the femoral heads and acetabular cups was found to be 35.999±0.002mm and 36.083±0.001mm respectively. The radius of curvature of the femoral heads was found to be slightly greater in the polar region than the equatorial region; it is believed this variation is caused during polishing of the head in manufacturing.

It must be emphasised that despite this measured variation, all parts in this study met drawing and manufacturing specifications (DePuy International DWG-136553000 (Internal confidential drawing)) when measured as per the method specified in the internal quality process specification (QPS-040-LDS (Internal confidential specification)). The QPS technique for bearing diameter comprises an overall check using a vernier caliper, and a single roundness measurement using a Talyrond or Roundtest type machine. The measurement technique used in this study is significantly more detailed than standard metrology of manufactured parts, therefore it is more likely that deviations will be detected.

Wear on the femoral head is focused around the polar region on this wear simulator, as demonstrated previously by Hardaker et al. and confirmed by the photographic analysis of samples from this test in Figure 36 (Hardaker et al., 2006). Head and cup samples were therefore paired to achieve minimal variation in polar clearance between stations; mean polar clearance was 68.073±0.465µm. Changes in diametrical clearance of over approximately 40µm above nominal have been shown to cause a significant increase in bearing wear; below this level clearance changes do not have a significant effect (Dowson et al., 2004b), therefore it is expected that the tight range of diametrical clearances achieved in this study will not have any effect on bearing wear.

Wear of the samples in this test was bi-phasic, with a significantly higher rate of wear over the first million cycles compared with the second half of the test. This is normal characteristic behaviour for metal-on-metal bearings (Dowson et al., 2004a), and is due to the parts bedding in to an optimal geometrical conformity with each other (Hu et al., 2004). After exclusion of an outlier station with high wear due to equipment malfunction, the mean bedding in and steady state wear rates for this test were $0.11\pm0.08mm^3$/mc and $0.03\pm0.02mm^3$/mc respectively. This represents a statistically significant difference between the two phases of the test (Paired Sample t-test, $p=0.04$). It is generally accepted that once in the steady state wear period, bearings will continue to wear at this low rate, therefore the wear volume in the bedding in period is of primary concern when evaluating overall performance of a bearing (Isaac et al., 2006; Leslie et al., 2008).

A previous study was performed in this laboratory on the same product, using an earlier design iteration of the ProSim wear simulator (Goldsmith et al., 2000). They presented steady state wear of $0.07\pm0.10mm^3$/mc, which is not significantly different from the present data, giving good confidence in the results generated by the new wear simulator. Similar results were also observed on three previously unpublished internal DePuy studies performed by the author on the same implant design and using an earlier generation design of the ProSim Hip Wear Simulator (Figure 43) (DePuy International, 2006, 2008a, 2008b).

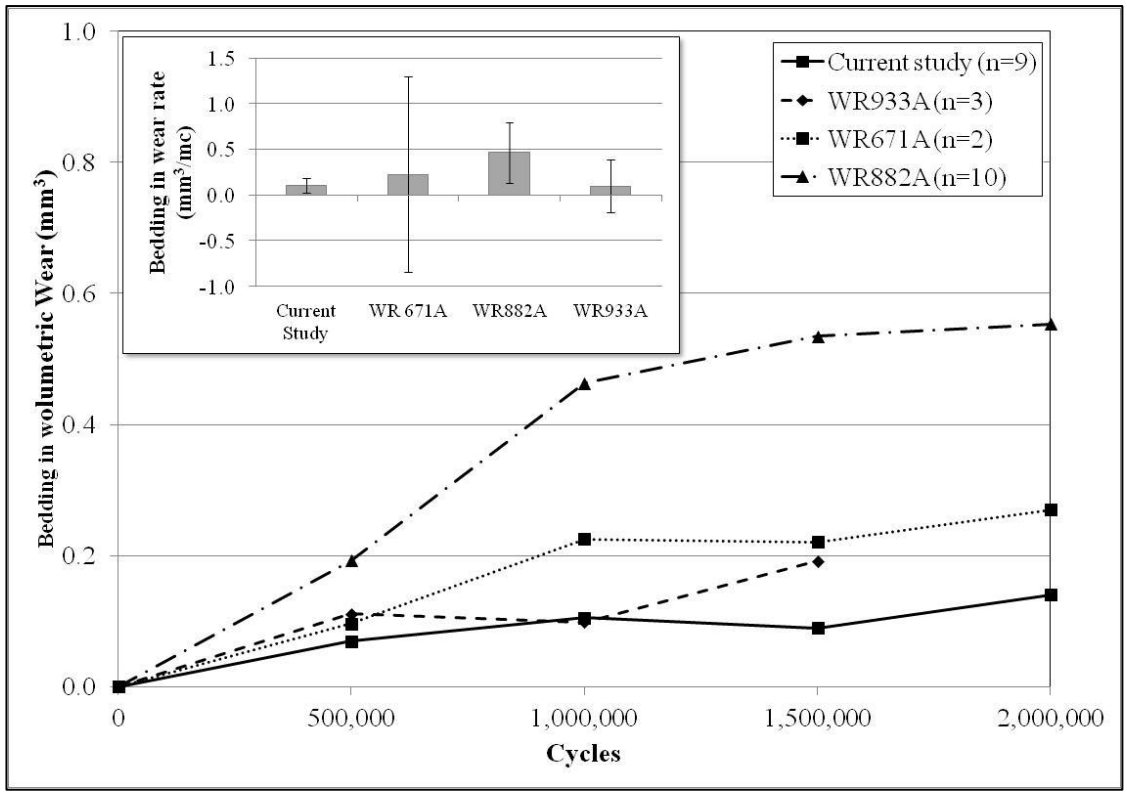

Figure 43: Comparison of results from the present study with previous tests using the same implants and wear simulator protocol (DePuy International, 2006, 2008a, 2008b)

Scratching was observed on all samples following wear testing. The degree of scratching ranged from a few isolated discrete marks, to a distinct area of concentrated damage, and this appeared to correlate with the overall volume of wear measured during the test. This correlation is believed to be due to a greater degree of scratching being indicative of more damage of the surface and thus a greater measured volumetric wear on the sample.

Scratching always appeared focused on the pole of the femoral head, but slightly away from the pole on the acetabular cup. This was due to relative positioning of the components in the simulator. The head was positioned vertically (a non anatomical position), however the cup was oriented at 35º from the horizontal. Load was applied vertically through the entire construct, therefore the primary contact zone between the head and cup was in line with this axis: on the pole of the head and 35º from the pole on the cup. The appearance of wear scars in these areas is in good agreement with earlier studies on similar devices (Hardaker et al., 2006; Williams et al., 2008).

Surface roughness measurements were taken of the heads and cups pre- and post-testing. Measurements were taken at the head on the pole and at four equispaced points

30º from the pole. This was not possible on the cup due to limitations with the interferometer used for the measurement and difficulty accessing the inner surface of the cups. Roughness was presented in terms of S_q (root mean square 3D roughness). A statistically significant increase in roughness was seen on femoral heads over the first million cycles of the test, but roughness appeared to plateau between 1mc and 2mc. It is believed this is due to the bedding-in behaviour identified with the gravimetric wear volume measurement. From 0-1mc, wear was at a relatively high rate and significant quantities of material were being removed from the bearing surfaces. The mechanisms of wear discussed in Chapter 1, including abrasion, where asperities or loose particles gouge the opposing material, result in scratching of the surface, which would increase proportionally with the volume of material lost. As volumetric wear was very low in the period from 1-2mc, damage to the surfaces must also have been relatively low, therefore roughness was not seen to increase further. This is in agreement with the study by Leslie et al. on similar bearings, which identified an increase in roughness in the first million cycles of *in vitro* wear, but no significant increase thereafter (Leslie et al., 2009).

The roughness of the femoral heads at the pole was compared with the same components 30º from the pole. A slight but non significant increase was observed on the pole. It has been shown that contact stress in the wear region increases towards the pole (Jalali-Vahid et al., 2006), therefore it is believed that the stress correlates with greater wear and an increased degree of scratching.

No significant increase in surface roughness was seen on the acetabular cups throughout the test. Following testing it was realised that measurement of the roughness of the cup at the pole was not appropriate since the wear was observed to form at 35º from the pole, in line with the positioning of the components *in vitro*. Since the testing had been undertaken, the interferometer used for roughness measurement had been modified to facilitate oblique measurements within cups, therefore the remaining four cups from this test were measured at 35º from the pole. S_q was 28.8±45.1nm. The error bars (95% confidence intervals) are significantly larger due to the small number of samples available, however the mean magnitude of roughness is very close to that of the heads at the same interval, suggesting a similar surface damage mechanism is occurring on both the femoral heads and acetabular liners.

3.5 Conclusion

This test evaluated wear of 36mm metal-on-metal total hip replacements under a standard walking cycle, using a new design of ProSim Hip Wear Simulator. Good agreement with previous studies was found for volumetric wear, visual appearance and surface roughness of the samples tested. It was concluded that the new design of simulator was performing as required, and provided reliable control data for standard walking conditions to compare with the multi-profile studies planned later in this study.

CHAPTER 4. WEAR OF 36MM METAL-ON-METAL TOTAL HIP REPLACEMENTS UNDER STOP-DWELL-START CONDITIONS – EFFECT OF DWELL DURATION

4.1 Introduction

This chapter describes development and application of a protocol for clinically relevant stop-dwell-start (SDS) type wear simulation, and the effect of this activity on the wear of 36mm MOM total hip replacements. In particular it describes the investigation of the effect of the duration of the dwell period. Typical clinical conditions for stop-dwell-start activity of real patients were derived from the literature and used to generate three scenarios with different relative durations of dwell and motion inputs for *in vitro* testing. A pause, or dwell, was introduced into a standard walking simulation protocol every 10 steps, with a dwell load of 1250N.

It was hypothesised that introduction of a pause, or dwell, into a wear simulation would increase *in vitro* wear of MOM THR, and that wear would increase proportionally with the pause duration, as previously suggested in the literature (Medley et al., 2002). Initial results from the 5s dwell did not agree with the hypothesis, therefore an increase in duration of dwell was introduced with the 30s and 60s dwell periods. The test protocol was developed iteratively throughout the study as further results became available.

4.2 Methods and Materials

4.2.1 Hip Simulator

Ten 36mm Pinnacle MOM total hip replacements from DePuy International (UK) were used for this study (DePuy International, Product code 136553000, DWG-136553000 (Internal confidential drawing)). Each individual component was assigned a unique reference number for identification in the format yy_xxxx, where yy represents the year of initial sourcing of the parts, and xxxx is a unique identifier assigned consecutively.

The samples were prepared and mounted as described in Chapter 2. A standard walking wear test adapted from ISO 14242-1:2002 (International Standards Organisation, 2002) was used for the basis of the SDS test. Load was applied to the components in a twin peak Paul-type waveform with a peak load of 3kN and swing phase load of 300N. Flexion / extension and internal / external rotation were applied in a sinusoidal waveform over +30º/-15º and ±10º respectively, as described in Chapter 2. This cycle was applied at a frequency of 1Hz.

4.2.2 Stop-dwell-start (SDS) Protocol

The SDS conditions were created by introducing a dwell period into the standard walking test at regular intervals. Data from the work of Morlock et al. discussed in Chapter 1 was used to define the load and kinematic inputs.

4.2.2.1 Dwell Frequency

Patients have been reported to spend approximately 62 minutes of the waking day in motion (walking or stair climbing), during which around 6600 steps take place in 319 sequences, or ‘bursts’ of motion (Morlock et al., 2001). This equates to motion occurring in bursts of roughly 20 steps or 12s duration, and indicates a step frequency of approximately 1.7Hz.

The standard ISO walking simulation test defines a test frequency of 1Hz (International Standards Organisation, 2002) and it is known that a change in frequency can affect wear test results (Kamali et al., 2010). It was preferable to eliminate frequency as a variable in this investigation therefore a frequency of 1Hz was selected for continuity. To simplify test programming and cycle counts, motion sequences of 10 steps, with a dwell introduced after each 10 step sequence were defined for the present study.

4.2.2.2 Dwell duration

The most frequent duration of pause measured in patients during normal daily activity was 2-5s (58%), with longer dwells of 5-10s (21%), 10-30s (15%) and 30-60s (4%) occurring proportionally less frequently. A mean pause duration of 11.2 ± 3.0s was reported (Morlock et al., 2000).

Dwell periods of 5s, 30s and 60s were selected for the present *in vitro* test as being most representative of the clinical measurements of patients' activity, yet providing a wide range of variables.

4.2.2.3 Dwell loading and kinematics

The work of Morlock et al. indicated the majority of pause time in patients was spent sitting (54%), with the remainder standing (37%) or lying (9%) (Morlock et al., 2000). To aid simplification, a standing dwell position was used for this study, with an applied load equivalent to bi-lateral stance load of 1250N (Bergmann et al., 2001). The F/E and IER motion axes were held at 0º during each dwell period to represent a standing position.

4.2.2.4 Complete SDS Cycle

Three SDS tests were run in this study. These are detailed in Table 12. Dwell kinematics and load remained constant for all three tests, as did the dwell frequency. Dwell duration was varied for each of the three tests, with durations of 5s, 30s and 60s evaluated. The first two tests were each run for a minimum of 2mc, however due to the low ratio of motion:dwell cycles on the last test, the amount of time required to generate two million motion cycles was excessively long (approximately six months) therefore this test was shortened to 0.5mc.

Table 12: Test run order for effect of dwell duration study

Test	Nomenclature	n
10s walking, 5s dwell (3mc)	SDS 10W 5D	9
10s walking, 30s dwell (2mc)	SDS 10W 30D	10
10s walking, 60s dwell (0.5mc)	SDS 10W 60D	10

A nomenclature was used to aid with identification of parameters for each test. Every SDS test was identified using the format SDS xW yD where x denotes the number of

walking cycles between dwell periods, and y indicates the duration in seconds of each dwell period, therefore SDS 10W 5D was a test where ten walking steps were followed by a 5s dwell in a repeated loop.

When counting cycles on multi profile stop start tests, only cycles where the walking cycle was running were counted for the purposes of calculating wear rates, on the assumption that no wear would occur during the dwell period, as no motion is present. If the dwell cycles had been included this would incorrectly have deflated the final calculated wear per cycle.

4.2.3 Effect of Bedding In

The SDS 10W 5D test was also used for a further investigation of the effect of bedding in of samples on the *in vitro* wear under SDS conditions. Five samples from this test were new, unworn bearings, and five were previously worn under standard walking conditions for 2mc. These samples were those previously tested and described in Chapter 3. A statistical comparison of the pre-worn and new samples was undertaken using a T-test.

4.2.4 Geometric Analysis

All samples were measured using the CMM prior to testing to define sample diameter and bearing clearance. The Zeiss CMM was used for these measurements as described in Chapter 2.

4.2.5 Gravimetric Analysis

All samples were weighed following cleaning using the techniques described in Chapter 2 every 500,000 cycles throughout the test.

4.3 Results

4.3.1 Effect of 5 Second Pause

A wear simulation was run for 3 million cycles (mc) on 36mm MOM hip bearings applying an SDS 10W 5D protocol. This incorporated 10 cycles of standard walking conditions at 1Hz followed by five seconds of dwell.

Shortly before 1mc into the test a major machine breakdown occurred. This was caused by a software malfunction. All samples were removed from the simulator and weighed at that time. During repair and resolution of the cause of this malfunction, several samples were damaged when excessively high loads were accidentally applied and several stations were dislocated. At this stage it was decided that four of the bearing pairs (Stations 3, 6, 9 & 10) were too severely damaged to provide any useful information, they were therefore removed from the test. The remaining samples were weighed again, before continuing the test to 1mc, with dummy specimens replacing the damaged samples. At 1mc the dummy specimens were replaced with four new bearing pairs. The test was then run for a further 2mc, therefore half of the samples from this test were run to 3mc, and half to 2mc. The data presented is for the ten samples which completed the test; the data from the damaged samples is not presented.

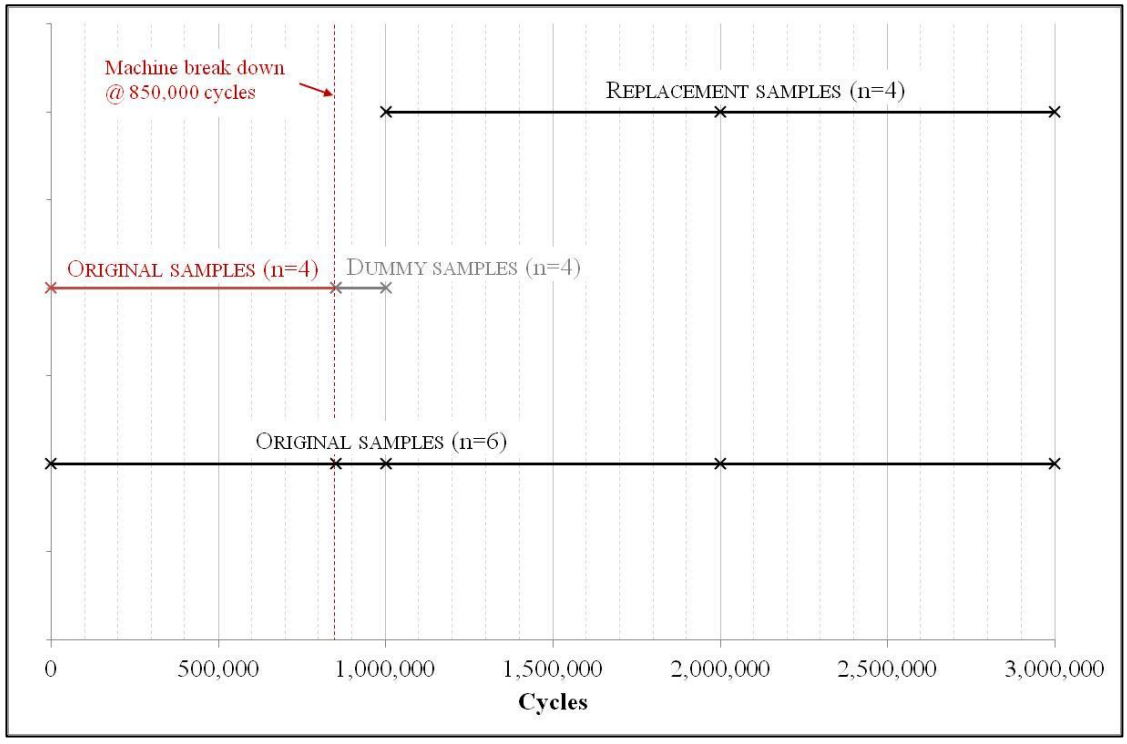

Figure 44: Schematic illustrating sample loss and replacement following machine breakdown during SDS 10W 5D test

4.3.1.1 Geometric analysis

Ten 36mm MOM bearing pairs were used in the SDS 10W 5D test. The acetabular components were found to have a mean diameter of 36.084±0.001mm (±95% confidence interval) with a mean form of 0.004±0.001mm (Table 13).

The femoral heads had a mean global diameter of 36.000±0.003mm with a mean sphericity of 0.008±0.001mm (Table 14). The femoral head polar diameter and form were 36.016±0.002mm and 0.006±0.001mm respectively. The femoral head equatorial diameter and form were 35.998±0.003mm and 0.006±0.001mm respectively.

As discussed in Chapter 3, the difference between polar and equatorial geometry can have an effect on bearing wear *in vitro*, therefore samples were paired using polar geometry, as with the Walking test described in Chapter 3. Mean polar clearance was 67.831±0.602µm (Table 15).

Table 13: CMM results for SDS 10W 5D acetabular components prior to testing

Station	Sample No.	Diameter (mm)	Form (mm)
1	**08_1460**	36.080	0.009
2	**08_1427**	36.082	0.003
3	**08_1445**	36.085	0.004
4	**08_1441**	36.083	0.002
5	**08_1437**	36.085	0.005
6	**08_1459**	36.086	0.004
7	**08_1453**	36.084	0.003
8	**08_1467**	36.084	0.003
9	**08_1444**	36.086	0.002
10	**08_1433**	36.086	0.003
Average		36.084	0.004
95% Confidence		0.001	0.001

Table 14: CMM results for SDS 10W 5D femoral components prior to testing

Station	Sample No.	Global Diameter (mm)	Global Sphericity (mm)	Polar Diameter (mm)	Polar Sphericity (mm)	Equatorial Diameter (mm)	Equatorial Sphericity (mm)
1	**08_1475**	36.001	0.008	36.012	0.006	36.000	0.005
2	**08_1476**	35.999	0.008	36.012	0.004	35.998	0.007
3	**08_1471**	36.000	0.008	36.014	0.003	35.998	0.006
4	**08_1489**	36.000	0.008	36.014	0.003	35.998	0.007
5	**08_1477**	35.996	0.009	36.015	0.004	35.994	0.007
6	**08_1474**	35.995	0.011	36.016	0.006	35.993	0.008
7	**08_1518**	36.004	0.006	36.016	0.001	36.002	0.003
8	**08_1479**	35.992	0.011	36.016	0.003	35.990	0.007
9	**08_1493**	36.002	0.008	36.016	0.004	36.001	0.006
10	**08_1058**	36.004	0.006	36.017	0.002	36.003	0.003
Average		36.000	0.008	36.016	0.003	35.998	0.006
95% Confidence		0.003	0.001	0.002	0.001	0.003	0.001

Table 15: Calculated clearance between head and cup for global, polar and equatorial geometries for SDS 10W 5D components prior to testing

Station	Global clearance (µm)	Polar clearance (µm)	Equatorial clearance (µm)
1	78.704	68.333	79.997
2	82.413	69.835	83.973
3	89.487	67.544	91.493
4	82.549	68.416	84.303
5	79.681	67.122	80.904
6	83.385	67.101	84.485
7	79.843	67.470	81.106
8	91.566	67.809	93.665
9	83.228	67.217	84.443
10	92.794	67.464	94.733
Average	84.365	67.831	85.910
95% Confidence	3.639	0.602	3.865

4.3.1.2 Gravimetric analysis

The raw volumetric wear data for all samples is presented in Figure 45 and Figure 46. The original samples which were tested for 3mc are shown in Figure 45. The simulator breakdown occurred at 850,000 cycles, and an extra wear measurement was taken at this stage. This is highlighted by the red circle. Station 7 was damaged at 1.5mc and removed from the test. The replacement samples which were tested for 2mc are shown in Figure 46.

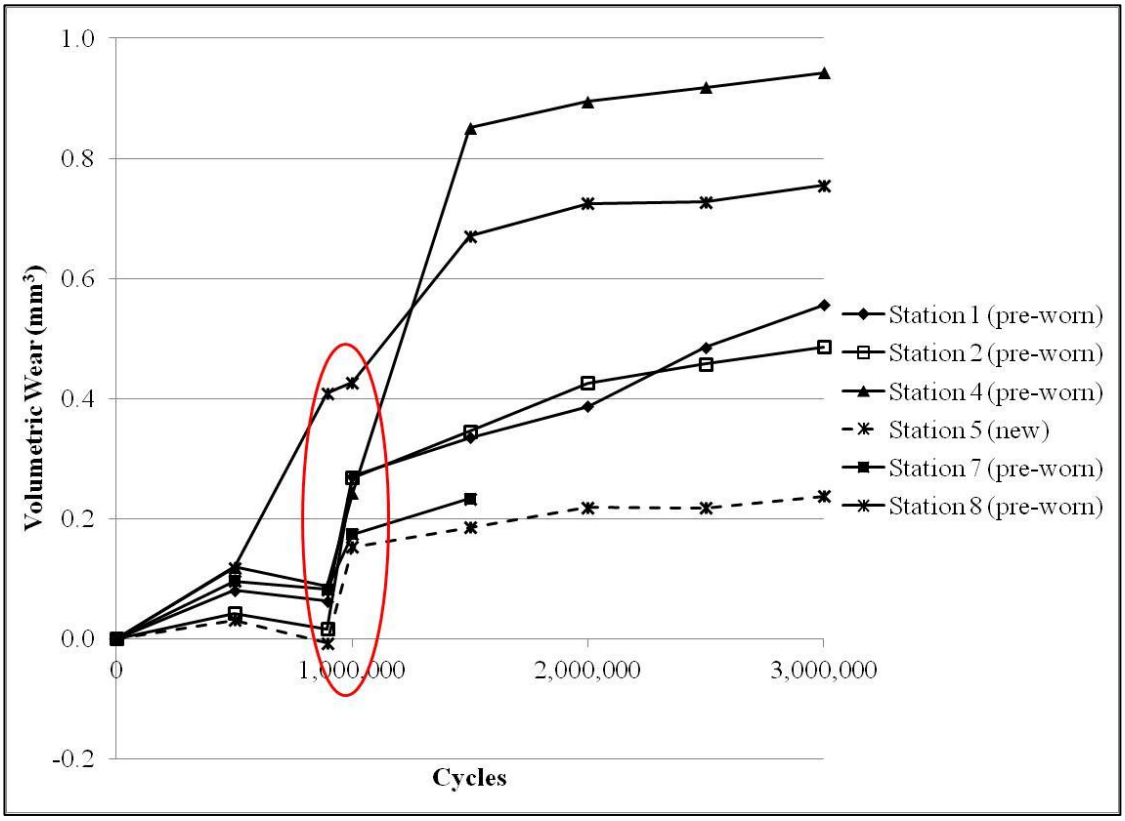

Figure 45: Cumulative individual volumetric wear of 36mm MOM under SDS 10W 5D protocol (original samples)

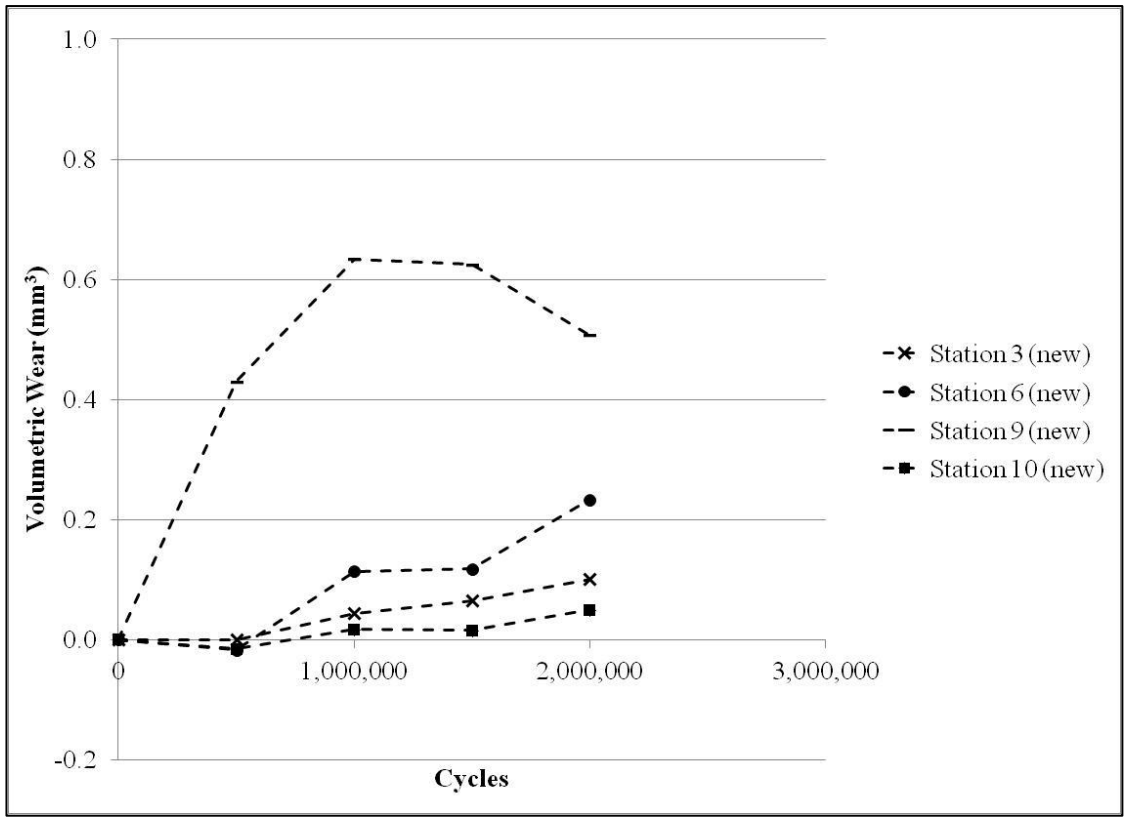

Figure 46: Cumulative individual volumetric wear of 36mm MOM under SDS 10W 5D protocol (replacement samples)

A significant increase in wear was observed at the time of the simulator breakdown, this can be observed in a jump in the graph between 0.85mc and 1mc (Figure 45). This was attributed to further damage caused by the machine breakdown which was not identified by visual inspection at the time. To allow comparison of the two data sets, the wear occurring at the time of the breakdown was excluded. The volume of wear measured between 0.85mc and 1mc was calculated for the six original samples and this value subtracted from each subsequent wear measurement point to provide corrected wear values.

The individual wear of all samples, both the original six with corrected wear data, and the replacement four parts are shown in Figure 47. The mean wear of all samples is shown in Figure 48. The mean volumetric total wear of all samples was 0.31±0.21mm^3 at 2mc (n=9) and 0.45±0.31mm^3 at 3mc (n=5). Three stations (3, 4 & 8) appeared to have slightly higher wear than the other stations. This was examined using a Grubbs' Outlier Test and these stations were found to be not significant as outliers at the 5% significance level (T_n = 1.57, Table value = 1.71).

Bedding in and steady state wear rates were calculated from 0-1mc and 1-3mc respectively. These wear rates were 0.15±0.15mm^3/mc and 0.04±0.14mm^3/mc respectively. There was no significant difference in wear of the samples between the different phases of the test (P=0.661, Paired T-test).

Wear under the SDS 10W 5D protocol from 0-2mc was compared with wear under standard walking conditions from 0-1mc. There was no significant difference between the tests at the 5% significance level (P=0.220, T-test).

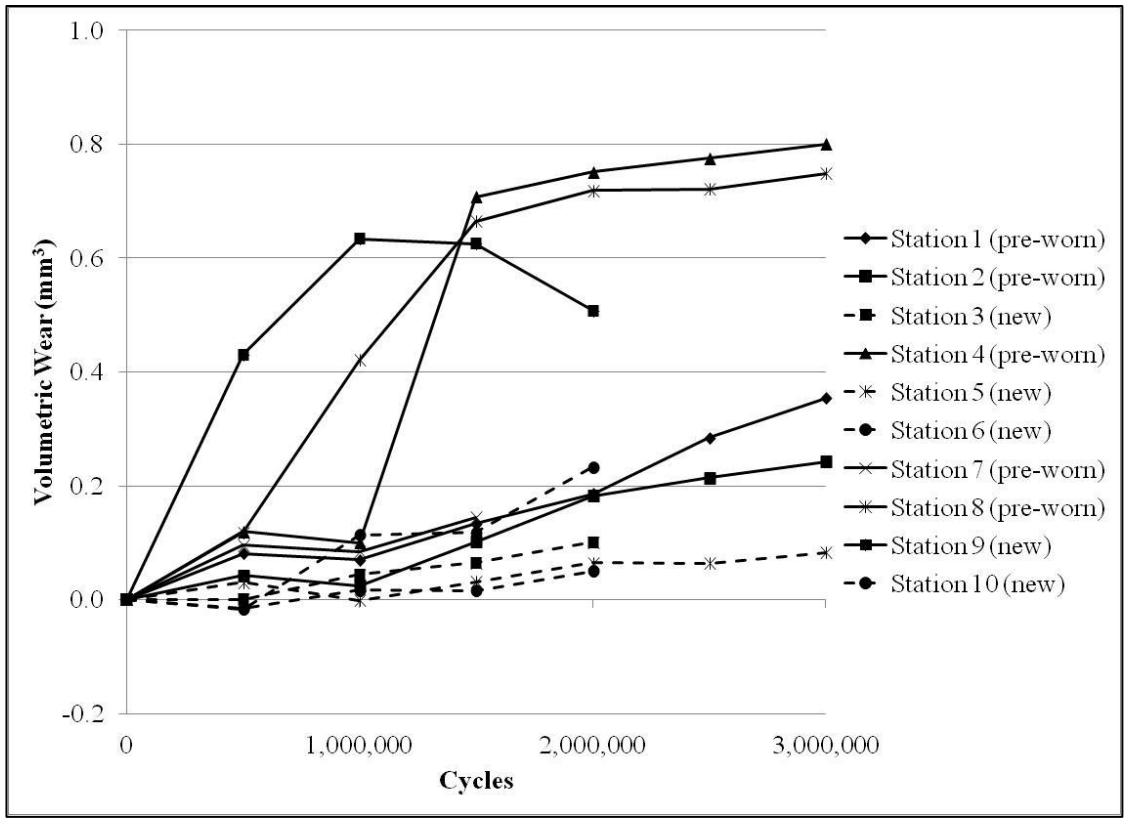

Figure 47: Cumulative individual volumetric wear of 36mm MOM under SDS 10W 5D protocol (corrected original and replacement samples)

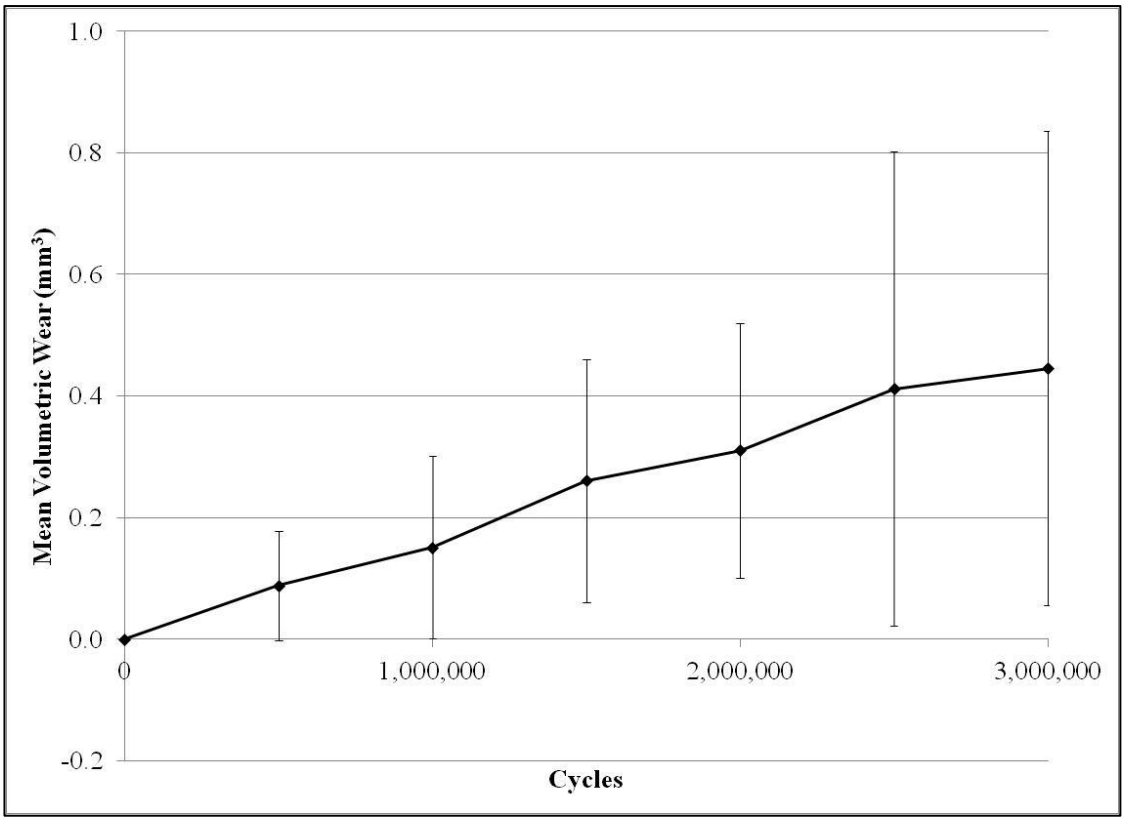

Figure 48: Cumulative mean volumetric wear of 36mm MOM under SDS 10W 5D protocol (corrected original and replacement samples) (0-1.5mc n=10, 1.5-2mc n=9, 2-3mc n=5, ±95% confidence limits)

4.3.2 Effect of Bedding In

Five samples from the SDS 10W 5D test had previously undergone 2mc of standard walking simulation as described in Chapter 3. The remaining five samples from this test were new and unworn. The mean wear rates for the two groups from 0-1mc were 0.13±0.2mm^3/mc and 0.16±0.33mm^3/mc for the pre-worn and new samples respectively (Figure 49). Overall wear rates from 0-3mc were 0.16±0.11mm^3/mc and 0.04±0.04mm^3/mc for the pre-worn and new samples respectively.

Significantly higher overall wear rates were measured on pre-worn samples compared with new samples (P=0.016, T-test), however this difference was not significant on wear rates from 0-1mc (P=0.880, T-test).

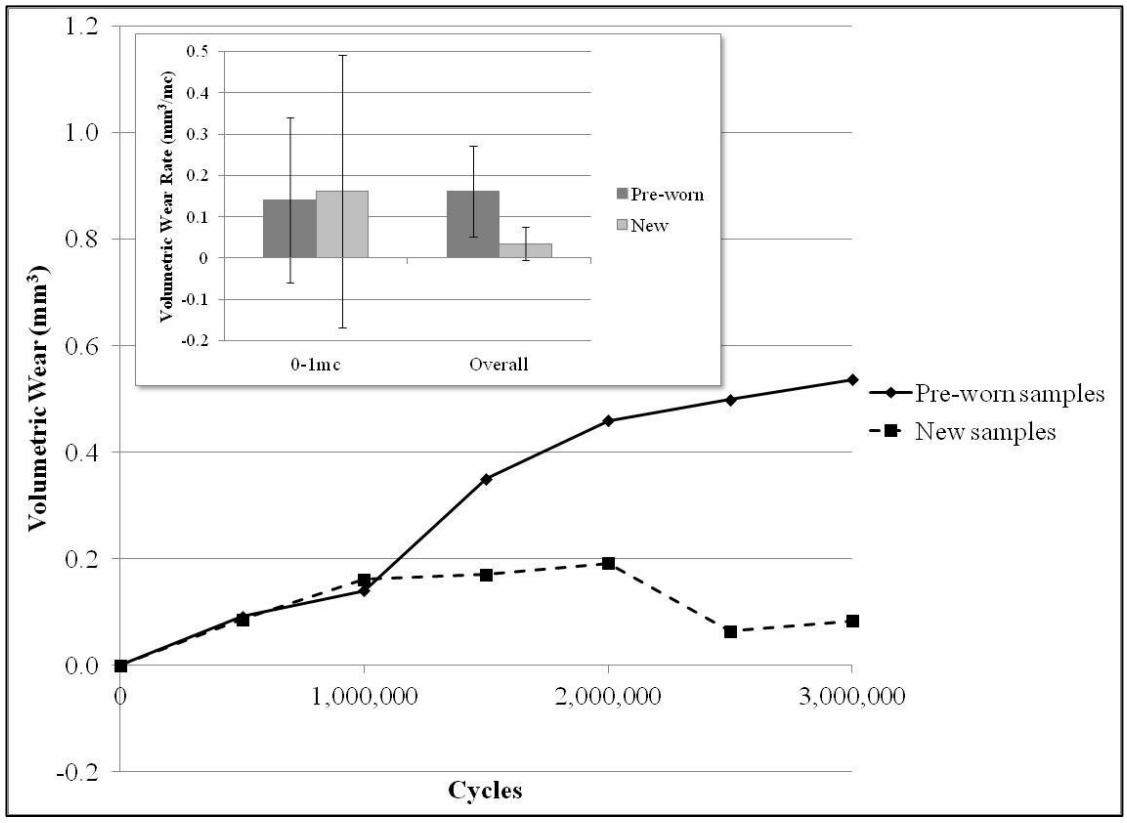

Figure 49: Cumulative mean volumetric wear of 36mm MOM under SDS 10W 5D protocol comparing pre-worn and new samples (0-1.5mc n=10, 1.5-2mc n=9, 2-3mc n=5, ±95% confidence limits)

4.3.3 Effect of 30 Second Pause

4.3.3.1 Geometric analysis

Ten 36mm MOM bearing pairs were used in the SDS 10W 30D test. The samples for the SDS 10W 30D test were taken from the SDS 10W5D test hence were pre-worn components. One new bearing pair was added to replace the damaged samples from Station 7. The acetabular components were found to have a mean diameter of 36.085±0.001mm (±95% confidence interval) with a mean form of 0.005±0.002mm (Table 16).

The femoral heads had a mean global diameter of 36.002±0.003mm with a mean sphericity of 0.008±0.003mm (Table 17). The femoral head polar diameter and form were 36.017±0.001mm and 0.003±0.002mm respectively. The femoral head equatorial diameter and form were 36.000±0.001mm and 0.006±0.003mm respectively.

As discussed in Chapter 3, the difference between polar and equatorial geometry can have an effect on bearing wear *in vitro*, therefore samples were paired using polar geometry, as with the Walking test described in Chapter 3. Mean polar clearance was 67.954±0.615µm (Table 18).

Table 16: CMM results for SDS 10W 30D acetabular components prior to testing

Station	Sample No.	Diameter (mm)	Form (mm)
1	**08-1460**	36.080	0.009
2	**08-1427**	36.082	0.003
3	**08-1440**	36.087	0.006
4	**08-1441**	36.083	0.002
5	**08-1449**	36.085	0.005
6	**08-1435**	36.087	0.002
7	**08_1461**	36.087	0.003
8	**08-1467**	36.084	0.003
9	**08-1431**	36.088	0.008
10	**08-1464**	36.087	0.003
Average		36.085	0.005
95% Confidence		0.001	0.002

Table 17: CMM results for SDS 10W 30D femoral components prior to testing

Station	Sample No.	Global Diameter (mm)	Global Sphericity (mm)	Polar Diameter (mm)	Polar Sphericity (mm)	Equatorial Diameter (mm)	Equatorial Sphericity (mm)
1	**08 1475**	36.001	0.008	36.012	0.006	36.000	0.005
2	**08 1476**	35.999	0.008	36.012	0.004	35.998	0.007
3	**08 1481**	35.999	0.010	36.019	0.003	35.996	0.007
4	**08 1489**	36.000	0.008	36.014	0.003	35.998	0.007
5	**08 1510**	36.006	0.007	36.018	0.001	36.004	0.004
6	**08 1472**	36.007	0.009	36.019	0.004	36.005	0.006
7	**08_1496**	36.004	0.007	36.020	0.002	36.003	0.004
8	**08 1479**	35.992	0.011	36.016	0.003	35.990	0.007
9	**08 1500**	36.006	0.007	36.021	0.003	36.004	0.005
10	**08 1480**	36.005	0.007	36.019	0.004	36.004	0.005
Average		36.002	0.008	36.017	0.003	36.000	0.006
95% Confidence		0.003	0.003	0.001	0.002	0.001	0.003

Table 18: Calculated clearance between head and cup for global, polar and equatorial geometries for SDS 10W 30D components prior to testing

Station	Global clearance (µm)	Polar clearance (µm)	Equatorial clearance (µm)
1	78.704	68.333	79.997
2	82.413	69.835	83.973
3	88.090	68.040	90.122
4	82.549	68.416	84.303
5	79.681	67.122	80.904
6	80.109	67.995	81.478
7	83.217	67.717	84.165
8	91.566	67.809	93.665
9	82.278	66.575	83.892
10	81.593	67.695	83.168
Average	83.020	67.954	84.567
95% Confidence	2.823	0.615	3.021

The SDS 10W 30D test was run to 1mc. Due to the long pause duration, this test took approximately four months to run. Time constraints prevented the test being run for a longer period.

4.3.3.2 Gravimetric analysis

Individual wear for all samples is shown in Figure 50. One bearing pair, Station 4, exhibited higher wear than the other samples from 0.5-1mc. This was shown to be a significant outlier using Grubbs' Outlier Test (T_n = 2.37, Table value = 2.29). This high wear was found to be due to a load cell failure identical to that encountered in the Walking test and described in Chapter 3. This sample was therefore excluded from the summary statistics for the SDS 10W 30D test.

Mean wear for the SDS 10W 30D test is presented in Figure 51. Overall mean wear at 1mc excluding the outlier station was 0.19±0.11mm^3, representing a wear rate of 0.19±0.11mm^3/mc.

Wear under the SDS 10W 30D test conditions was compared with wear under standard walking conditions from 0-1mc (Chapter 3). There was no significant difference between the sample sets at the 5% significance level (P=0.193, T-test).

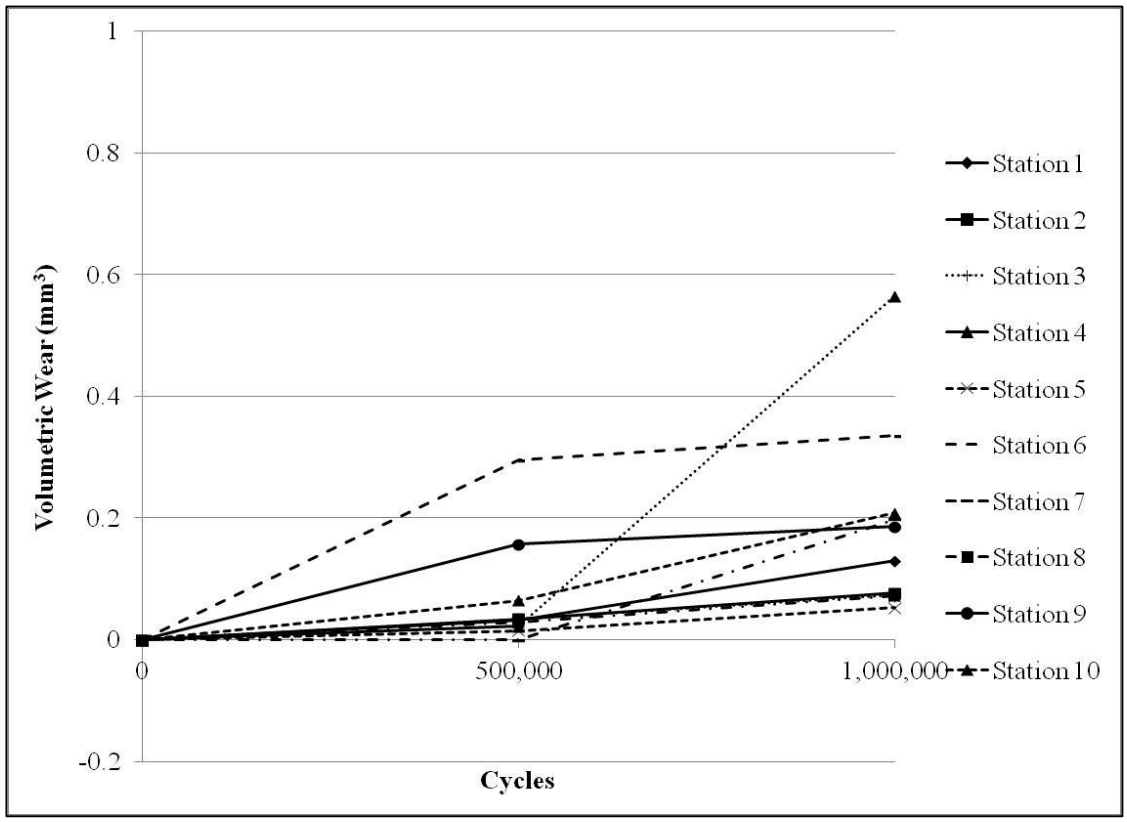

Figure 50: Cumulative individual volumetric wear of 36mm MOM under SDS 10W 30D protocol

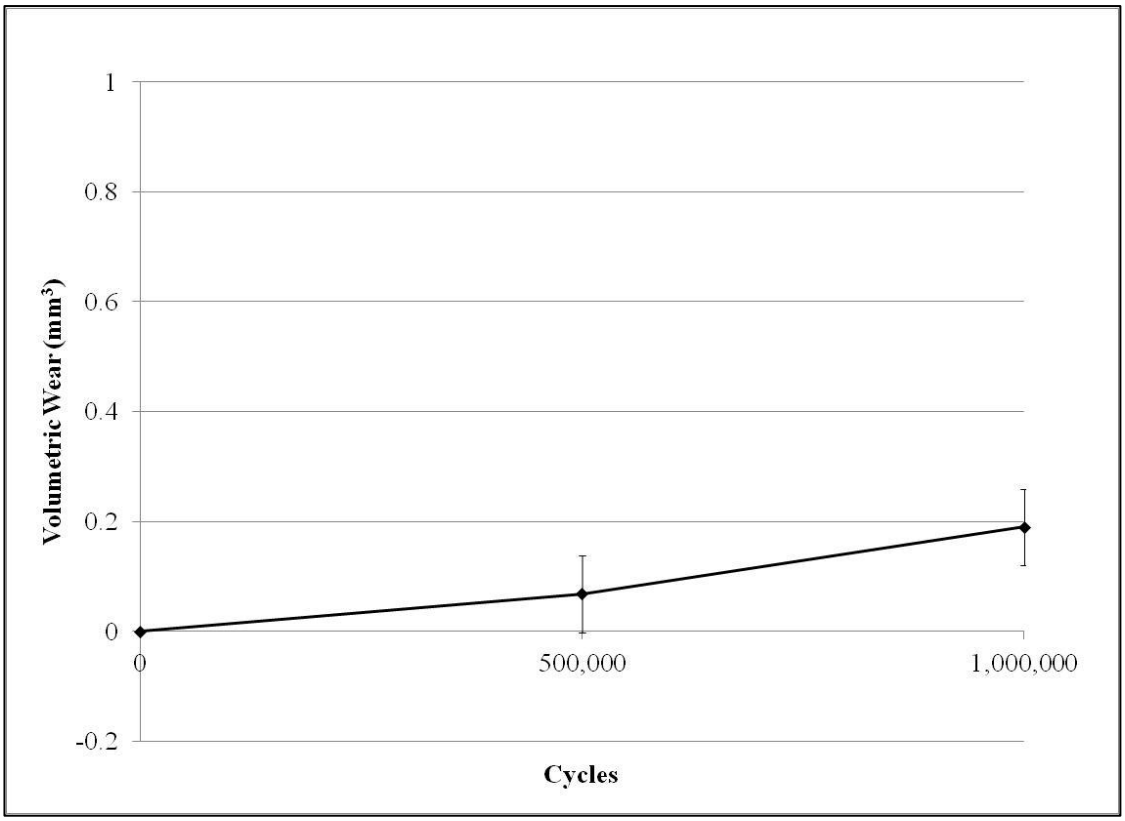

Figure 51: Cumulative mean volumetric wear of 36mm MOM under SDS 10W 30D protocol (n=9, ±95% confidence limits)

4.3.4 Effect of 60 Second Pause

4.3.4.1 Geometric analysis

The samples for the SDS 10W 60D test were taken from the SDS 10W 30D test. The acetabular components were found to have a mean diameter of 36.085±0.001mm (±95% confidence interval) with a mean form of 0.005±0.002mm (Table 16). The femoral head polar diameter and form were 36.017±0.001mm and 0.003±0.002mm respectively. Mean polar clearance was 67.954±0.615µm (Table 18).

The SDS 10W 60D test was run to 0.5mc. Due to the long pause duration, this test took approximately seven months to run. Time constraints prevented the test being run for a longer period.

4.3.4.2 Gravimetric analysis

Individual and mean wear for samples tested under the SDS 10W 60D test are presented in Figure 52 and Figure 53. Mean overall wear at 0.5mc was 0.05±0.01mm^3, representing a wear rate of 0.09±0.02mm^3/mc.

Wear under the SDS 10W 60D test conditions was compared with wear under standard walking conditions from 0-0.5mc. There was no significant difference between the samples sets at the 5% significance level (P=0.420, T-test).

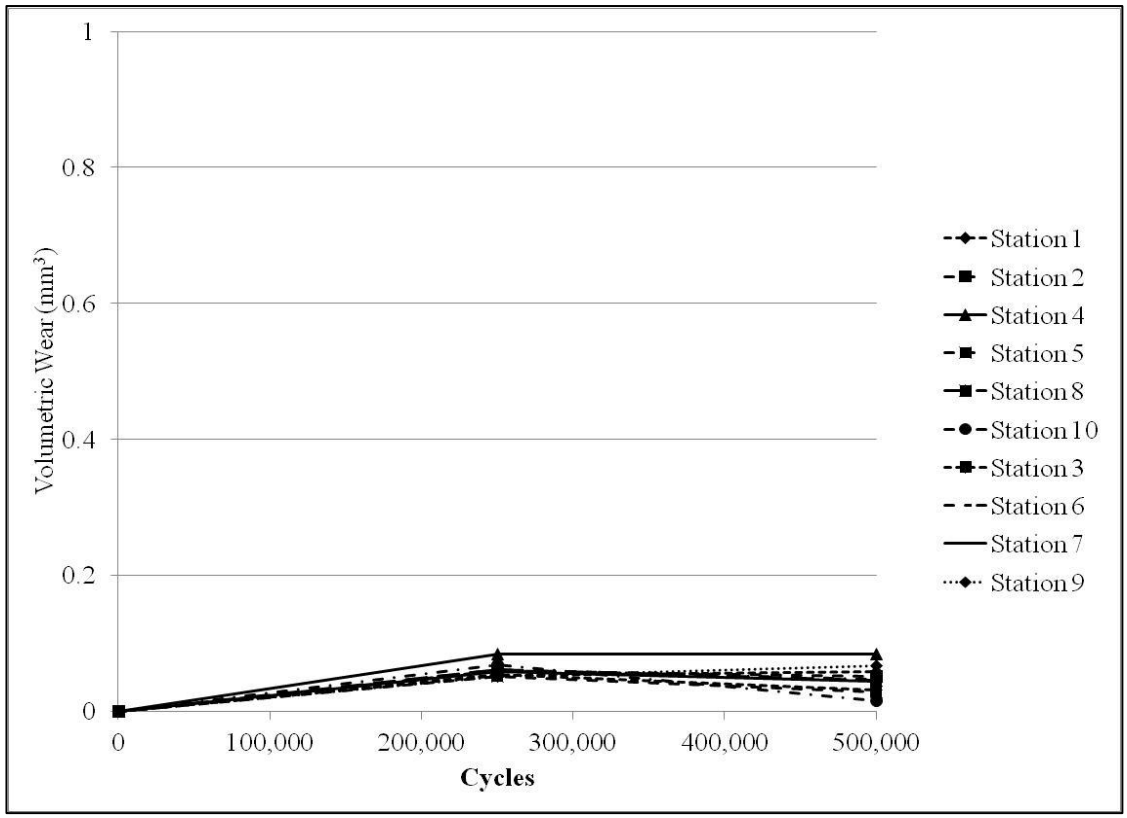

Figure 52: Cumulative individual volumetric wear of 36mm MOM under SDS 10W 60D protocol

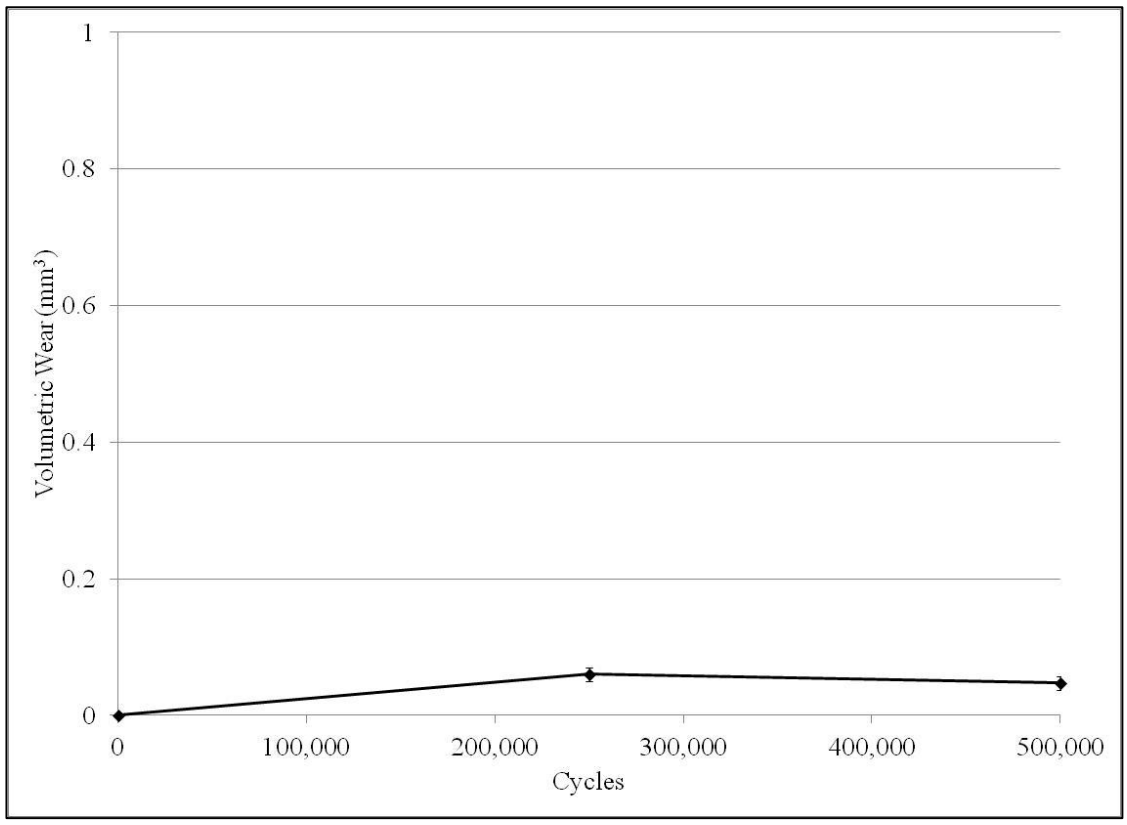

Figure 53: Cumulative mean volumetric wear of 36mm MOM under SDS 10W 60D protocol (n=10, ±95% confidence limits)

4.3.5 Summary of Results

Three wear simulation tests have been run to examine the effect of dwell duration on the wear of 36mm MOM hip bearings under SDS conditions. The mean wear for each of these tests is presented in Figure 54, and compared with the data for a standard walking test presented in Chapter 3.

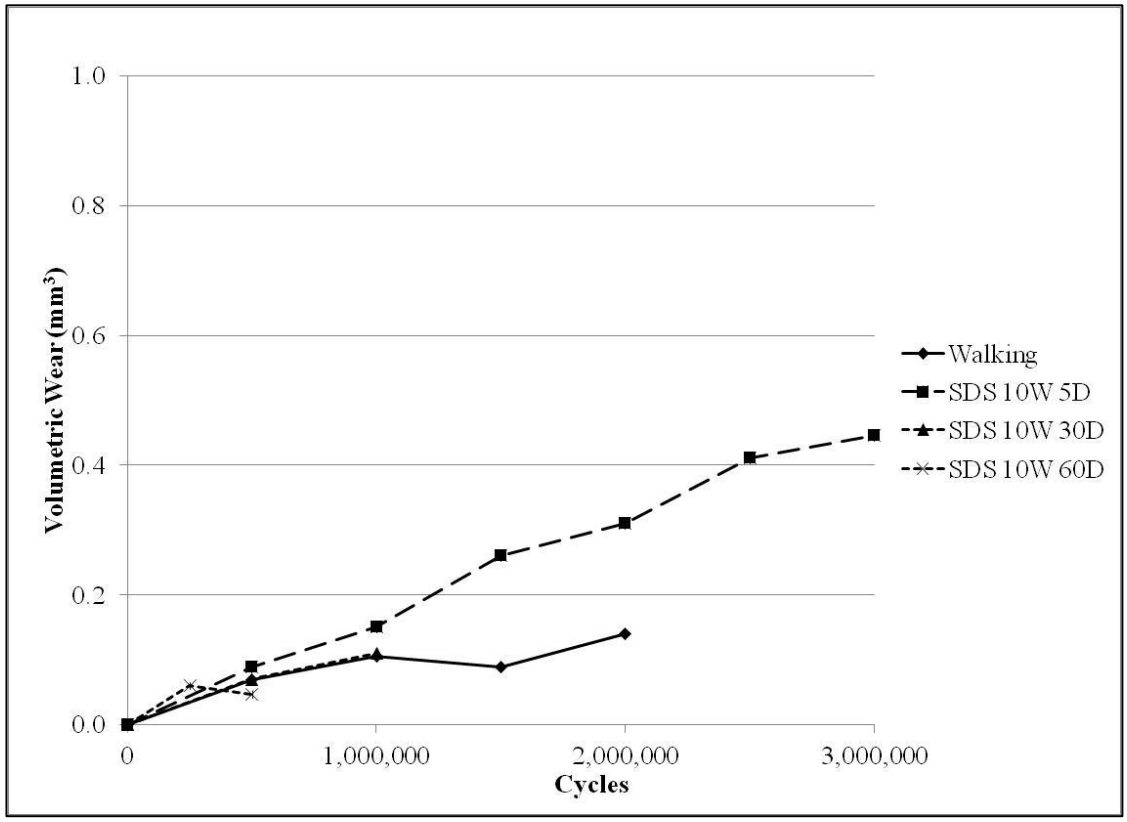

Figure 54: Cumulative mean volumetric wear of 36mm MOM under SDS conditions comparing three different dwell periods of 5s, 30s and 60s

Mean volumetric wear rates for the 5s, 30s and 60s dwell period tests were 0.15±0.15mm^3/mc, 0.19±0.11mm^3/mc and 0.09±0.02mm^3/mc respectively. Due to the different test durations, to allow simple comparison these were calculated over the first 1mc of the test. The SDS 10W 60D test was only run for 0.5mc, therefore the wear rate was extrapolated to 1mc for comparison with the other data sets.

Results for all three tests were compared with the wear rate for samples under standard walking conditions presented in Chapter 3. The wear rate for the standard walking test from 0-1mc was 0.11±0.08mm^3/mc. There was no significant difference between the wear rate under standard walking conditions and any of the SDS conditions examined here.

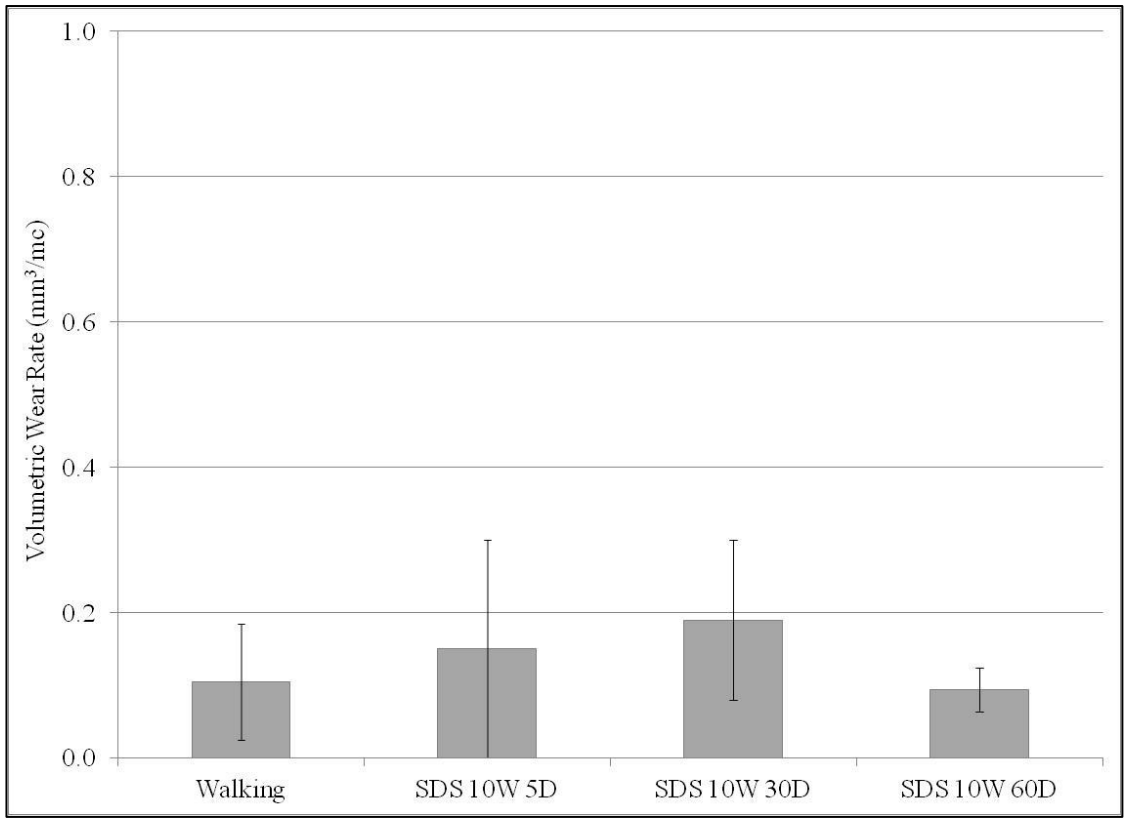

Figure 55: Mean volumetric wear of 36mm MOM under SDS conditions (±95% confidence limits)

Walking: **0-1mc, n=9**

SDS 10W 5D: **0-1mc, n=9**

SDS 10W 30D **0-1mc, n=9**

SDS 10W 60D **0-0.5mc, n=10**

4.4 Discussion

4.4.1 SDS Protocol Development

This chapter describes the development of three new protocols for stop-dwell-start (SDS) wear simulation for total hip replacements. The wear of 36mm diameter MOM bearings was examined under these conditions and compared with *in vitro* wear behaviour under standard walking conditions as described in Chapter 3. The focus of the study was to evaluate the effect of the dwell duration in an SDS protocol.

Data from the literature was used to identify typical activity of real patients and generate simulator profiles. A degree of compromise was necessary to adapt patient activity into simulator inputs. With respect to test frequency, measurements indicated the average walking frequency in THA patients was 1.7Hz (Morlock et al., 2001), whereas the standard walking simulation was specified to run at 1Hz (International Standards Organisation, 2002). Limited studies exist in the literature examining the effect of a change in frequency on the wear of THR *in vitro*, however indications are that an increased frequency may cause an increase in wear (Kamali et al., 2010). It was desirable to minimise additional variables in the present study which may have confounded with the primary area of interest of the SDS protocols, therefore it was decided to maintain the ISO recommended frequency of 1Hz for this study.

The frequency of dwell periods, or number of steps between dwells, was also a critical factor in the testing. Patient measurements in the literature indicated patients paused every 20 steps or 12s of motion, however high variability between different patients was reported in this data (Morlock et al., 2001). The motion sequence of 10 steps between dwells used in this study was slightly lower than the mean values reported in real patients but remained within one standard deviation of the mean. This allowed a simplified test protocol while maintaining clinical relevance in the simulator inputs.

Three dwell durations were selected for evaluation in this study; as before, these inputs were primarily derived from patient measurements in the literature. Dwell durations of 5s, 30s and 60s were examined for their effect on bearing wear. The shortest duration of 5s was clinically relevant, being the most frequently occurring reported duration of pause in patients (Morlock et al., 2000). The longer durations of 30s and 60s were also shown to occur in real patients albeit less frequently.

It was hypothesised that introduction of a pause into a wear test would increase *in vitro* wear, due to interruption of the squeeze film action retaining lubricant in the bearing during the walking cycle and depletion of the thickness of the squeeze film during the dwell period, leading to sub-optimal lubrication conditions when motion re-starts. This was supported by an increase in wear reported in some SDS tests in the literature (Medley et al., 2002). The Hamrock and Dowson equation presented in Chapter 1 also supports this hypothesis. As entraining velocity between the components tends to zero, the lubricant film thickness will also reduce, leading to greater asperity contact and potentially increased wear.

It was also hypothesised that an increase in the duration of the pause would increase wear further. Studies in the literature have shown that friction in the bearing increases with pause duration (Wimmer et al., 2001); the Stribeck curve presented in Chapter 1 indicates that with increasing friction and a lower entraining velocity, the lubrication regime will deteriorate towards the boundary end of the spectrum, potentially leading to an increase in wear.

Kinematic and kinetic inputs for the dwell period were again derived from patient data in the literature (Morlock et al., 2000). This data showed that patients pause more frequently in a sitting position compared with a standing position. Early trials to introduce a sitting pause into a walking test on the simulator used in this study highlighted a number of limitations in motor response, meaning that a transition to a sitting position with the hip flexed to approximately 60^{o} would take several seconds longer than a pause in a standing position and caused undesirable interruptions to the test.

The current study was run with all dwell periods in a standing position with both motion axes at 0^{o}, however it was also recognised that positioning of the bearing components during the dwell may have an effect on wear. A distinct wear scar is evident on both components in the contact region as described previously, and coincides with an area of altered surface roughness and geometry on the bearing. When the wear simulation is paused in a standing position these wear scars will be coincident, whereas in a sitting position the scar on the femoral head will be oriented posteriorly. These different relative positions may have an effect on tribological conditions at the contact region during a pause, due to different equivalent radii and composite surface roughness in the contact zone, and thus have a subsequent effect on wear. Equipment limitations

restricted this test to applying a pause in a standing position, however the effect of different positions would be of interest in future studies.

4.4.2 SDS Wear Simulation

All tests in this chapter were undertaken on 36mm MOM total hip replacements identical to those used in Chapter 3. All samples were geometrically characterised prior to testing. The radius of curvature of the femoral heads was found to be slightly greater in the polar region than the equatorial region; it is believed this variation is caused during polishing of the head in manufacturing, however all parts were within drawing and manufacturing specifications (DePuy International DWG-136553000 (Internal confidential drawing)).

Head and cup samples were paired to achieve minimal variation in polar clearance between stations to eliminate bearing clearance as a test variable. Individual and mean clearances for each test are described in the Results section of this Chapter, however all polar clearances were approximately 68µm with 95% confidence limits of less than 1µm.

Wear of 36mm MOM bearings under all three SDS protocols was not found to be statistically different from wear under standard walking conditions. Equivalent wear rates from 0-1mc for the Walking, SDS 10W 5D, SDS 10W 30D and SDS 10W 60D tests were $0.11\pm0.08mm^3$/mc, $0.15\pm0.15mm^3$/mc, $0.19\pm0.11mm^3$/mc and $0.09\pm0.02mm^3$/mc respectively.

Several simulator breakdowns were encountered during this study. This was attributed largely to the simulator being designed to a unique specification and was the first of its type to be manufactured. These early failures were all addressed by the manufacturers during the course of this study. The breakdown at 0.85mc in the SDS 10W 5D test was caused by a software malfunction. During repair it was necessary to run trials with the test samples *in situ* to ensure loads were being applied correctly. A further malfunction during these trials caused accidental application of extremely high loads and flexion angles to the simulator. Several samples were severely damaged and some fixtures and spigots badly bent. An additional gravimetric analysis point had been taken prior to the repair trials to characterise the samples; a further point was taken immediately after, and four stations exhibiting high wear which could be directly attributed to the simulator

breakdown were removed from the test and replaced by dummy samples as described previously.

The six remaining stations did not exhibit significant volumetric material loss at the time of the simulator breakdown, however some did present with significantly higher wear rates on subsequent measurement points (Figure 30, Stations 4 & 5). One of the new samples introduced to replace the damaged stations also exhibited higher wear (Figure 46, Station 9). Simulator load cell logs were examined to find a possible cause for this high wear and no anomalies were found. It is believed this high wear may have been due to damage caused to the fixtures during the simulator breakdown which was not identified at the time. At the end of the SDS 10W 5D test all fixtures were exchanged for new components, and no subsequent effect was observed on the SDS 10W 30D and SDS 10W 60D tests. It would have been ideal to repeat the SDS 10W 5D test however restricted resources and time prevented this.

The SDS 10W 5D test was also used to evaluate the effect on wear of pre bedding-in of samples prior to an SDS test. Half of the samples tested were taken from the standard walking test described in Chapter 3, where they had previously undergone 2mc of standard walking and were exhibiting typically low steady state wear rates. The other five samples for the current test were new with no previous wear. The wear behaviour of the new and pre-worn samples were not statistically different in the early stage of the test from 0-1mc, however from 1-3mc a significant difference was observed.

It would be expected that the pre-worn samples would wear at a lower rate than the new samples in the early stages of the test, due to the effects of bedding in optimising bearing conformity and reducing wear. Improved bearing conformity and lower contact stress gives rise to a larger effective bearing radius and lubricant film thickness in the contact zone, thereby reducing wear. In this test however both sample sets appear to wear at a similar rate to the bedding in phase of the walking test described in Chapter 3. The pre-worn samples which previously exhibited lower steady state wear now exhibited an increased wear rate under the SDS conditions. These results suggest that under SDS conditions the entraining velocity has a more dominant effect over film thickness than relative radius of the bearings.

The wear behaviour of the pre-worn and new samples was significantly different from 1mc onwards. This difference was dominated by the three stations believed to have

damaged fixtures: Stations 3, 4 and 5. It is believed that had these stations not been damaged, the volumetric wear from pre-worn and new samples would have been statistically similar throughout the test. This test indicated that pre-worn parts do not perform significantly differently to new samples, therefore it was considered acceptable to reuse components for subsequent tests.

In summary, no significant difference was observed between wear performance of 36mm MOM bearings under standard walking or SDS conditions. Pre-worn parts performed similarly to new components. These findings contradict some earlier SDS studies which demonstrated increased wear (Chan, Bobyn, Medley, and Krygier, 1999; Medley et al., 2002), however are in agreement with other studies which found no increase in wear under SDS conditions (Liao et al., 2004). The primary difference between these studies was the load applied during the dwell phase. In the studies reporting an increased wear rate under SDS conditions a dwell load of 3kN was used, whereas the Liao study used a dwell load of 1250N in common with the present work. The lower dwell load is more clinically relevant and derived from patient data, however it is unlikely a patient would be exerting a peak load of 3kN through the hip when stationary. All of the earlier studies differed significantly from the current work in that long dwell periods of around a minute were used, and interspersed with long walking periods of 5-10 minutes. Patient measurements in the literature suggest this is not very clinically relevant (Morlock et al., 2000, 2001). No earlier studies have been found in the literature which applied shorter dwell and walking periods as in the present study.

The hypothesis at the commencement of this study predicted that the introduction of dwell periods would increase wear of MOM bearings. These results found in the study do not support the hypothesis; under all SDS conditions wear was similar to rates measured under the bedding in phase of a standard walking test. No reduction of wear rate from a bedding in to steady state phase was observed in any of the SDS tests. It is important to note that the application of the dwell period and variation in the dwell period, with an applied load of 1250N, as used in this study, did not produce a statistically significant increase in wear that could be detected by the methods adopted in this study. The SDS wear rates of less than $0.2mm^3$/mc were of a similar order to the bedding in wear rate under normal walking reported in Chapter 3 and other published wear rates (Goldsmith et al., 2000).

The lubrication behaviour of MOM bearings under start up conditions has been modelled previously, and results suggest that although the lubricant film does deteriorate during a dwell, the film is restored very swiftly, in two or three steps after motion restarts (Jalali-Vahid et al., 2006). This may explain the results in the current study. It is postulated that the lubricant film was disrupted during the dwell, but irrespective of the dwell duration the bearing returns to optimal lubrication conditions two or three steps after motion restarts. While wear in the bearing may be higher in those two or three steps, when averaged out across ten steps, where most were exhibiting normal wear, the overall wear rate of the bearing appeared not to be statistically different from standard walking, given the variation and confidince limits of the wear rate data.

4.5 Conclusion

The wear of 36mm MOM total hip replacements was examined under three newly proposed simulator protocols for stop-dwell-start (SDS) conditions. These tests introduced a dwell period every ten steps of a standard walking cycle. Three dwell durations of 5s, 30s and 60s were evaluated. The load during the dwell was 1250N for all tests. No significant increase in wear under SDS conditions was observed for any of the tests. In all three tests wear was similar to that of identical bearings during the bedding in phase of a standard walking test, as demonstrated in Chapter 3. No reduction in wear to a steady state level was observed during any of the SDS tests. It was postulated there was some effect on tribological conditions in the bearing caused by the SDS tests, however this effect only lasts for a few walking cycles after each dwell and the effect was therefore not measurable in this study.

CHAPTER 5. WEAR OF 36MM METAL-ON-METAL TOTAL HIP REPLACEMENTS UNDER STOP-DWELL-START CONDITIONS – EFFECT OF WALKING DURATION

5.1 Introduction

This chapter describes development and application of a protocol for clinically relevant stop-dwell-start (SDS) type wear simulation, and the effect of this activity on the wear of 36mm MOM total hip replacements. In particular it describes the investigation of the effect of the frequency of dwell periods, or the number of walking steps between each dwell.

In the previous study in Chapter 4 it was shown that introduction of a dwell period every ten walking steps did not cause a statistically significant increase in bearing wear compared with wear under standard walking conditions, irrespective of the duration of the dwell. The results were attributed to the dwell period only potentially increasing wear rates over two or three steps following the pause, after which time the wear rate returns to normal, therefore overall average wear rates were similar to those for walking tests.

This chapter describes an alteration of the SDS protocol to maintain a fixed dwell period, but reduce the number of cycles between the dwells to test the conclusions of the preceding chapter. It was hypothesised that as the number of walking cycles between each dwell period was reduced, wear would increase.

5.2 Methods and Materials

5.2.1 Hip Simulator

Ten 36mm Pinnacle MOM total hip replacements from DePuy International (UK) were used for this study (DePuy International, Product code 136553000, DWG-136553000 (Internal confidential drawing)). Each individual component was assigned a unique reference number for identification in the format yy_xxxx, where yy represents the year of initial sourcing of the parts, and xxxx is a unique identifier assigned consecutively.

The samples were prepared and mounted as described in Chapter 2. A standard walking wear test adapted from ISO 14242-1:2002 (International Standards Organisation, 2002) was used for the basis of the SDS test. Load was applied to the components in a twin peak Paul-type waveform with a peak load of 3kN and swing phase load of 300N. Flexion / extension and internal / external rotation were applied in a sinusoidal waveform over +30º/-15º and ±10º respectively, as described in Chapter 2. This cycle was applied at a frequency of 1Hz.

5.2.2 Stop-dwell-start (SDS) Protocol

The SDS conditions were created by introducing a dwell period into the standard walking test at regular intervals. Three SDS tests were run in this study, using two protocols. One of the protocols was repeated on both new and pre-worn implants. The tests are detailed in Table 12. Dwell kinematics and load remained constant for all three tests, as did the dwell duration, which was fixed at 10s. The number of steps between dwell periods was varied for each of the tests, with one-step and two-step walking sequences evaluated. All tests were each run for a minimum of 0.5mc. Longer tests were not possible due to the extended period of time these tests took to run.

Table 19: Test run order for effect of dwell duration study

Test	Nomenclature	n
1s walking, 10s dwell (0.5mc, pre-worn samples)	SDS 1W 10D (WORN)	10
1s walking, 10s dwell (0.6mc, new samples)	SDS 1W 10D (NEW)	10
2s walking, 10s dwell (0.5mc, pre-worn samples)	SDS 10W 60D	10

A nomenclature was used to aid with identification of parameters for each test. Every SDS test was identified using the format SDS xW yD where x denotes the number of

walking cycles between dwell periods, and y indicates the duration in seconds of each dwell period, therefore SDS 1W 10D was a test where one walking step was followed by a 10s dwell in a repeated loop.

When counting cycles on multi profile stop start tests, only cycles where the walking cycle was running were counted for the purposes of calculating wear rates, on the assumption that no wear would occur during the dwell period, as no motion is present. If the dwell cycles had been included this would incorrectly have deflated the final calculated wear per cycle.

5.2.3 Geometric Analysis

All samples were measured using CMM prior to testing to define sample diameter and bearing clearance. The Zygo CMM was used for these measurements as described in Chapter 2.

5.2.4 Gravimetric Analysis

All samples were weighed following cleaning using the techniques described in Chapter 2 throughout the test. All samples were weighed at 0 cycles, 50,000 cycles, 100,000 cycles and every 100,00 cycles thereafter. The SDS 1W 10D (Worn) and SDS 2W 10D tests did not have measurement intervals at 400,000 cycles; the tests were run through from 300,000 to 500,000 cycles without measurement.

5.2.5 Surface Roughness Analysis

Surface roughness measurements of the samples from the SDS 1W 10D (New) test were taken after testing only, following the procedure described in Chapter 2. Chapter 3 describes the alteration necessary to the surface roughness measurement of acetabular cups whereby measurements were taken at 35º from the pole, and coincident with the wear scar rather than directly at the pole. That measurement technique was duplicated for this study.

5.3 Results

5.3.1 Effect of Single Step Gait on Pre-worn Samples

A wear simulation was run for 0.5 million cycles (mc) on 36mm MOM hip bearings applying an SDS 1W 10D protocol. This incorporated 1 cycle of standard walking conditions at 1Hz followed by a ten second dwell.

5.3.1.1 Geometric Analysis

The samples for the SDS 1W 10D test were taken from the SDS 10W 60D test and were hence pre-worn. The acetabular components were found to have a mean diameter of 36.085±0.001mm (±95% confidence interval) with a mean form of 0.005±0.002mm. The femoral head polar diameter and form were 36.017±0.001mm and 0.003±0.002mm respectively. Mean polar clearance was 67.954±0.615µm (Chapter 4 Table 18).

5.3.1.2 Gravimetric Analysis

Individual and mean wear for samples tested under the SDS 1W 10D test are presented in Figure 56 and Figure 57. Mean overall wear at 0.5mc was 0.77±0.29mm^3. Wear appeared to be bi-phasic (Figure 57) with a higher rate of wear from 0-200,000 cycles (2.96±1.12mm^3/mc) than from 200,000 to 500,000 cycles (0.59±0.36mm^3/mc) (Figure 58). The difference between these wear rates was statistically significant (P=0.001, Paired T-test).

Wear under the SDS 1W 10D (Worn) test conditions was compared with wear under standard walking conditions from 0-1mc, i.e. the bedding in phase. There was a significant difference between the wear under standard walking conditions and wear in the high wearing phase of the SDS 1W 10D (Worn) test from 0 to 200,000 cycles at the 5% significance level (P=0.000, T-test). Wear in the second, lower wearing phase of the SDS 1W 10D (Worn) test from 200,000 to 500,000 cycles was also significantly greater than wear under standard walking conditions during the bedding in phase (P=0.011, T-test).

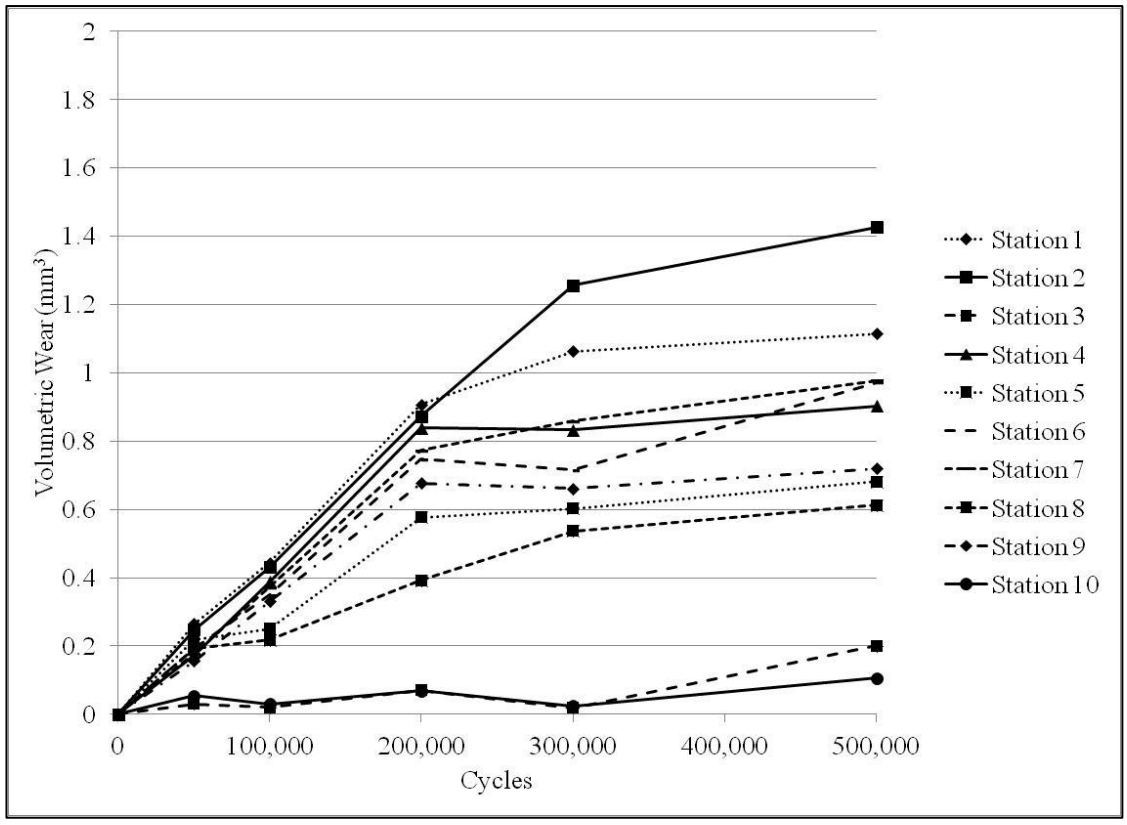

Figure 56: Cumulative individual volumetric wear of 36mm MOM under SDS 1W 10D (Worn) protocol

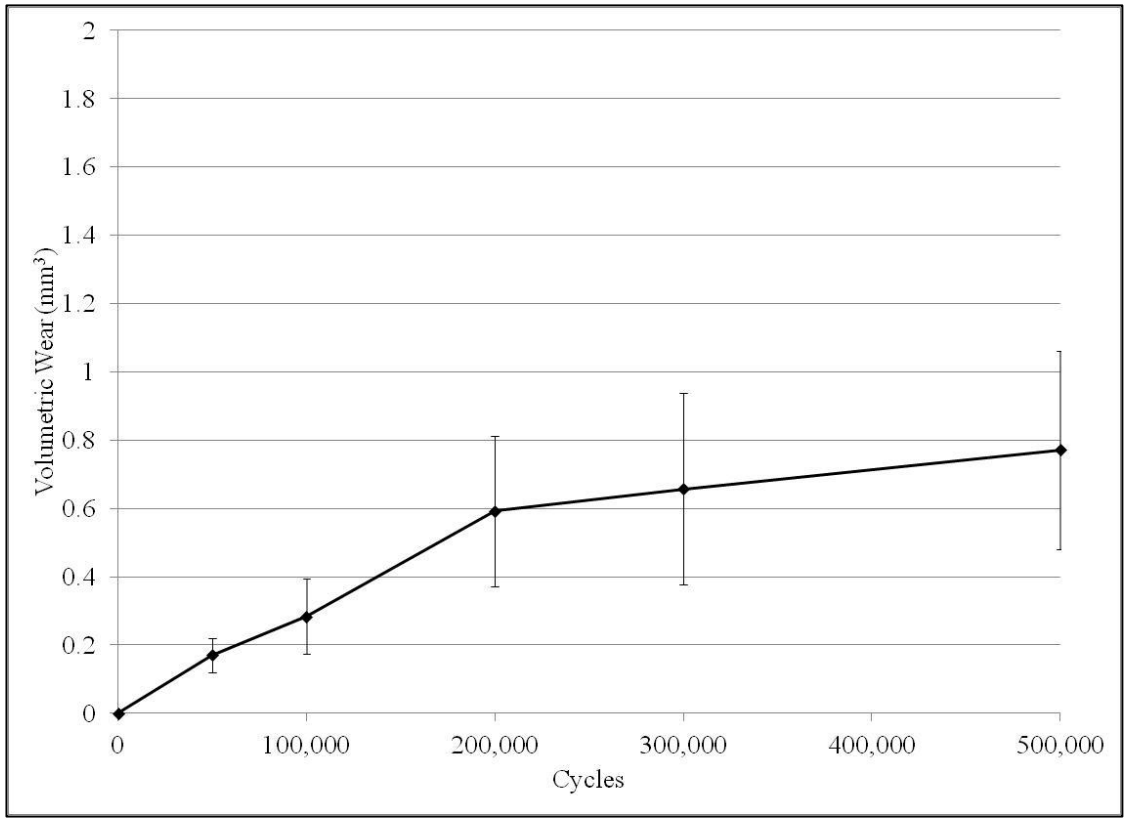

Figure 57: Cumulative mean volumetric wear of 36mm MOM under SDS 1W 10D (Worn) protocol (n=10, ±95% confidence limits)

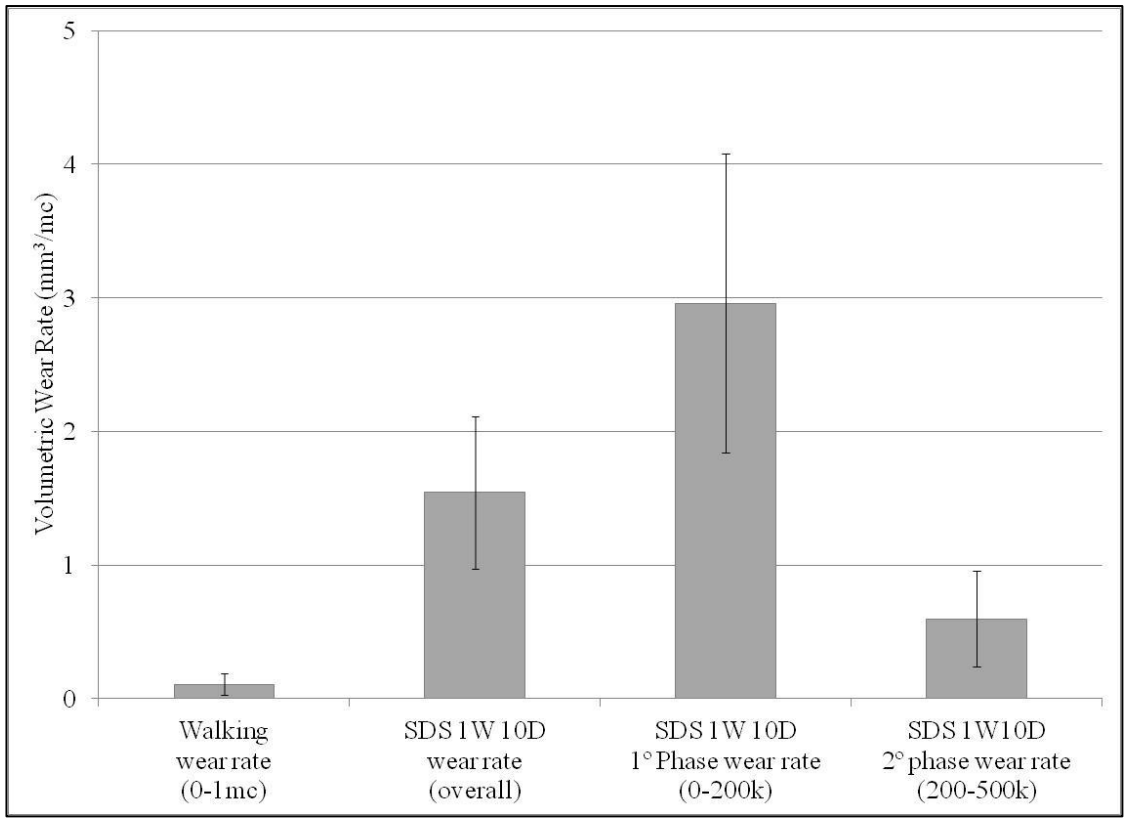

Figure 58: Mean volumetric wear rate of 36mm MOM under SDS 1W 10D protocol compared with standard walking conditions (Walking n=9, SDS n=10, ±95% confidence limits)

5.3.2 Effect of Single Step Gait on New Samples

The SDS 1W 10D test was repeated on a new set of ten unworn 36mm MOM bearings. This test was run for 0.6mc. As before, the test incorporated 1 cycle of standard walking conditions at 1Hz followed by a ten second dwell.

5.3.2.1 Geometric Analysis

All samples for the SDS 1W 10D test were new and previously untested. The acetabular components were found to have a mean diameter of 36.091±0.001mm (±95% confidence interval) with a mean form of 0.005±0.001mm (Table 20).

The femoral heads had a mean global diameter of 36.005±0.003mm with a mean sphericity of 0.012±0.002mm (Table 21). The femoral head polar diameter and form were 36.029±0.004mm and 0.005±0.008mm respectively. The femoral head equatorial diameter and form were 36.002±0.003mm and 0.006±0.002mm respectively.

As discussed in Chapter 3, the difference between polar and equatorial geometry can have an effect on bearing wear *in vitro*, therefore samples were paired using polar geometry, as with the Walking test described in Chapter 3. Mean polar clearance was 62.026±7.675µm (Table 22).

Table 20: CMM results for SDS 1W 10D (New) acetabular components prior to testing

Station	Sample No.	Diameter (mm)	Form (mm)
1	**08_1436**	36.090	0.007
2	**08_1422**	36.091	0.004
3	**08_1469**	36.091	0.009
4	**08_1446**	36.091	0.003
5	**08_1428**	36.092	0.004
6	**08_1463**	36.092	0.003
7	**08_1456**	36.089	0.004
8	**08_1429**	36.089	0.005
9	**08_1420**	36.095	0.004
10	**08_1421**	36.092	0.006
Average		36.091	0.005
95% Confidence		0.001	0.001

Table 21: CMM results for SDS 1W 10D (New) femoral components prior to testing

Station	Sample No.	Global Diameter (mm)	Global Sphericity (mm)	Polar Diameter (mm)	Polar Sphericity (mm)	Equatorial Diameter (mm)	Equatorial Sphericity (mm)
1	**08_1512**	36.006	0.007	36.025	0.008	36.005	0.004
2	**08_1516**	36.004	0.009	36.025	0.002	36.002	0.005
3	**08_1499**	36.007	0.007	36.025	0.002	36.005	0.004
4	**08_1498**	36.002	0.010	36.025	0.003	36.000	0.006
5	**08_1517**	36.001	0.011	36.025	0.002	35.999	0.006
6	**08_1511**	36.002	0.012	36.027	0.004	35.999	0.008
7	**08_1505**	36.008	0.022	36.033	0.006	36.001	0.008
8	**08_1507**	36.008	0.008	36.047	0.005	35.998	0.005
9	**08_1509**	36.009	0.016	36.048	0.005	36.005	0.004
10	**08_1483**	36.004	0.019	36.013	0.015	36.003	0.006
Average		36.005	0.012	36.029	0.005	36.002	0.006
95% Confidence		0.003	0.002	0.004	0.008	0.003	0.002

Table 22: Calculated clearance between head and cup for global, polar and equatorial geometries for SDS 1W 10D (New) components prior to testing

Station	Global clearance (µm)	Polar clearance (µm)	Equatorial clearance (µm)
1	83.890	65.381	85.456
2	86.972	66.136	88.838
3	84.075	66.258	85.647
4	89.556	66.214	91.053
5	91.073	66.821	93.033
6	90.464	65.083	92.771
7	81.048	56.048	88.595
8	81.576	42.476	90.813
9	86.089	46.789	89.635
10	88.357	79.057	89.786
Average	86.310	62.026	89.563
95% Confidence	2.569	7.675	1.844

5.3.2.2 Gravimetric Analysis

Individual and mean wear for samples tested under the SDS 1W 10D (New) test are presented in Figure 59 and Figure 60. Mean overall wear at 0.6mc was 1.11±0.26mm^3. Wear appeared to occur in three phases (Figure 60) with a lower rate of wear from 0 to 100,000 and 400,000 to 600,000 cycles and a higher rate from 100,000 to 400,000 cycles.

The mean wear rate from 0 to 100,000 cycles was 0.53±1.00mm^3/mc. This was compared with the mean wear rate during the bedding in phase of a standard walking test (Chapter 3) and no significant difference was found between the rates (P=0.375, T-test).

The second wear phase of the SDS 1W 10D (New) test exhibited a higher wear rate between 100,000 and 400,000 cycles of 3.35±0.49mm^3/mc. This was found to be significantly greater than both the bedding phase of the standard walking test (P=0.000, T-test) and the SDS 1W 10D (New) test from 0 to 100,000 cycles (P=0.000, T-test).

The wear rate during the third wear phase of the SDS 1W 10D (New) test was again lower at 0.24±0.33mm^3/mc. This was significantly lower than the secondary wear phase (P=0.000, T-test), but did not differ significantly from the primary phase (P=0.541, T-test) or walking bedding in phase wear rates (P=0.469, T-test).

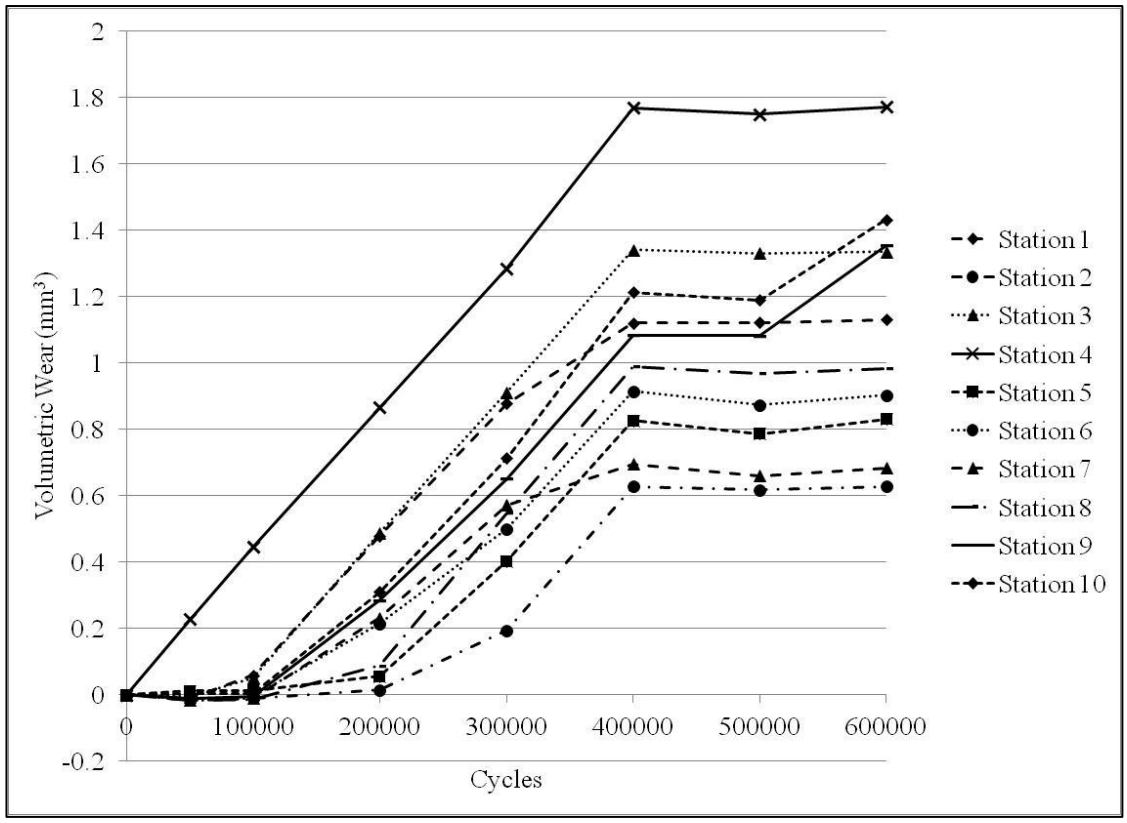

Figure 59: Cumulative individual volumetric wear of 36mm MOM under SDS 1W 10D (New) protocol

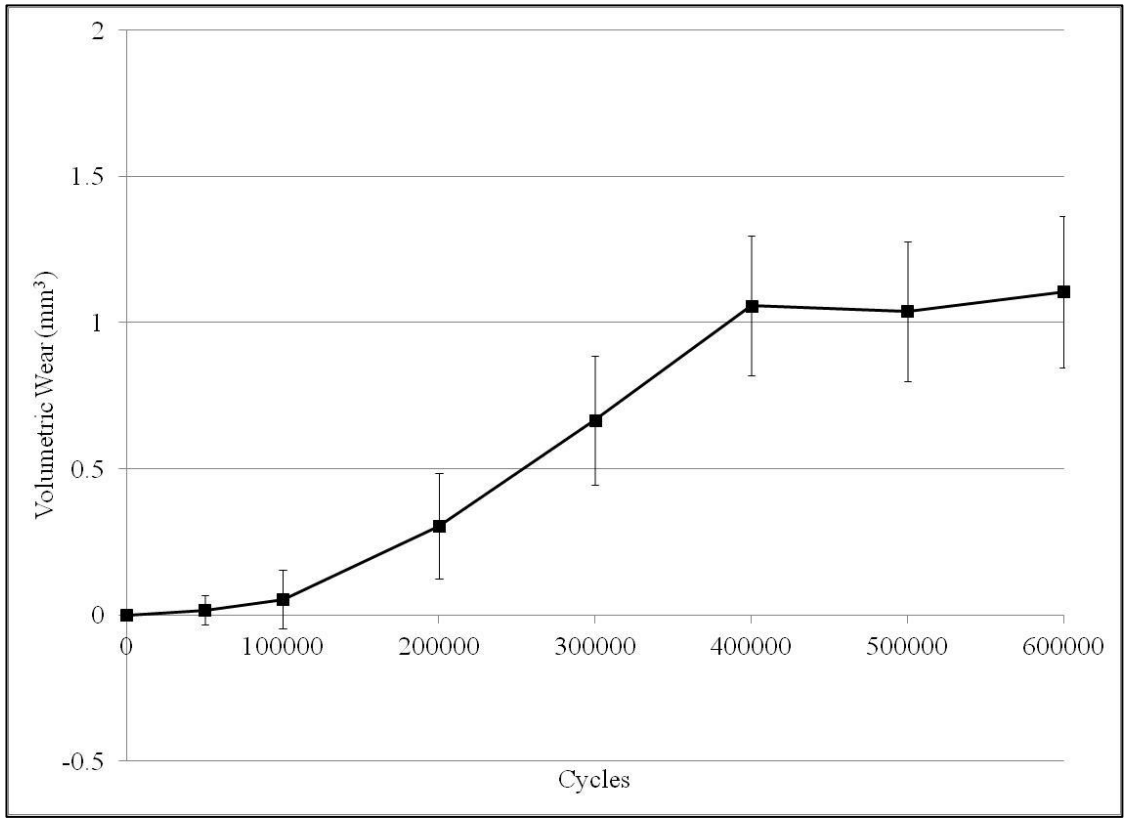

Figure 60: Cumulative mean volumetric wear of 36mm MOM under SDS 1W 10D (New) protocol (n=10, ±95% confidence limits)

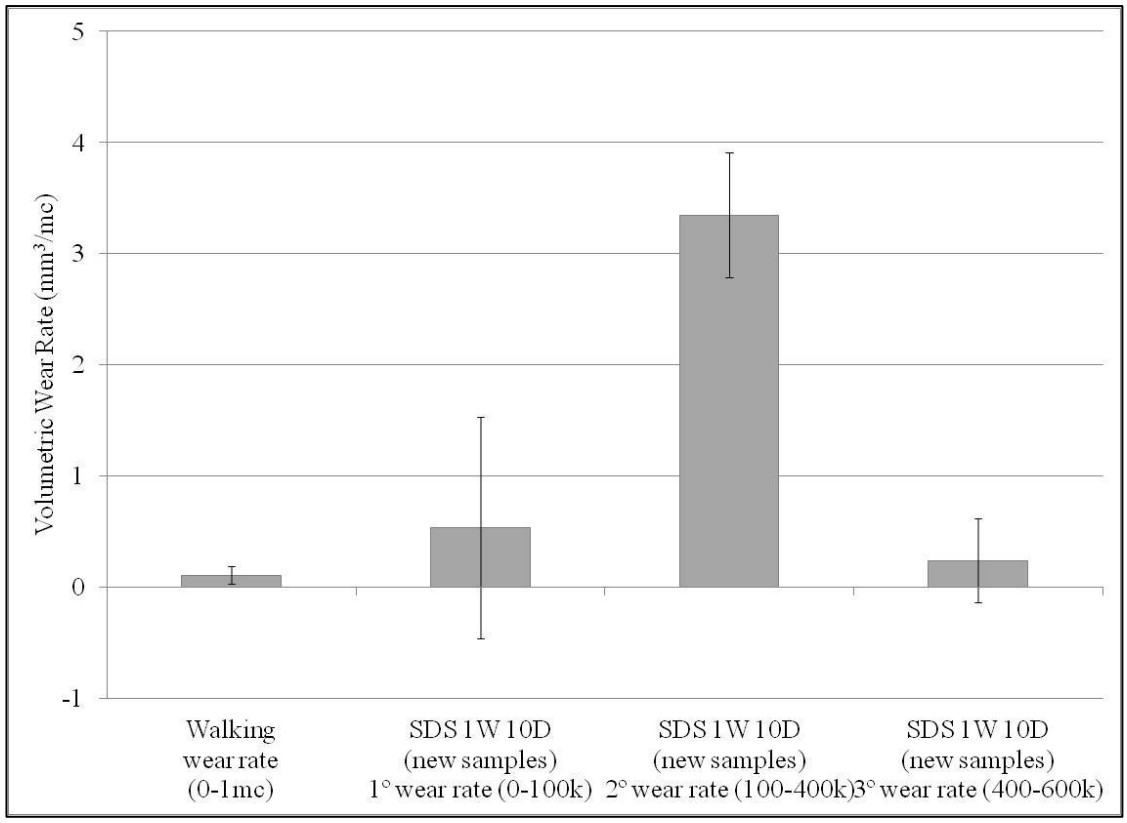

Figure 61: Mean volumetric wear rates of 36mm MOM under SDS 1W 10D (New) protocol compared with wear rates under standard walking conditions during the bedding in phase (n=10, ±95% confidence limits)

5.3.3 Effect of Double Step Gait

5.3.3.1 Geometric Analysis

Ten 36mm MOM bearing pairs were used in the SDS 2W 10D test. Five of the sample pairs were taken from the SDS 1W 10D (Worn) test, and hence were pre-worn components, while five bearing pairs were new. The acetabular components were found to have a mean diameter of 36.087±0.001mm (±95% confidence interval) with a mean form of 0.005±0.002mm (Table 23).

The femoral heads had a mean global diameter of 36.002±0.003mm with a mean sphericity of 0.009±0.002mm (Table 24). The femoral head polar diameter and form were 36.019±0.001mm and 0.004±0.003mm respectively. The femoral head equatorial diameter and form were 36.000±0.002mm and 0.006±0.002mm respectively.

As discussed in Chapter 3, the difference between polar and equatorial geometry can have an effect on bearing wear *in vitro*, therefore samples were paired using polar geometry, as with the Walking test described in Chapter 3. Mean polar clearance was 67.311±0.611µm (Table 25).

Table 23: CMM results for SDS 2W 10D acetabular components prior to testing

Station	Sample No.	Diameter (mm)	Form (mm)
1	**08_1460**	36.080	0.009
2	**08_1452**	36.089	0.004
3	**08_1440**	36.087	0.006
4	**08_1441**	36.083	0.002
5	**08_1454**	36.088	0.003
6	**08_1438**	36.088	0.003
7	**08_1461**	36.087	0.003
8	**08_1432**	36.089	0.004
9	**08_1431**	36.088	0.008
10	**08_1448**	36.087	0.003
Average		36.087	0.005
95% Confidence		0.001	0.002

Table 24: CMM results for SDS 2W 10D femoral components prior to testing

Station	Sample No.	Global Diameter (mm)	Global Sphericity (mm)	Polar Diameter (mm)	Polar Sphericity (mm)	Equatorial Diameter (mm)	Equatorial Sphericity (mm)
1	**08_1475**	36.001	0.008	36.012	0.006	36.000	0.005
2	**08_1501**	36.004	0.010	36.022	0.009	36.002	0.007
3	**08_1481**	35.999	0.010	36.019	0.003	35.996	0.007
4	**08_1489**	36.000	0.008	36.014	0.003	35.998	0.007
5	**08_1492**	36.000	0.010	36.022	0.003	35.998	0.007
6	**08_1514**	36.004	0.007	36.021	0.001	36.003	0.004
7	**08_1496**	36.004	0.007	36.020	0.002	36.003	0.004
8	**08_1513**	36.004	0.009	36.023	0.001	36.003	0.006
9	**08_1500**	36.006	0.007	36.021	0.003	36.004	0.005
10	**08_1490**	36.000	0.009	36.019	0.003	35.998	0.006
Average		36.002	0.009	36.019	0.004	36.000	0.006
95% Confidence		0.003	0.002	0.001	0.003	0.002	0.002

Table 25: Calculated clearance between head and cup for global, polar and equatorial geometries for SDS 2W 10D components prior to testing

Station	Global clearance (µm)	Polar clearance (µm)	Equatorial clearance (µm)
1	78.704	68.333	79.997
2	85.097	66.117	86.997
3	88.090	68.040	90.122
4	82.549	68.416	84.303
5	79.681	67.122	80.904
6	83.920	66.754	85.491
7	83.217	67.717	84.165
8	84.500	66.269	86.172
9	82.278	66.575	83.892
10	87.088	67.762	89.254
Average	83.512	67.311	85.130
95% Confidence	2.102	0.611	2.312

5.3.3.2 Gravimetric Analysis

Individual and mean wear for samples tested under the SDS 2W 10D test are presented in Figure 62 and Figure 63. Mean overall wear at 0.5mc was 0.27±0.19mm3, which was extrapolated to give a wear rate of 0.54±0.38mm^3/mc.

Wear under the SDS 2W 10D protocol was compared with wear under standard walking conditions during the bedding in phase (0-1mc). Wear under SDS conditions was shown to be significantly higher than during a standard walking test (P=0.028, T-test).

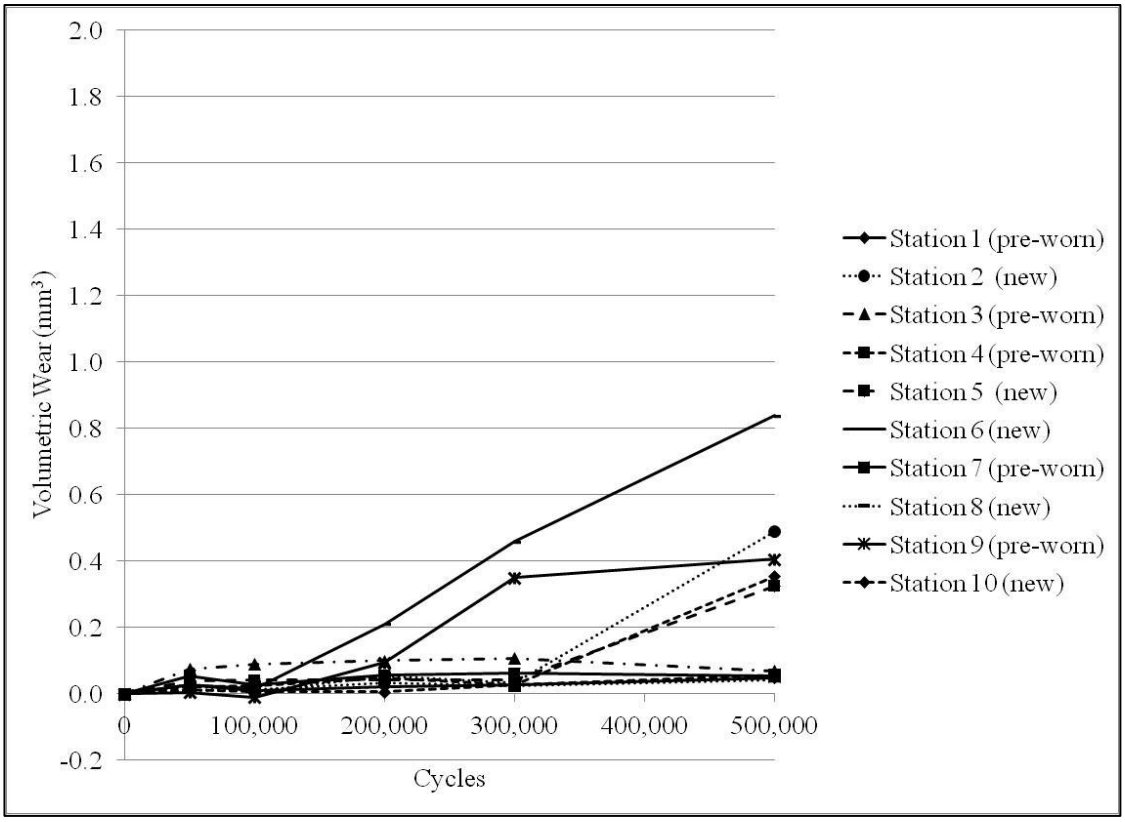

Figure 62: Cumulative individual volumetric wear of 36mm MOM under SDS 2W 10D protocol

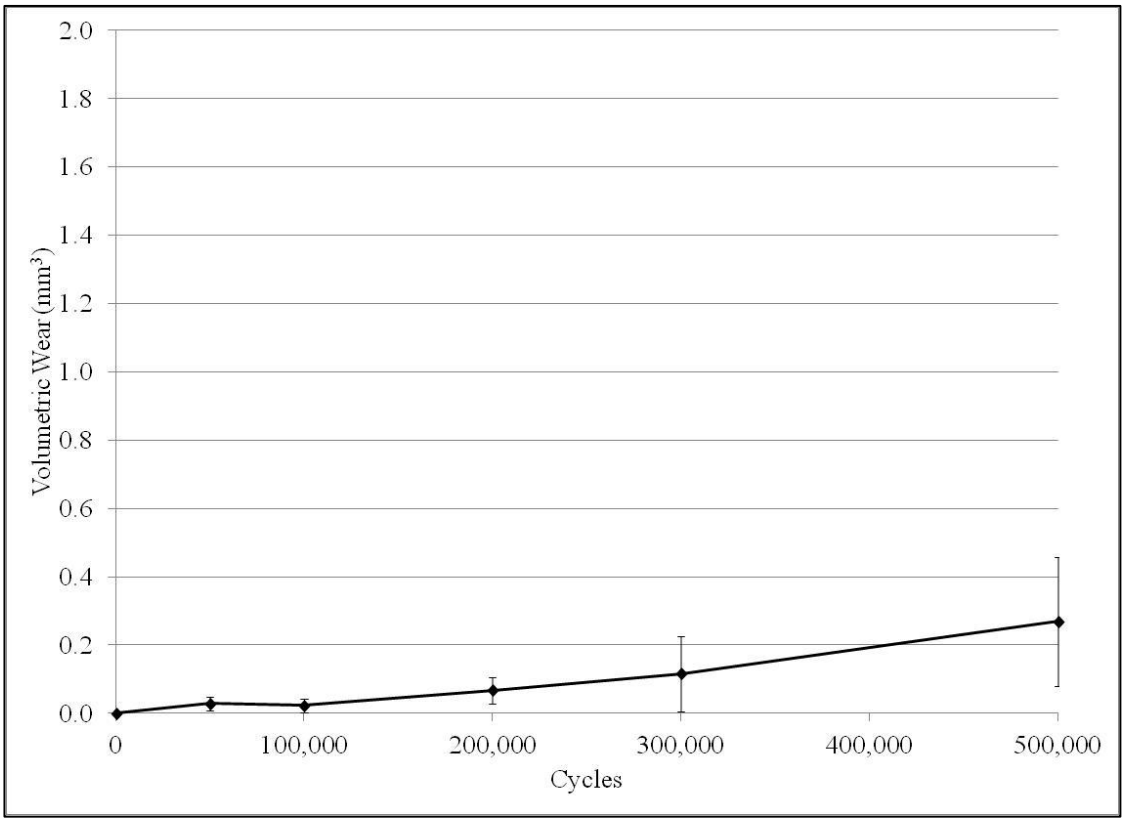

Figure 63: Cumulative mean volumetric wear of 36mm MOM under SDS 2W 10D protocol (n=10, ± 95% confidence limits)

5.3.4 Comparison of Pre-Worn and New Samples under SDS Conditions

The results from the SDS 1W 10D (Worn) and SDS 1W 10D (New) tests were compared up to 0.5mc. Overall mean wear for both tests is presented in Figure 64. Overall mean wear rates were calculated for each test (Figure 65). There was found to be no significant difference between the overall wear rates of worn (1.54±0.57mm^3/mc) and new samples (1.84±0.43mm^3/mc) under SDS 1W 10D conditions (P=0.369, T-test).

Similarly, the wear behaviour of pre-worn and new samples from the SDS 2W 10D test was compared (Figure 66). The overall mean wear rates of the worn and new samples were 0.25±0.39mm^3/mc and 0.82±0.72mm^3/mc respectively (Figure 67); there was no significant difference between these groups at the 5% significance level (P=0.091, T-test).

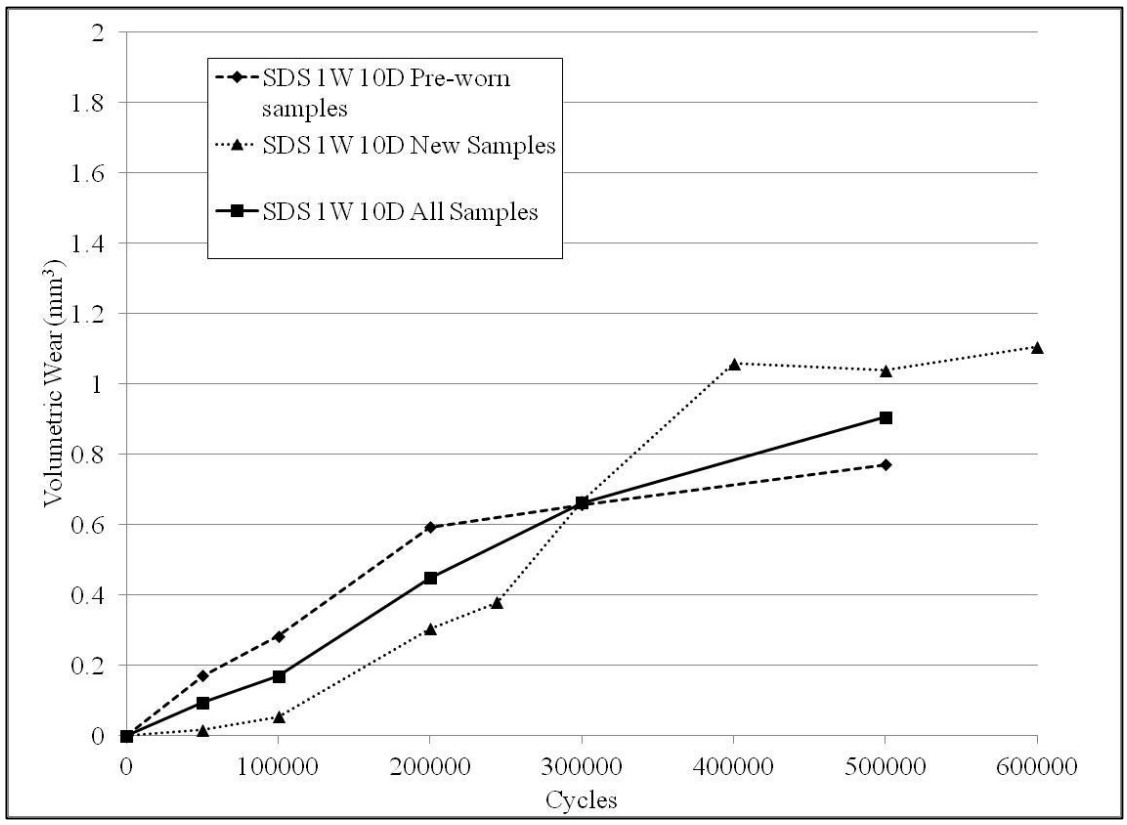

Figure 64: Cumulative mean volumetric wear of 36mm MOM under SDS 1W 10D (Worn) and SDS 1W 10D (New) protocol (n=20)

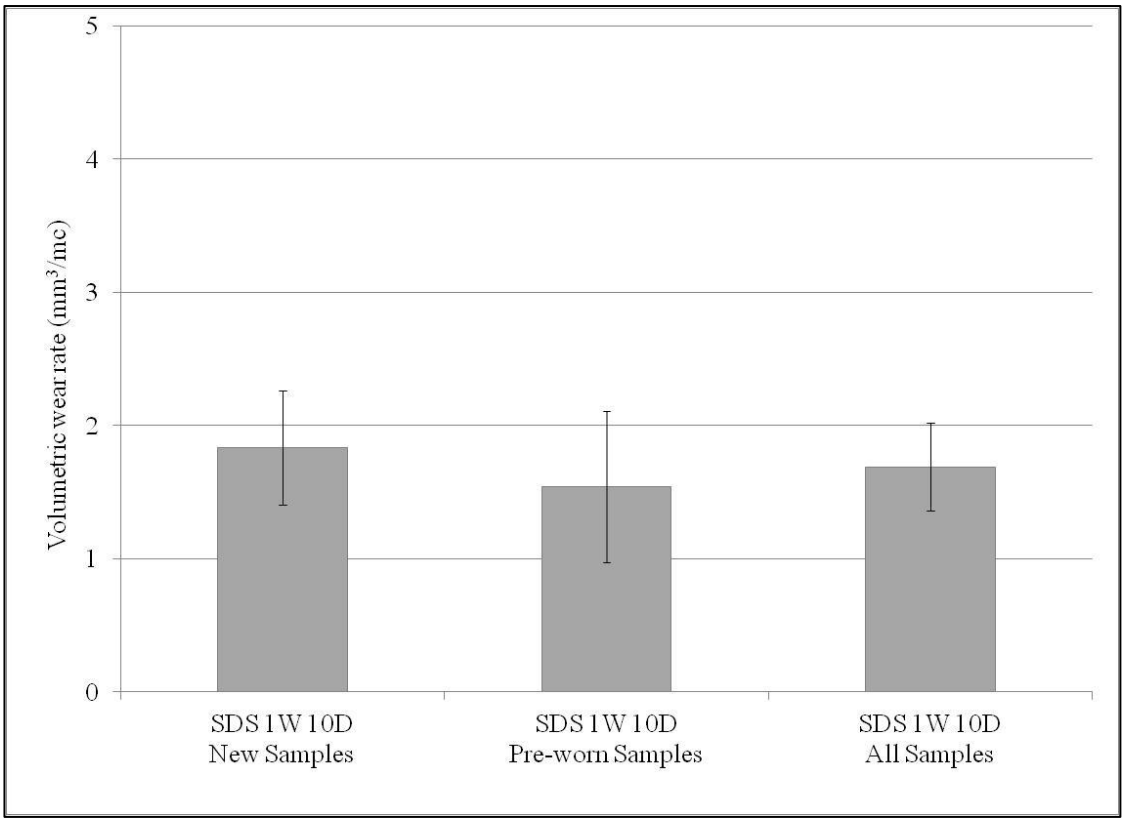

Figure 65: Mean volumetric wear rates of 36mm MOM under SDS 1W 10D (Worn) and SDS 1W 10D (New) protocol (n=20, ±95% confidence limits)

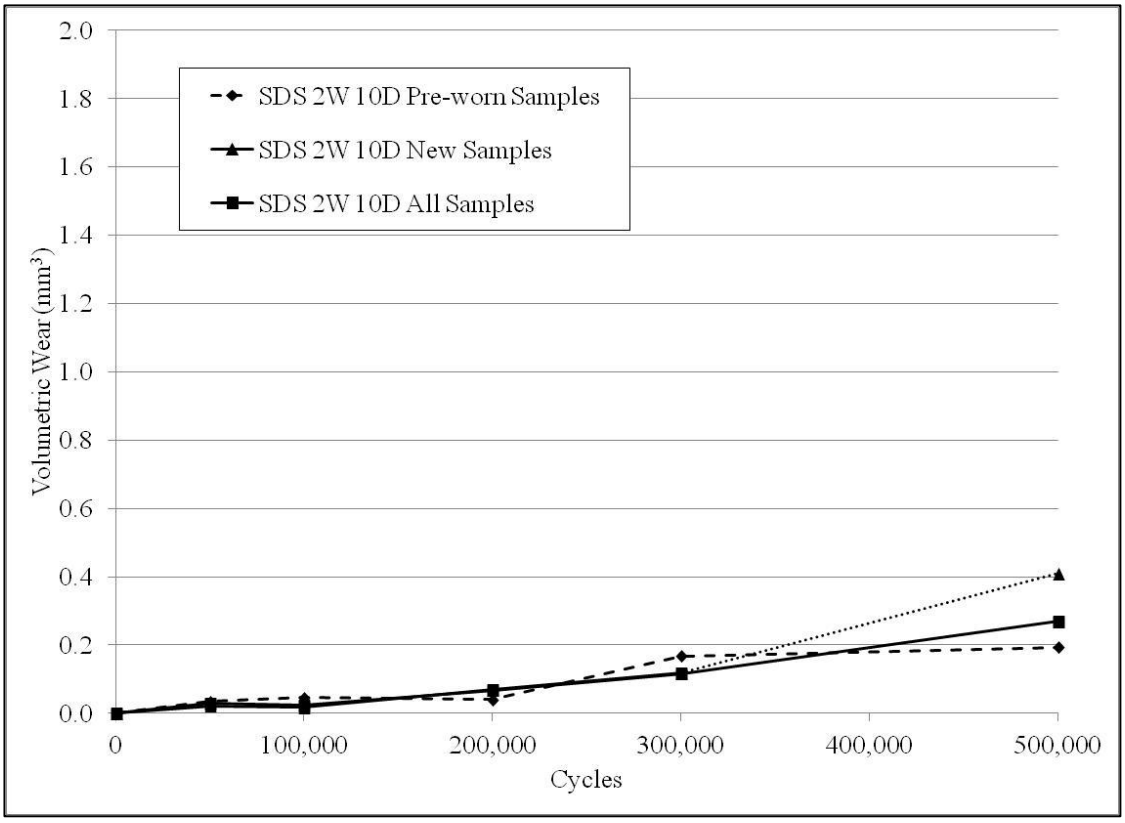

Figure 66: Cumulative mean volumetric wear of pre-worn and new 36mm MOM under SDS 2W 10D protocol (n=10)

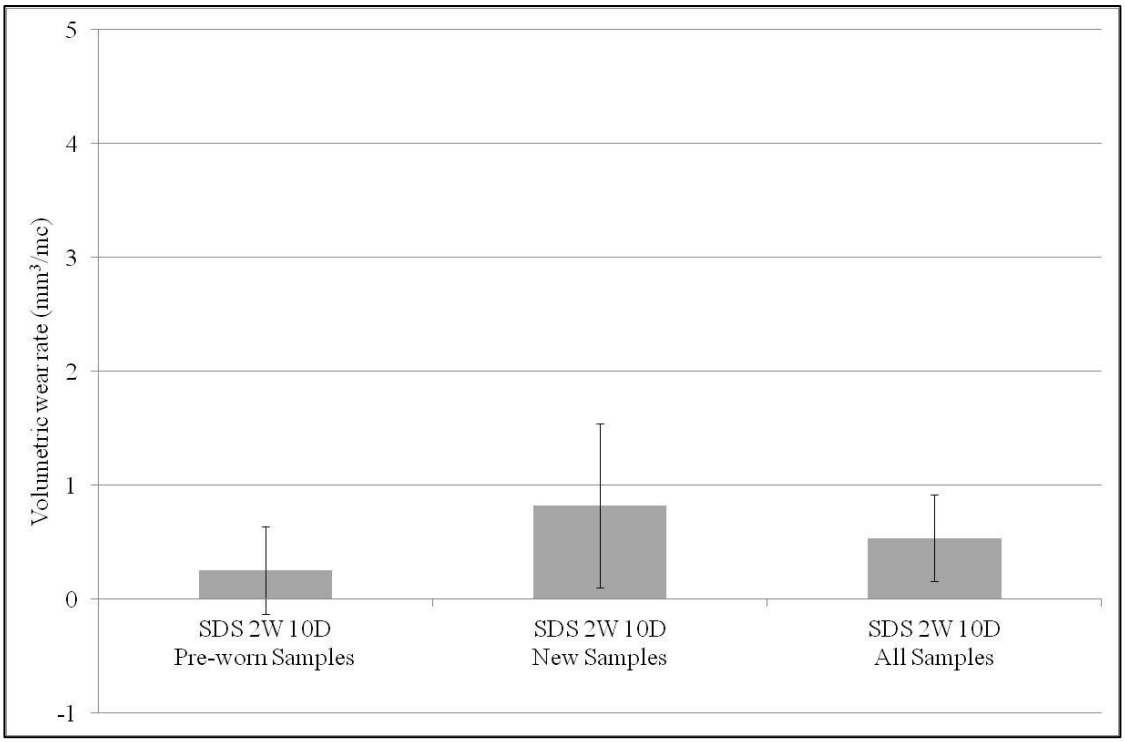

Figure 67: Mean volumetric wear rates of pre-worn and new 36mm MOM under SDS 2W 10D protocol (n=10, ±95% confidence limits)

5.3.5 Surface Roughness Analysis

Surface roughness was measured on the SDS 1W 10D (New) samples following testing. Femoral heads were measured at the pole and at 30º from the pole; acetabular cups were measured at 35º from the pole to coincide with the wear regions.

Surface roughness is presented in terms of S_q (root mean square areal roughness) in Figure 68. Samples from the SDS 1W 10D test at 0.6mc (end of test) were compared with samples from the walking test described in Chapter 3 at the beginning of the test (unworn) and at 0.5mc which is the closest measurement in terms of cycle count to the SDS 1W 10D results.

The mean S_q of the femoral heads following the SDS 1W 10D test was 39.5±16.3nm, which was significantly greater than the roughness of heads under standard walking conditions at a similar number of cycles (P=0.000, T-test), and significantly greater than unworn samples (P=0.000, T-test).

In contrast, the S_q of the acetabular liners following the SDS 1W 10D test was 12.7±2.3nm which was not found to be significantly different from roughness of cups under standard walking conditions at 0.5mc (P=0.524, T-test), or from unworn samples (P=0.053, T-test).

To examine the surface roughness further, samples were also compared with respect to S_z (areal ten point average peak to valley height) (Figure 69). S_z of the acetabular liners was 373.7±83.9nm, which in this instance was found to be significantly greater than S_z of the cups when unworn (P=0.000, T-test) and after 0.5mc of a standard walking test (P=0.000, T-test).

Similarly the S_z of femoral heads after the SDS 1W 10D test (1155.6±320.3nm) was significantly greater than heads pre-test (P=0.000, T-test), or after 0.5mc of a standard walking test (P=0.000, T-test).

It should be noted that due to a change in measurement technique for acetabular liners during a previous test (Chapter 3) the measurements for the SDS 1W 10D samples were taken at 35º from the pole, whereas the comparison data from the walking tests was taken at the cup pole.

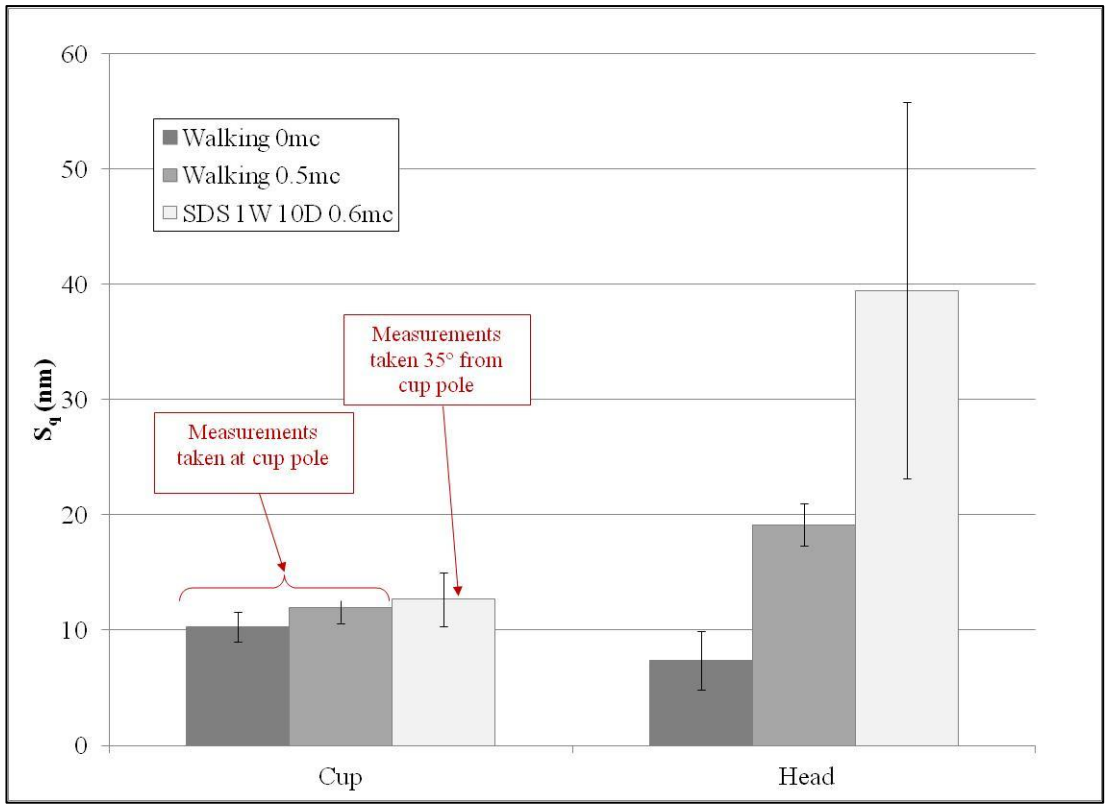

Figure 68: Surface roughness (S_q) of femoral heads in the polar region and at 30° from pole, and acetabular liners at 35° from pole, during the SDS 1W 10D (New) test, and compared with results from a standard walking test (n=10, ±95% confidence intervals)

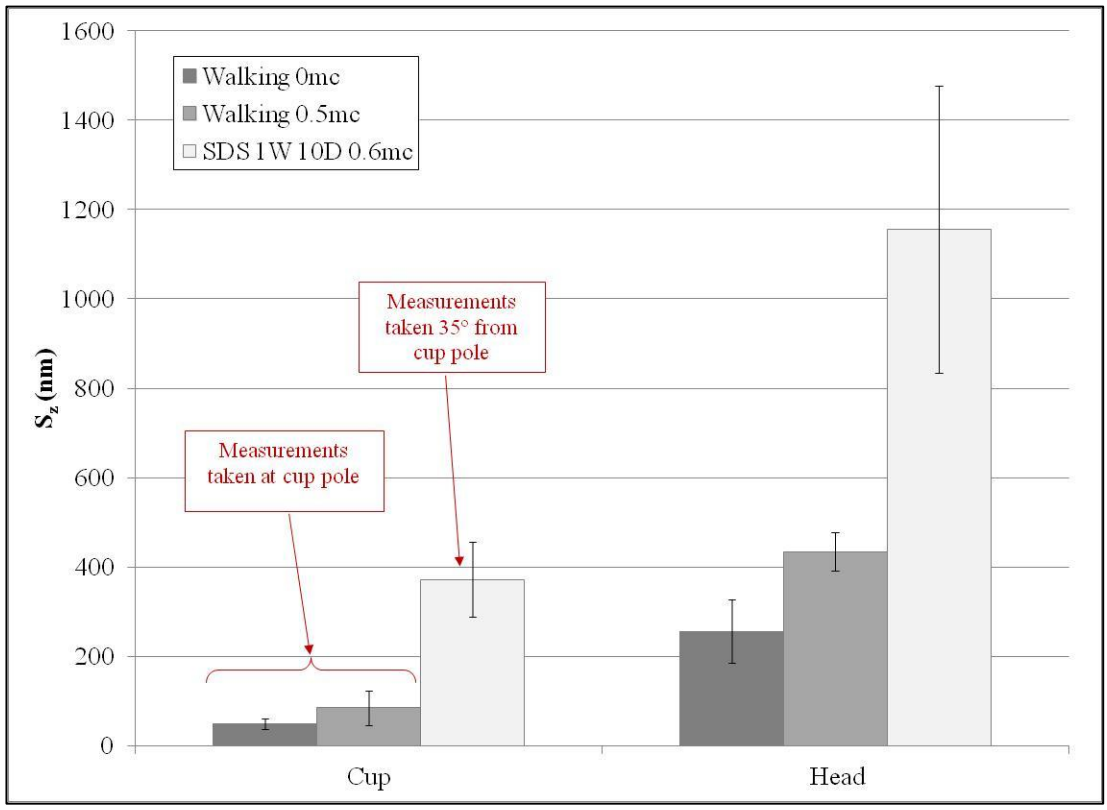

Figure 69: Surface roughness (S_z) of femoral heads in the polar region and at 30° from pole, and acetabular liners at 35° from pole, during the SDS 1W 10D (New) test, and compared with results from a standard walking test (n=10, ±95% confidence intervals)

5.3.6 Summary of Results

Two wear simulation tests have been run to examine the effect of dwell frequency, or the number of walking steps between dwell periods, on the wear of 36mm MOM hip bearings under SDS conditions. The mean wear for each of these tests is presented in Figure 70, and compared with the data for a standard walking test presented in Chapter 3. Each test was run on both new and pre-worn samples.

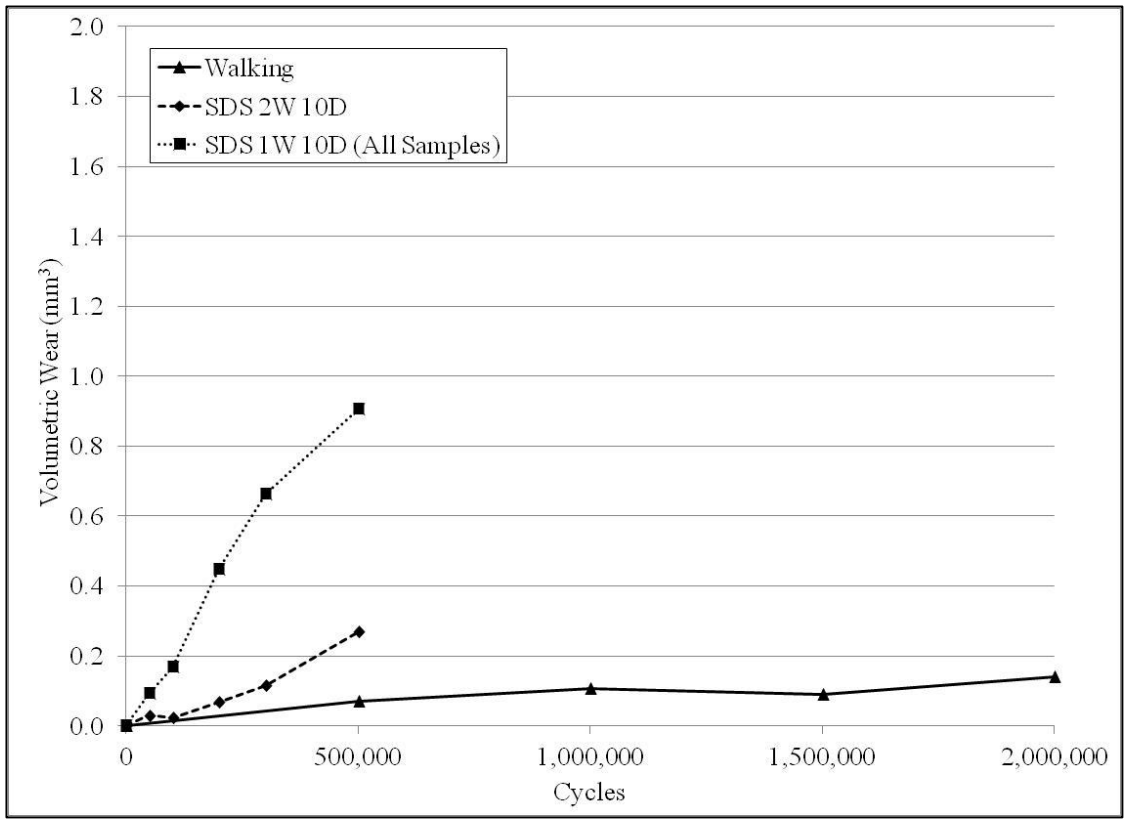

Figure 70: Cumulative mean volumetric wear of 36mm MOM under SDS conditions comparing two different dwell frequencies

Mean volumetric wear rates for the SDS 1W 10D and SDS 2W 10D tests for both new and worn samples combined were 1.68±0.33mm^3/mc and 0.53±0.38mm^3/mc respectively (Figure 71). These results were compared with the wear rate for samples under standard walking conditions presented in Chapter 3. The wear rate for the standard walking test from 0-1mc was 0.11±0.08mm^3/mc. There was no significant difference between the wear rates of new and pre-worn samples on either test.

Wear under SDS 1W 10D conditions was found to be significantly higher than both SDS 2W 10D (P=0.000, T-test) and walking (P=0.000, T-test) wear test wear rates.

Wear under SDS 2W 10D test conditions was also found to be significantly greater than under standard walking conditions (P=0.028, T-test).

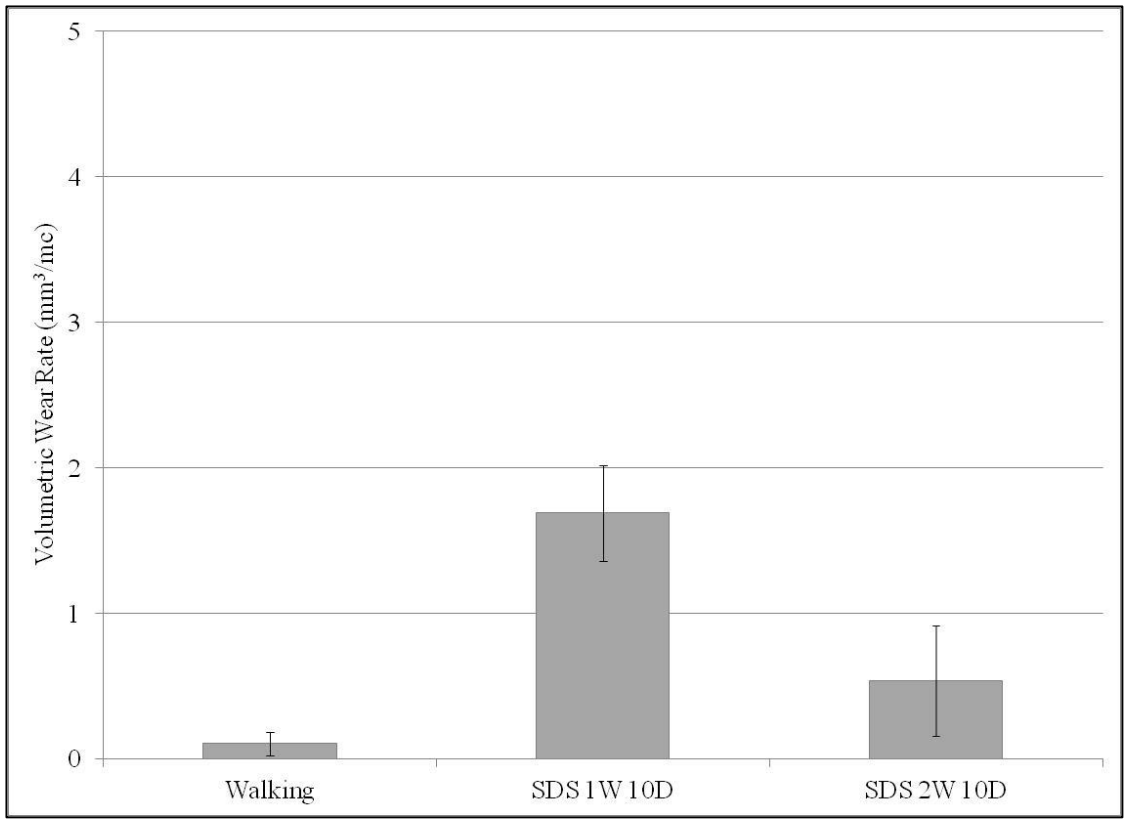

Figure 71: Mean volumetric wear of 36mm MOM under SDS conditions (±95% confidence limits)

Walking: 0-1mc, n=9

SDS 1W 10D: 0-0.5mc, n=20

SDS 2W 10D 0-0.5mc, n=10

5.4 Discussion

This chapter described development and application of a protocol for clinically relevant stop-dwell-start (SDS) type wear simulation, and the effect of this activity on the wear of 36mm MOM total hip replacements. In the previous study in Chapter 4 it was shown that introduction of a dwell period every ten walking steps did not cause a statistically significant increase in bearing wear compared with wear under standard walking conditions, irrespective of the duration of the dwell. The results were attributed to the dwell period only potentially increasing wear rates over two or three steps following the pause, after which time the wear rate returns to normal, therefore overall average wear rates were similar to those for walking tests.

In the current study two protocols were developed to further understand the results from Chapter 4; the same basic SDS protocol was employed, however for these tests a fixed dwell period was used, and the number of steps between dwell periods was reduced.

A dwell period of 10s was selected based on results from the previous study. This duration fell within the range of dwell durations studied in earlier chapters, and it was believed that this would be unlikely to effect a change in bearing wear behaviour compared with a standard walking wear simulation.

In Chapter 4 a walking phase of 10 steps between dwell periods was used, however no significant increase in wear was observed compared with a standard walking wear simulation. It was believed based on the results from that study, that higher wear than normal was occurring in the first few steps after a dwell period, but wear was normal thereafter. When overall wear was calculated the averaging effects led to a wear rate little different from that of standard walking tests. It was hypothesised that if an SDS protocol was developed focusing on those first few steps after a dwell, it would be possible to measure the higher wear occurring in this period. Walking periods of one step and two steps between dwells were therefore selected to test this hypothesis.

Overall mean wear rates from the SDS 1W 10D and SDS 2W 10D tests were $1.68\pm0.33 mm^3/mc$ and $0.53\pm0.38 mm^3/mc$ respectively. These were both shown to be significantly greater than wear during a standard walking test during the bedding in phase ($0.11\pm0.08 mm^3/mc$). These findings support the hypothesis that a greater wear rate was occurring during the first few cycles after the dwell; very high wear occurs on

the first step, followed by slightly less on the next and so on. This is in agreement with models presented in the literature (Jalali-Vahid et al., 2006) indicating that a steady state elastohydrodynamic lubrication film reforms within two or three steps after a dwell. No previous studies could be found in the literature for comparison reproducing an SDS protocol *in vitro* with this small number of walking cycles between dwell periods.

The SDS 1W 10D test was run twice, one on pre-worn samples, and repeated on new, unworn bearings. The SDS 1W 10D (New) test was run for an extra 100,000 cycles due to the significant change in wear rate between 400,000 and 500,000 cycles; necessitating further investigation to confirm whether the measurement point at 500,000 cycles was genuine or anomalous. The wear rate between 400,000 and 600,000 cycles appeared relatively consistent, therefore it was concluded this was genuine data.

The overall average wear rate measured in the two tests was not significantly different, however slightly different wear patterns were observed between the two groups. The pre-worn samples exhibited a relatively high wear rate from 0-200,000 cycles, followed by a much lower wear rate from 200-500,000 cycles (Figure 52). In contrast the new samples exhibited low wear from 0-100,000 cycles, and from 400-600,000 cycles with a higher wear rate observed in the intervening period from 100-400,000 cycles.

The wear patterns in the early stages of these tests could be explained with reference to the work of Hu et al. (2004) and the changes in contact zone sizes and bearing conformity throughout a wear test. It would be expected that the pre-worn test specimens started the test with a worn region in the contact zone, and therefore a greater degree of bearing conformity than the new, unworn bearings. The wear test results show that SDS conditions with a short walking phase cause higher wear than standard walking conditions *in vitro,* suggesting the tribological conditions are more severe. The contact zone in the pre-worn bearings would have been higher, leaving a greater surface area susceptible to the aggressive wear conditions than in the new bearings with a relatively small contact zone, and thus leading to higher wear initially. The unworn bearings demonstrated an initial wear rate similar to that of identical samples in the bedding in phase of a walking test (Figure 61), before the wear rate increased significantly to a level similar to that of the pre-worn samples under SDS conditions (Figure 58, Figure 61). A possible explanation for this may be that the unworn samples may not be susceptible to the aggressive SDS wear conditions until a certain degree of

conformity and size of contact zone is achieved; up to this point wear will be similar to that occurring under normal walking conditions.

In the latter part of the SDS tests both sample groups exhibit a reduction in wear rate, similar to that observed in a standard walking test as bearings bed in to a steady state wear rate. This is believed to be due to improving conformity as the bearings wear down. With greater conformity the bearing clearance decreases but contact area increases, thereby reducing contact stress. The Stribeck curve tells us the lubrication regime tends from boundary towards fluid film under these conditions (Smith et al., 2001b), leading to a reduction in the wear rate. This occurs at a stage where the bearing geometry reaches an optimal point of conformity where contact stress and localised bearing clearance are low enough to permit sufficient separation of the surfaces by the lubricant and wear therefore reduces significantly. In the SDS 1W 10D (Worn) test, samples which had previously exhibited a low steady state wear rate in earlier tests (Chapter 3, Chapter 4) were observed to wear at a higher rate for a short period then 'bed in' to a lower rate once more. This suggests that the optimal conformity of the bearings may differ depending on the severity of the wear conditions. These results show that SDS conditions with a short walking phase cause higher wear than standard walking conditions *in vitro*, suggesting the tribological conditions are more severe. If the tribological conditions are more aggressive, other factors must alter to allow the bearing to reach steady state wear. If the material and lubricant properties, load and entraining velocities all remain the same, the bearing geometry is the only variable which can change to facilitate bedding in. The Hamrock and Dowson equation (Hamrock and Dowson, 1978) indicates that to increase film thickness, which is necessary for lower wear, the equivalent radius of the bearing must increase, or polar clearance must decrease. Therefore to reach steady state wear under the more aggressive SDS test conditions a greater degree of conformity is necessary, which could explain the second bedding in phase.

The SDS 1W 10D (New) samples appear to reach a low final wear rate at 400,000 cycles which is later than for the SDS 1W 10D (Worn) samples (200,000). This delay is believed to be due to the early low wear rate observed in the new samples, which then offsets the subsequent wear patterns compared with the pre-worn bearings.

The final wear rates of the SDS 1W 10D (Worn) and (New) tests were $0.59\pm0.36 mm^3/mc$ and $0.24\pm0.33 mm^3/mc$, which are both greater than the steady state

wear rate under standard walking conditions (0.03±0.02mm^3/mc), although this difference is not significant due to the relatively large degree of variability in the results. This difference may be due again to the increased severity of the tribological conditions during these SDS tests; although the opposing surfaces are optimally conforming, greater wear is still likely to occur due to the reduction in lubricant in the bearing caused by the pauses.

The SDS 2W 10D test was also run on both new and pre-worn test specimens. The overall wear rates of each group were not significantly different, and in contrast with the SDS 1W 10D tests, little difference was observed in wear patterns. No evidence of a change in wear rate was evident in either test, and no reduction in wear to a steady state level was measured. These differences may be attributable to the lower overall wear rate, whereby due to overall test variability, changes in wear pattern are harder to detect. Alternatively, a reduction in wear rate may occur at a later stage under these conditions, and it may be necessary to run the test longer to achieve bearing conformity. The proposed explanation discussed with respect to the SDS 1W 10D test may also apply here, whereby depending on the severity of the tribological conditions induced by the wear test, the degree of conformity necessary to achieve steady state wear will vary, hence the volume of wear necessary to reach steady state wear will also differ depending on the test conditions. Bedding in was observed at approximately 0.1mm^3 during the standard walking test and between approximately 0.6mm^3 and 1mm^3 in the SDS 1W 10D tests; the SDS 2W 10D test exhibited overall wear of approximately 0.2-0.4mm^3 during the test without bedding in; a reduction in wear rate of this test may occur after further cycles and greater volumetric wear.

Surface roughness was examined on the SDS 1W 10D samples following testing and compared with results from the standard walking test both pre-test and at 0.5mc, which was the closest point for comparison with the SDS samples run to 0.6mc. The measurement location for the cup was changed during the study, as described in Chapter 3, therefore the comparisons for the acetabular cup are not ideal, however some conclusions can still be drawn. A significant increase in S_q and S_z was observed on the head, compared with both an unworn surface, and with the samples exposed to a similar number of cycles but under standard walking conditions. In contrast the acetabular cups did not exhibit a significant increase in S_q, however a significant increase in S_z was measured.

The increase of both parameters on the femoral heads indicates all peaks and valleys on the surface have increased in height or depth, whereas the difference for the acetabular liners suggests that although the overall average peak and valley magnitude has not increased, the range of heights has done so, indicating isolated peaks and valleys, or scratches and ridges which are relatively high or deep. The difference between head and cup may be attributed to the kinematics and kinetics in the wear simulator, whereby the load is applied through the head, and the load vector remains constant with the head whilst varying with the cup. In both cases the increased roughness leads to a lower lambda ratio, therefore the bearing will be operating in a more severe wear lubrication condition which would explain the greater wear measured in the SDS tests.

In summary, a significant increase in wear from standard walking levels was observed on the SDS 1W 10D and SDS 2W 10D tests. Some slight differences were noted in the wear behaviour of pre-worn and unworn samples under these conditions, but the overall wear rates were similar. The significant reduction in wear rate from the single step test to the two step test suggests the lubrication regime is restored rapidly after a dwell. Following this trend it is postulated that if a test with three walking steps between dwell periods were to be run (SDS 3W 10D), wear would be lower still and possibly similar to that of a standard walking test.

5.5 Conclusion

The wear of 36mm MOM total hip replacements was examined under two new simulator protocols for stop-dwell-start (SDS) conditions. These tests introduced a 10s dwell period with a 1250N load during the standard walking cycle. The two tests incorporated either a single step or two steps between dwell periods (SDS 1W 10D or SDS 2W 10D). A significant increase in wear was observed for both tests when compared with wear under standard walking conditions. This increase was significantly greater for the single step test. It was postulated these differences were caused by deterioration of the lubricant film in the bearing during the dwell, leading to higher wear on the subsequent cycles, however the lubrication regime recovers rapidly after the dwell, and it is thought that by the third step wear rates would have returned to steady state levels.

CHAPTER 6. OVERALL DISCUSSION AND CONCLUSIONS

6.1 Discussion

This thesis has examined the *in vitro* wear behaviour of 36mm MOM total hip replacement bearings with the introduction of a pause into the wear test. It has been demonstrated that THA patients pause frequently during normal daily activity, and it was hypothesised that this pause may have a detrimental effect on tribology of the bearing, leading to an increase in measured bearing wear. It is desirable to minimise wear in any THA bearing material, but high wear in MOM bearings in particular can lead to metallosis, patient hypersensitivity, pain and implant loosening among others, all potentially leading to loss of joint function and early revision.

At the time of commencing this study, none of the commercially available hip wear simulation machines on the market were capable of running adapted cycles, such as the stop-dwell-start (SDS) of interest in this study. A specification for a new simulator was therefore developed and a collaboration was established with Simulation Solutions (Manchester, UK) to design and build the new machine. The ProSim Deep Flexion Wear Simulator was commissioned using a standard continuous walking wear simulation adapted from ISO 14242-1 (2002) and described in Chapter 3. MOM 36mm hip bearings from stock were run under standard conditions for 2mc, and overall wear rates found to be statistically similar to existing data for the same implant on an earlier generation of the ProSim Simulator. Characteristic bedding in and steady state wear phases were identified, in common with many of the existing studies of MOM devices. A relatively high rate of bedding in wear over the first million cycles of the test was followed by a period of steady state, relatively low wear, and this was attributed to the opposing bearing faces wearing in the contact zone until an optimal geometry for good lubrication and minimal wear was achieved. The results of this commissioning study confirmed that the simulator was operating within the required specification.

The development of an SDS cycle for the wear simulator and evaluation of the effects of this cycle on bearing wear were described in Chapters 4 & 5. The first SDS test was developed from measurements of real patient activity reported in the literature (Morlock et al., 2000, 2001). During this profile ten walking steps, or cycles, were applied followed by a 5s dwell at 1250N (SDS 10W 5D), equivalent to bi-lateral stance load

(Bergmann et al., 2001). This was similar to the mean frequency and duration of dwell periods in real patients reported in the literature. This profile differed significantly from earlier SDS studies in the literature (Chan, Bobyn, Medley, and Krygier, 1999; Medley et al., 2002; Liao et al., 2004) which tended to apply longer durations of walking cycles of five to ten minutes depending on the study, and longer dwell periods of up to one minute. Dwell loads were either 1250N, as in the current study, or 3kN, as per the peak load of the standard walking cycle. Results from earlier SDS studies varied depending on the parameters used; some groups reported a significant increase in wear under these conditions, however some could not measure any difference.

In the present study no significant increase in wear was observed in the first SDS test (SDS 10W 5D) compared with the bedding in period of the standard walking test. No evidence of bedding in was observed, although in the case of some of the shorter tests a greater number of test cycles may be necessary to confirm this finding. Initially the similarity in wear rates was attributed to the duration of the dwell not being long enough to cause sufficient deterioration of the lubricant film, therefore two further tests were run with dwell periods of 30s and 60s respectively. It was hypothesised that an increase in dwell duration would cause a more significant deterioration of the tribological conditions, however again no significant increase in bearing wear was observed. It was then postulated this lack of apparent effect was due not to the dwell duration, but to the number of steps between dwell periods, as suggested by models reported in the literature (Jalali-Vahid et al., 2006). These models suggested that during a pause, the tribological conditions in the bearing deteriorated as squeeze film and elastohydrodynamic actions were no longer present to generate a lubricant film separating the bearing surfaces and thus limiting wear. When motion was reinitiated, it took a number of cycles to re-establish the lubricant film, during which time the bearing surfaces were in greater contact and wear may have been higher. The Jalali-Vahid model indicated the lubricant film may reform in as little as 2-3 walking cycles, thus in the present study with a walking phase of 10 cycles, although high wear may be present on the first few, subsequent cycles all exhibit normal wear, and when overall mean wear rates are calculated the wear rate appears similar to that of standard walking.

To test this hypothesis, a further two SDS protocols were developed, maintaining a fixed dwell duration of 10s but varying the number of walking cycles between dwell periods. The SDS 1W 10D and SDS 2W 10D tests were both run on identical samples to those used previously, and wear rates were found to be significantly greater than

those reported for standard walking conditions, with an approximate 15-fold increase for the one step test, and approximately five fold for the two step test. This demonstrated good agreement with the theoretical models, and supported the hypothesis that high, but steadily reducing wear occurs on the first few cycles after a pause, and normal tribological conditions are established within a few cycles.

Several interesting patterns were identified throughout this study with respect to the changing of wear rates during each simulator test. In the standard walking test described in Chapter 3, an initial high wear rate during the first million cycles of the test was followed by a low wear rate over the second million cycles. As described previously, this is a commonly recognised phenomenon in metal-on-metal bearings and attributed to bedding-in of the bearing surfaces to an optimal geometry for good lubrication and low wear. In contrast, in the tests examining dwell duration in Chapter 4, no change in wear rate was observed, and samples continued to wear throughout the test at a similar rate to the bedding-in period of a standard walking test. This was suggested to be due to the changing wear rate throughout each walking phase, preventing the bearing from bedding in to an optimal geometry and thus reaching steady state wear. Wear was believed to be higher during the first few cycles after each dwell period, suggesting more aggressive tribological conditions, and lower thereafter until the next dwell, indicating more optimal tribology. This was supported by the results from Chapter 5 and also by comparison with theoretical models in the literature. It was postulated in Chapter 5 that an optimal bedding-in geometry depends on the severity of the test conditions; the changing conditions in the SDS 10W 5D, 30D and 60D tests mean that the bearing can never bed in to an optimal geometry since the tribological environment is changing during each walking phase.

Finally, in the tests investigating dwell frequency described in Chapter 5, a change in wear rate similar to that reported in the standard walking test was observed in the SDS 1W 10D test, with initially high wear reducing to a lower rate in later phases of the tests. This was again believed to be due to bearings bedding in to an optimal conformity for good lubrication and low wear. In contrast with the tests with longer dwell periods, it is postulated that severe tribological conditions were believed to be present on every walking cycle, and as the lubricant film was never able to re-establish, there was no conflict between optimal conformity for different tribological conditions, and the bearings were able to bed in and achieve a steady state wear rate. The steady state wear rate for this test was however significantly greater than that for a standard walking test;

it was proposed that this was due again to the more severe tribological conditions under the SDS test conditions. The SDS 2W 10D test did not exhibit any degree of bedding in. It is possible that a greater volume of wear and thus further wear cycles may have been needed to achieve optimal conditions and steady state wear; a longer wear test would corroborate this.

In some of the simulator tests in this study a comparison was made between the wear behaviour of new and pre-worn, i.e. bedded-in specimens. This was run on the standard walking test, and the SDS 5W 10D, SDS 1W 10D and SDS 2W 10D tests. On each of these tests no significant difference was observed between the overall wear rates of pre-worn and new samples. It had been hypothesised that pre-worn components would wear at a lower rate, as they were already bedded in to an optimal conformity, however these results suggested that the entraining velocity has a more dominant effect on bearing tribology and therefore wear, than the degree of geometrical conformity of the bearings under the conditions examined in this study. Some small differences were noted between pre-worn and new samples in the later stages of the SDS 10W 5D test; these were suggested to be due to damage caused during the simulator breakdown in the earlier part of the test, however a repeat of this test would be necessary to confirm or reject this as a possible cause. A small difference between new and pre-worn samples was also noted in the first 100,000 cycles of the SDS 1W 10D test. A possible explanation for this could be the lower conformity and small contact area of new samples, leaving the surfaces less susceptible to the aggressive SDS conditions until a threshold contact region is achieved through wear, at which point wear rates accelerate rapidly. This effect may not be unique to the SDS 1W 10D test, but it may be that only at the high wear rates of this test that this effect can be distinguished, and under less aggressive test conditions with lower wear the effect is masked by normal variance.

Surface roughness of wear test specimens was examined during the standard walking test, and following the SDS 1W 10D study. A change in measurement technique was found to be necessary on the acetabular cups, moving the measurement point from the cup pole to 35º from the pole to coincide with the wear scar. Due to this change some of the comparisons of surface metrology for the liners were between 0º pre-test and 35º post-test and therefore not ideal. The continuous machining and polishing techniques used in manufacturing of these components and the drawing specification for surface finish, permit the assumption that roughness pre-test was relatively constant across the

entire surface, therefore it was considered reasonable to use the polar measurements for comparison when time and resource constraints prevented a repeat of the test.

Roughness was seen to increase significantly during the bedding in period of the walking test, then stabilise once steady state conditions were reached. The Lambda ratio described in Chapter 1 suggests that this increase in surface roughness would lead to a less optimal tribological situation, thereby increasing wear. At the same time, as the bearings bed in, it is known that localised clearance in the contact region decreases, leading to an improvement in the lubrication regime, as demonstrated by the Somerfeld relationship. These results indicate that the bearing geometry may have a more dominant effect on the lubrication of the bearing than the surface roughness under these test conditions.

The surface roughness of samples from the SDS 1W 10D test was found to be significantly higher than those from the standard walking test after a similar number of wear cycles. This was attributed to the more aggressive tribological conditions under the SDS protocol facilitating increased counterface scratching of the bearings due to a thinner lubricant film. As before, it is known that increased surface roughness in turn also leads to less optimal lubrication, and this may help to explain the greater steady state wear rate measured in the SDS 1W 10D test compared with standard walking; the damage caused to the bearing surfaces early in the test could have been contributing to increased wear at a later stage.

6.1.1 Review of Thesis Aims

The main aims of this study detailed in Chapter 1 were to develop and utilise a clinically relevant wear simulation method to understand the performance of large diameter metal-on-metal bearings under stop-start conditions. A key area of focus was to ensure clinical relevance in this work and match simulator parameters to real patient activity patterns, an aspect which was believed to be absent in previous SDS studies in the literature.

For this study patient activity patterns and kinematics and kinetics were derived from the literature to generate inputs for the simulator protocols. This did however present some limitations. One key set of data from Bergmann et al. (2001) was used for kinematics and kinetics. There are other studies available in the literature however this was found to be the most comprehensive, although the sample size of patients was small

at n=4. No data in the literature could be found reporting the kinematics of stopping and starting during walking, therefore inputs for these aspects of the SDS tests were estimated. The activity patterns of patients were taken from the data of Morlock et al. (2000, 2001). These studies covered a greater number of patients (n=30-40), but no other studies measuring the same parameters could be found in the literature to corroborate the data.

During the development process for the wear simulator to run the SDS protocols, a number of challenges were encountered. The choice of manufacturer was limited to Simulation Solutions due to the need to maintain consistency in manufacturer with existing simulators in the laboratory. The new simulator design was loosely based on existing technology used by Simulation Solutions. This limited the simulator design to a pneumatic system, as opposed to hydraulic, which can limit the load response times for kinetic inputs. Similarly only two motion axes were available as opposed to three as described by ISO 14242:2 (2002), however as discussed previously, this does not necessarily lead to a difference in wear rate *in vitro*.

A number of simulator breakdowns were encountered during this study, which have impacted results in some cases. Breakdowns were due to a variety of reasons including issues with quality of externally sourced components such as load cells, and incorrect specification of certain elements at the design stage such as the pneumatic valves. A number of software bugs were also encountered which at times caused the machine to crash and damage samples. Resource and time constraints prevented repeats of the affected tests, therefore some of the conclusions from the data are not as solid as would be preferred. It is evident that when developing new simulators in future a significantly longer and more robust commissioning test is necessary to prevent any failures affecting research studies.

When considering clinical relevance of this study, the SDS 10W 5D was deemed to be most similar to the mean reported patient activity patterns in the literature. The other tests were primarily designed to further the understanding of the effect of the relative parameters, however all of the SDS tests fell within the range of reported activity patterns measured in patients (Morlock et al., 2000, 2001). The SDS 10W 5D, 30D and 60D tests could be most closely equated to the activity of relatively normally functioning patients walking in bursts of steps before pausing. This study suggests that under these conditions while wear is not significantly greater than that during the

bedding-in phase of a continuous walking test, under these SDS conditions the bearings do not appear to bed in, thus overall wear may be greater. It is known that the SDS pattern is far more realistic than the continuous walking employed in standard *in vitro* studies therefore this may go some way to explaining the discrepancy frequently reported between the *in vitro* and *in vivo* wear behaviour of MOM bearings.

In contrast, the test where greatest wear was observed in this study: SDS 1W 10D and SDS 2W 10D, could be considered less clinically relevant with respect to well functioning patients, however these tests may be more realistic when considering less well functioning subjects. The use of just one or two steps between pauses could be characteristic of patients in the very early stages of recovery post-surgery, or the elderly or infirm with other medical complications, who are unable to sustain continuous walking for any length of time. The results of this study suggest that under those conditions MOM bearings may wear at a significantly higher rate than is desirable to avoid the complications such as metallosis, necrosis and pain.

6.1.2 Further work

There is significant scope for further development and extension of the research described in this thesis. Most crucially, a repeat of some of the tests affected by simulator breakdowns would be desirable. The primary aim of this study was to define and evaluate new protocols for SDS testing, however many further studies are of interest to develop the understanding of the wear behaviour presented here. A examination of the effect of these cycles on different bearing material combinations would be of interest to clinicians in particular. This could be supported with more detailed *in vit*ro analysis of serum ion levels, wear particle morphology, and changes in bearing geometry and surface finish. Furthermore study of the effect of geometrical changes such as bearing clearance and conformity may yield useful information. On a more detailed level, measurements of changes in lubrication film thickness during the different cycles would help to confirm the suggested potential causes of this wear behaviour as discussed earlier. Similarly, more detailed measurements of the geometry of the contacting regions of the bearings would help to confirm whether the hypothesis regarding differing conformities of bearings depending on the severity of the wear conditions is correct. Longer term these SDS protocols would be of interest when run in conjunction with other activity simulations presented in the literature such as running. A complex daily living cycle incorporating a number of different patient activities may

give a significantly more accurate prediction of *in vivo* bearing performance than the current techniques offer.

6.2 Conclusion

This thesis has described the development of a number of clinically relevant stop-dwell-start protocols for *in vitro* wear simulation of total hip replacement bearings. A new wear simulator was developed and commissioned to allow application of these complex cycles, and data from the literature examined to characterise activity patterns of real THA patients.

A number of different stop-dwell-start test scenarios were investigated, examining the effect on wear of altering both the duration of dwell periods, and the number of walking cycles between dwells. Wear did not appear to increase significantly with a longer dwell period, however it was observed that bearings did not bed in under these conditions therefore overall wear volumes may be higher. This may provide an explanation for the discrepancy between clinical wear measurements of metal-on-metal hips, when patients typically employ a variety of activities, and laboratory data created using continuous standard walking cycles.

A significant increase in wear was observed when the number of cycles between dwell periods was reduced down to one or two cycles; this is believed to be due to deterioration of the lubricant film during the dwell, leading to severe lubrication conditions at start-up, and subsequent high wear of the bearing surfaces. These findings may be particularly relevant to the use of MOM devices in very infirm patients, or those in the early stages of recovery, for whom walking in a single step pattern may be more common.

These results have clinical relevance in the loads and cycle combinations used, compared with earlier studies. Both the number of walking and dwell cycles, and the dwell period load are based on data from real hip patients in the literature, showing that activity bursts are generally short and change frequently, and the load during a pause is low compared with peak loads during walking.

It is believed this use of more clinically relevant activity simulations for pre-clinical *in vitro* testing of hip replacement bearings is vital for improved understanding of bearing tribology and more accurate prediction of implant performance *in vivo.*

REFERENCES

Amstutz, H.C., Grigoris, P., 1996. Metal on metal bearings in hip arthroplasty. Clinical Orthopaedics & Related Research S11–34.

Anissian, H.L., Stark, A., Gustafson, A., Good, V., Clarke, I.C., 1999. Metal-on-metal bearing in hip prosthesis generates 100-fold less wear debris than metal-on-polyethylene. Acta Orthopaedica Scandinavica 70, 578–582.

ASTM, 2011. Annual Book of ASTM Standards 2011 Section 13 Medical Devices and Services.

August, A.C., Aldam, C.H., Pynsent, P.B., 1986. The McKee-Farrar hip arthroplasty. A long-term study. The Journal of bone and joint surgery. British volume 68, 520–7.

Barbour, P.S.M., Stone, M.H., Fisher, J., 1999. A hip joint simulator study using simplified loading and motion cycles generating physiological wear paths and rates. Proceedings of the Institution of Mechanical Engineers Part H Journal of engineering in medicine 213, 455–467.

Bergmann, G., 2002. Realistic test scenarios for hip implants, in: Institution of Mechanical Engineers: Engineers and Surgeons: Joined at the Hip. London, p. C601/029.

Bergmann, G., Deuretzbacher, G., Heller, M., Graichen, F., Rohlmann, A., Strauss, J., Duda, G.N., 2001. Hip contact forces and gait patterns from routine activities. Journal of Biomechanics 34, 859–871.

Bergmann, G., Graichen, F., Rohlmann, A., 1993. Hip joint loading during walking and running, measured in two patients. Journal of Biomechanics 26, 969–990.

Bergmann, G., Graichen, F., Rohlmann, A., 1995. Is staircase walking a risk for the fixation of hip implants? Journal of Biomechanics 28, 535–553.

Van den Bogert, A.J., Read, L., Nigg, B.M., 1999. An analysis of hip joint loading during walking, running, and skiing. Medicine and science in sports and exercise 31, 131–142.

Bowsher, J.G., Hussain, A., Williams, P.A., Shelton, J.C., 2006. Metal-on-metal hip simulator study of increased wear particle surface area due to “severe” patient activity. Proceedings of the Institution of Mechanical Engineers Part H Journal of engineering in medicine 220, 279–287.

Bowsher, J.G., Nevelos, J., Williams, P.A., Shelton, J.C., 2006. “Severe” wear challenge to “as-cast” and “double heat-treated” large-diameter metal-on-metal hip bearings. Proceedings of the Institution of Mechanical Engineers Part H Journal of engineering in medicine 220, 135–143.

Bowsher, J.G., Shelton, J.C., 2001. A hip simulator study of the influence of patient activity level on the wear of crosslinked polyethylene under smooth and roughened femoral conditions. Wear 250, 167–179.

Bragdon, C.R., O’Connor, D.O., Lowenstein, J.D., Jasty, M., Syniuta, W.D., 1996. The importance of multidirectional motion on the wear of polyethylene. Proceedings of the Institution of Mechanical Engineers. Part H, Journal of engineering in medicine 210, 157–65.

Brand, R.A., Pedersen, D.R., Davy, D.T., Kotzar, G.M., Heiple, K.G., Goldberg, V.M., 1994. Comparison of hip force calculations and measurements in the same patient. The Journal of Arthroplasty 9, 45.

Brockett, C., Fisher, J., Williams, S., Jin, Z., Isaac, G., 2006. Friction of total hip replacements with different bearings and loading conditions. Journal of Biomedical Materials Research Part B: Applied Biomaterials 81B, 508–515.

Browne, J.A., Bechtold, C.D., Berry, D.J., Hanssen, A.D., Lewallen, D.G., 2010. Failed metal-on-metal hip arthroplasties: a spectrum of clinical presentations and operative findings. Clinical orthopaedics and related research 468, 2313–20.

Burroughs, B.R., Hallstrom, B., Golladay, G.J., Hoeffel, D., Harris, W.H., 2005. Range of Motion and Stability in Total Hip Arthroplasty With 28-, 32-, 38-, and 44-mm Femoral Head Sizes: An In Vitro Study. The Journal of Arthroplasty 20, 11.

Bűscher, R., Tager, G., Dudzinski, W., Gleising, B., Wimmer, M.A., Fischer, A., 2005. Subsurface microstructure of metal-on-metal hip joints and its relationship to wear

particle generation. Journal of biomedical materials research Part B Applied biomaterials 72, 206–214.

Campbell, P.A., Wang, M., Amstutz, H.C., Goodman, S.B., 2002. Positive cytokine production in failed metal-on-metal total hip replacements. Acta orthopaedica Scandinavica 73, 506–512.

Catelas, I., Bobyn, J.D., Medley, J.B., Krygier, J.J., Zukor, D.J., Huk, O.L., 2003. Size, shape, and composition of wear particles from metal-metal hip simulator testing: effects of alloy and number of loading cycles. Journal of Biomedical Materials Research Part A 67, 312–327.

Catelas, I., Medley, J.B., Campbell, P.A., Bobyn, J.D., Huk, O.L., 2002. Comparison of Metal-Metal Wear Particles from a Hip Simulator with Those from Periprosthetic Tissue, in: Institution of Mechanical Engineers: Engineers and Surgeons: Joined at the Hip. London, p. C601/095.

Catelas, I., Medley, J.B., Campbell, P.A., Huk, O.L., Bobyn, J.D., 2004. Comparison of in vitro with in vivo characteristics of wear particles from metal-metal hip implants. Journal of biomedical materials research. Part B, Applied biomaterials 70B, 167–178.

Chan, F.W., Bobyn, J.D., Medley, J., Krygier, J.J., 1999. Simulator wear of metal-metal hip implants under adverse load conditions, in: 45th Annual Meeting, Orthopaedic Research Society. Anaheim, California, p. 310.

Chan, F.W., Bobyn, J.D., Medley, J.B., Krygier, J.J., Tanzer, M., 1999. The Otto Aufranc Award. Wear and lubrication of metal-on-metal hip implants. Clinical Orthopaedics and Related Research 10–24.

Chan, F.W., Bobyn, J.D., Medley, J.B., Krygier, J.J., Yue, S., Tanzer, M., 1996. Engineering issues and wear performance of metal on metal hip implants. Clinical Orthopaedics & Related Research 96–107.

Charnley, J., 1961. Arthroplasty of the hip. A new operation. Lancet 1, 1129–32.

Charnley, J., 1982. Long-term results of low-friction arthroplasty. The Hip 42–9.

Clarke, I.C., 1981. Wear of artificial joint materials IV: Hip Joint Simulator Studies. Engineering in Medicine 10, 189–198.

Clarke, I.C., Good, V., Anissian, L., Gustafson, A., 1997. Charnley wear model for validation of hip simulators— ball diameter versus polytetrafluoroethylene and polyethylene wear. Proceedings of the Institution of Mechanical Engineers, Part H: Journal of Engineering in Medicine 211, 25–36.

Clarke, I.C., Good, V., Williams, P., Schroeder, D., Anissian, L., Stark, A., Oonishi, H., Schuldies, J., Gustafson, G., 2000. Ultra-low wear rates for rigid-on-rigid bearings in total hip replacements. Proceedings of the Institution of Mechanical Engineers, Part H: Journal of Engineering in Medicine 214, 331–347.

Clarke, M.T., Lee, P.T., Arora, A., Villar, R.N., 2003. Levels of metal ions after small- and large-diameter metal-on-metal hip arthroplasty. Journal of bone and joint surgery. British volume 85, 913–917.

Crowninshield, R.D., 2006. The New Orthopaedic Hip Patient. Hip international: the journal of clinical and experimental research on hip pathology and therapy 16, S3–S8.

Crowninshield, R.D., Brand, R.A., Johnston, R.C., 1978. The Effects of Walking Velocity and Age on Hip Kinematics and Kinetics. Clinical Orthopaedics & Related Research 132, 140–144.

Crowninshield, R.D., Rosenberg, A.G., Sporer, S.M., 2006. Changing demographics of patients with total joint replacement. Clinical Orthopaedics & Related Research 443, 266–272.

Cuckler, J.M., Moore, K.D., Lombardi Jr., A. V, McPherson, E., Emerson, R., 2004. Large versus small femoral heads in metal-on-metal total hip arthroplasty. The Journal of arthroplasty 19, 41–44.

D Shetty, V., N Villar, R., 2006. Development and problems of metal-on-metal hip arthroplasty. Proceedings of the Institution of Mechanical Engineers Part H Journal of engineering in medicine 220, 371–377.

Davy, D.T., Kotzar, G.M., Brown, R.H., Heiple, K.G., Goldberg, V.M., Heiple Jr., K.G., Berilla, J., Burstein, A.H., 1988. Telemetric force measurements across the hip after total arthroplasty. The Journal of Bone and Joint Surgery Am 70, 45–50.

Delaunay, C.P., 2004. Metal-on-metal bearings in cementless primary total hip arthroplasty. The Journal of arthroplasty 19, 35–40.

Dennis, D., Komistek, R., Northcut, E., Ochoa, J., Ritchie, A., 2001. “In vivo” determination of hip joint separation and the forces generated due to impact loading conditions. Journal of Biomechanics 34, 623–629.

DePuy International, 2006. WR671A (Internal report).

DePuy International, 2007. DePuy International Reconstructive Products UK Price List. Leeds.

DePuy International, 2008a. WR882A (Internal report).

DePuy International, 2008b. WR933A (Internal report).

DePuy Synthes, 2012. DePuy Pinnacle Hip System [WWW Document]. URL http://www.depuy.com/pinnaclepatient

Devitt, A., OSullivan, T., Quinlan, W., 1997. 16- to 25-year follow-up study of cemented arthroplasty of the hip in patients aged 50 years or younger. The Journal of Arthroplasty 12, 479–489.

Dowson, D., 2001. New joints for the Millennium: wear control in total replacement hip joints. Proceedings of the Institution of Mechanical Engineers Part H Journal of engineering in medicine 215, 335–358.

Dowson, D., Hardaker, C., Flett, M., Isaac, G., 2004a. A hip joint simulator study of the performance of metal-on-metal joints: Part I: The role of materials. The Journal of Arthroplasty 19, 118.

Dowson, D., Hardaker, C., Flett, M., Isaac, G., 2004b. A hip joint simulator study of the performance of metal-on-metal joints: Part II: Design. The Journal of Arthroplasty 19, 124.

Dowson, D., Jin, Z.M., 2006. Metal-on-metal hip joint tribology. Proceedings of the Institution of Mechanical Engineers Part H Journal of engineering in medicine 220, 107–118.

Dowson, D., Jobbins, B., 1988. Design and development of a versatile hip joint simulator and a preliminary assessment of wear and creep in Charnley total replacement

hip joints. Proceedings of the Institution of Mechanical Engineers. Part H, Journal of engineering in medicine 17, 111–117.

Dowson, D., Wright, V., 1981. An Introduction to the bio-mechanics of joints and joint replacement. Mechanical Engineering Publications, London.

Dumbleton, J.H., Manley, M.T., 2005. Metal-on-Metal total hip replacement: what does the literature say? The Journal of arthroplasty 20, 174–188.

Ernsberger, C., 2008. Low Ion Release Aspheric Metal on Metal Hip Design, in: Wear. 54th Annual Meeting of the Orthopaedic Research Society.

Fabi, D., Levine, B., Paprosky, W., Della Valle, C., Sporer, S., Klein, G., Levine, H., Hartzband, M., 2012. Metal-on-Metal Total Hip Arthroplasty: Causes and High Incidence of Early Failure. Orthopedics 35, e1009–16.

Firkins, P., Tipper, J., Saadatzadeh, M., Ingham, E., 2001. Quantitative analysis of wear and wear debris from metal-on-metal hip prostheses tested in a physiological hip joint simulator. Biomedical materials and engineering 11, 143–157.

Firkins, Tipper, Ingham, Stone, Farrar, Fisher, 2001. Influence of simulator kinematics on the wear of metal-on-metal hip prostheses. Proceedings of the Institution of Mechanical Engineers. Part H, Journal of engineering in medicine 215, 119–21.

Fischer, A., Wimmer, M.A., 2006. Differences in wear mechanisms between main contact areas and stripe wear regions in metal-on-metal hip joints. Journal of Biomechanics 39, S139.

Food and Drug Administration (FDA), 2012. Information for All Health Care Professionals who Provide Treatment to Patients with a Metal-on-Metal Hip Implant System [WWW Document].

URL:http://www.fda.gov/MedicalDevices/ProductsandMedicalProcedures/ImplantsandProsthetics/MetalonMetalHipImplants/ucm241744.htm

Gluck, T., 1891. Report on the positive results obtained by the modern surgical experiment regarding the suture and replacement of defects of superior tissue, as well as the utilization of re-absorbable and living tamponade in surgery [In German]. Arch klin chir. 41, 187–239.

Goldsmith, A.A., Dowson, D., 1999. Development of a ten-station, multi-axis hip joint simulator. Proceedings of the Institution of Mechanical Engineers Part H Journal of engineering in medicine 213, 311–316.

Goldsmith, A.A., Dowson, D., Isaac, G.H., Lancaster, J.G., 2000. A comparative joint simulator study of the wear of metal-on-metal and alternative material combinations in hip replacements. Proceedings of the Institution of Mechanical Engineers Part H Journal of engineering in medicine 214, 39–47.

Goldsmith, A.A., Dowson, D., Wroblewski, B.M., Siney, P.D., Fleming, P.A., Lane, J.M., 2001. The effect of activity levels of total hip arthroplasty patients on socket penetration. The Journal of arthroplasty 16, 620–627.

Gray, H., 1918. Anatomy of the Human Body, 20th ed. Lea & Febiger, Philadelphia.

Hall, R.M., Unsworth, A., 1994. Frictional Characterisation of explanted Charnley hip prostheses. Wear 175, 159–166.

Hallab, N.J., Anderson, S., Caicedo, M., Skipor, A., Campbell, P., Jacobs, J.J., 2004. Immune responses correlate with serum-metal in metal-on-metal hip arthroplasty. The Journal of arthroplasty 19, 88–93.

Hamrock, B.J., Dowson, D., 1978. Elastohydrodynamic Lubrication of Elliptical Contacts for Materials of Low Elastic-Modulus I - Fully Flooded Conjunction. Trans. ASME, Journal of Lubrication Technology 100, 236–245.

Hardaker, C., Dowson, D., Isaac, G.H., 2006. Head replacement, head rotation, and surface damage effects on metal-on-metal total hip replacements: a hip simulator study. Proceedings of the Institution of Mechanical Engineers, Part H: Journal of Engineering in Medicine 220, 209–217.

Harris, W.H., 1969. Traumatic Arthritis of the Hip after Dislocation and Acetabular Fractures: Treatment by Mold Arthroplasty An end result study using a new method of result evaluation. The Journal of Bone & Joint Surgery 51, 737–755.

Heller, M.O., Bergmann, G., Deuretzbacher, G., Durselen, L., Pohl, M., Claes, L., Haas, N.P., Duda, G.N., 2001. Musculo-skeletal loading conditions at the hip during walking and stair climbing. Journal of Biomechanics 34, 883–893.

Howie, D.W., McCalden, R.W., Nawana, N.S., Costi, K., Pearcy, M.J., Subramanian, C., 2005. The long-term wear of retrieved McKee-Farrar metal-on-metal total hip prostheses. The Journal of arthroplasty 20, 350–357.

Hu, Isaac, Fisher, 2004. Changes in the contact area during the bedding-in wear of different sizes of metal on metal hip prostheses. Biomed Mater Eng 14, 145–149.

Huk, O.L., Catelas, I., Mwale, F., Antoniou, J., Zukor, D.J., Petit, A., 2004. Induction of apoptosis and necrosis by metal ions in vitro. The Journal of arthroplasty 19, 84–87.

Ingham, E., Fisher, J., 2000. Biological reactions to wear debris in total joint replacement. Proceedings of the Institution of Mechanical Engineers Part H Journal of engineering in medicine 214, 21–37.

International Standards Organisation, 2000. BS ISO 14242-2:2000 Implants for surgery - Wear of total hip-joint prostheses - Part 2: Methods of measurement.

International Standards Organisation, 2002. BS ISO 14242-1:2002 Implants for surgery - Wear of total hip-joint replacement prostheses - Part 1: Loading and displacement parameters for wear-testing machines and corresponding environmental conditions for test.

International Standards Organisation, 2009. BS ISO 14242-3:2009 Implants for surgery - Wear of total hip-joint replacement prostheses - Part 3: Loading and displacement parameters for orbital bearing type wear-testing machines and corresponding environmental conditions for test.

Isaac, G.H., Thompson, J., Williams, S., Fisher, J., 2006. Metal-on-metal bearings surfaces: materials, manufacture, design, optimization, and alternatives. Proceedings of the Institution of Mechanical Engineers, Part H: Journal of Engineering in Medicine 220, 119–133.

Jacobs, M.A., Schmidt, M.B., Farrar, R., 1998. The effect of clearance and diameter on debris generation in a metal-on-metal hip. The Journal of Arthroplasty 13, 224.

Jagatia, M., Jin, Z.M., 2001. Elastohydrodynamic lubrication analysis of metal-on-metal hip prostheses under steady state entraining motion. Proceedings of the Institution of Mechanical Engineers Part H Journal of engineering in medicine 215, 531–541.

Jalali-Vahid, D., Jin, Z., Dowson, D., 2004. Elastohydrodynamic lubrication analysis of metal-on-metal hip implants under start-up and stopping conditions, in: Dalmaz, G., Lubrecht, A.A., Dowson, D., Priest, M. (Eds.), Transient Processes in Tribology (Eds). pp. 751–758.

Jalali-Vahid, D., Jin, Z.M., Dowson, D., 2006. Effect of start-up conditions on elastohydrodynamic lubrication of metal-on-metal hip implants. Proceedings of the Institution of Mechanical Engineers, Part J: Journal of Engineering Tribology 220, 143–150.

Jin, Z.M., Dowson, D., Fisher, J., 1997. Analysis of fluid film lubrication in artificial hip joint replacements with surfaces of high elastic modulus. Proceedings of the Institution of Mechanical Engineers Part H Journal of engineering in medicine 211, 247–256.

Kamali, A., Hussain, A., Li, C., Pamu, J., Daniel, J., Ziaee, H., McMinn, D.J.W., 2010. Tribological performance of various CoCr microstructures in metal-on-metal bearings: the development of a more physiological protocol in vitro. The Journal of bone and joint surgery. British volume 92, 717–25.

Khan, M., Takahashi, T., Kuiper, J.H., Sieniawska, C.E., Takagi, K., Richardson, J.B., 2006. Current in vivo wear of metal-on-metal bearings assessed by exercise-related rise in plasma cobalt level. Journal of Orthopaedic Research 24, 2029–2035.

Knight, L.A., Pal, S., Coleman, J.C., Bronson, F., Haider, H., Levine, D.L., Taylor, M., Rullkoetter, P.J., 2007. Comparison of long-term numerical and experimental total knee replacement wear during simulated gait loading. Journal of Biomechanics 40, 1550–1558.

Ladon, D., Doherty, A., Newson, R., Turner, J., Bhamra, M., Case, C.P., 2004. Changes in metal levels and chromosome aberrations in the peripheral blood of patients after metal-on-metal hip arthroplasty. The Journal of arthroplasty 19, 78–83.

Langton, D.J., Jameson, S.S., Joyce, T.J., Gandhi, J.N., Sidaginamale, R., Mereddy, P., Lord, J., Nargol, A.V.F., 2011. Accelerating failure rate of the ASR total hip replacement. The Journal of bone and joint surgery. British volume 93, 1011–6.

Leslie, I., Williams, S., Brown, C., Isaac, G., Jin, Z., Ingham, E., Fisher, J., 2008. Effect of bearing size on the long-term wear, wear debris, and ion levels of large diameter metal-on-metal hip replacements-An in vitro study. Journal of biomedical materials research. Part B, Applied biomaterials 87, 163–72.

Leslie, I.J., Williams, S., Brown, C., Anderson, J., Isaac, G., Hatto, P., Ingham, E., Fisher, J., 2009. Surface engineering: a low wearing solution for metal-on-metal hip surface replacements. Journal of biomedical materials research. Part B, Applied biomaterials 90, 558–65.

Liao, Y.S., Hanes, M., Fryman, C., Turner, L., 2004. Effects of Clearance, Head Size and Start-Stop Protocol on Wear of Metal-on-Metal Hip Joint Bearings in a Physiological Anatomical Hip Joint Simulator, in: 50th Annual Meeting of the Orthopaedic Research Society. San Diego, p. 1454.

Long, W.T., 2005. The clinical performance of metal-on-metal as an articulation surface in total hip replacement. The Iowa Orthopaedic Journal 25, 10–16.

MacDonald, S.J., 2004. Can a safe level for metal ions in patients with metal-on-metal total hip arthroplasties be determined? The Journal of Arthroplasty 19, 71–77.

Matthies, A.K., Skinner, J.A., Osmani, H., Henckel, J., Hart, A.J., 2012. Pseudotumors Are Common in Well-positioned Low-wearing Metal-on-Metal Hips. Clinical orthopaedics and related research 470, 1895–906.

MatWeb, 2011. MatWeb [WWW Document]. URL:http://www.matweb.com/search/DataSheet.aspx?MatGUID=d78c582672c748c18a72d4169b02d273&ckck=1

McKee, G.K., 1982. Total hip replacement--past, present and future. Biomaterials 3, 130–135.

McKee, G.K., Watson-Farrar, J., ., 1966. Replacement of arthritic hips by the McKee-Farrar prosthesis. The Journal of bone and joint surgery. British volume 48, 245–59.

McKellop, H., Park, S.H., Chiesa, R., Doorn, P., Lu, B., Normand, P., Grigoris, P., Amstutz, H., 1996. In vivo wear of three types of metal on metal hip prostheses during two decades of use. Clinical Orthopaedics & Related Research 329 Suppl, S128–40.

McMinn, D.J.W., Daniel, J., Ziaee, H., Pradhan, C., 2011. Indications and results of hip resurfacing. International orthopaedics 35, 231–7.

Medicines and Healthcare Products Regulatory Agency (MHRA), W. mhra. gov. u., 2012. Medical Device Alert: All metal-on-metal (MoM) hip replacements (MDA/2012/036).

Medley, J., Bobyn, J.D., Krygier, J.J., Roter, G.E., Cheung, N.Y., Chan, F.W., 2002. Intermittent motion as a simulator protocol for hip implants made from high elastic modulus materials, in: Institution of Mechanical Engineers: Engineers and Surgeons: Joined at the Hip. London, p. C601/094.

Medley, J.B., Bobyn, J.D., Krygier, J.J., Tanzer, M., Chan, F.W., Roter, G.E., 2001. Elastohydrodynamic lubrication and wear of metal-metal hip implants. Invited lecture at the World Tribology Forum, Montreux, Switzerland, October 5- 7, 2000. pp 125–136.

Medley, J.B., Chan, F.W., Krygier, J.J., Bobyn, J.D., 1996. Comparison of alloys and designs in a hip simulator study of metal on metal implants. Clinical Orthopaedics & Related Research 329 Suppl, S148–59.

Mejia, L.C., Brierley, T.J., 1994. A hip wear simulator for the evaluation of biomaterials in hip arthroplasty components. Bio-medical materials and engineering 4, 259–71.

Merritt, K., Brown, S.A., 1996. Distribution of cobalt chromium wear and corrosion products and biologic reactions. Clinical Orthopaedics & Related Research 329 Suppl, S233–43.

Morlock, M., Nassutt, R., Bluhm, A., Vollmer, M., Honl, M., Mueller, V., Hille, E., Schneider, E., 2000. Quantification of Hip Joint Resting Periods During Daily Activities: Could They Play a Role For The Failure of Total Hip Prostheses Due To The Increase In Static Friction?, in: 46th Annual Meeting, Orthopaedic Research Society, March 12-15, 2000, Orlando, Florida. Orlando, Florida, p. 497.

Morlock, M., Schneider, E., Bluhm, A., Vollmer, M., Bergmann, G., Muller, V., Honl, M., 2001. Duration and frequency of every day activities in total hip patients. Journal of Biomechanics 34, 873–881.

Mäkelä, K.T., Visuri, T., Pulkkinen, P., Eskelinen, A., Remes, V., Virolainen, P., Junnila, M., Pukkala, E., 2012. Risk of cancer with metal-on-metal hip replacements: population based study. BMJ (Clinical research ed.) 345, e4646.

Nassutt, R., Wimmer, M.A., Schneider, E., Morlock, M.M., 2003. The influence of resting periods on friction in the artificial hip. Clinical Orthopaedics & Related Research 127–138.

National Joint Registry for England and Wales, 2011. Stats Online [WWW Document]. URL http://www.njrcentre.org.uk/njrcentre/Healthcareproviders/Accessingthedata/StatsOnline/tabid/117/Default.aspx

Naudie, D., Roeder, C.P., Parvizi, J., Berry, D.J., Eggli, S., Busato, A., 2004. Metal-on-metal versus metal-on-polyethylene bearings in total hip arthroplasty: a matched case-control study. The Journal of arthroplasty 19, 35–41.

Nordin, M., Frankel, V.H., 2001. Basic Biomechanics of the Musculoskeletal System. Lippincott Williams and Wilkins, Baltimore, Maryland.

Park, Y.S., Hwang, S.K., Choy, W.S., Kim, Y.S., Moon, Y.W., Lim, S.J., 2006. Ceramic failure after total hip arthroplasty with an alumina-on-alumina bearing. The Journal of Bone and Joint Surgery 88, 780–787.

Paul, J.P., 1966. Biomechanics. The biomechanics of the hip-joint and its clinical relevance. Proceedings of the Royal Society of Medicine. 59, 943–948.

Paul, J.P., 1967. Forces Transmitted by Joints in the Human Body. Proceedings of the Institution of Mechanical Engineers, Conference Proceedings 1966 181, 8–15.

Paul, J.P., 1976. Force actions transmitted by joints in the human body. Proceedings of the Royal Society of London. Series B, Containing papers of a Biological character 192, 163–172.

Paul, J.P., 2002. Analysis of Loading of the Hip Joint, in: Institution of Mechanical Engineers: Engineers and Surgeons: Joined at the Hip. London, p. C601/076.

Rasquinha, V.J., Ranawat, C.S., Weiskopf, J., Rodriguez, J.A., Skipor, A.K., Jacobs, J.J., 2006. Serum metal levels and bearing surfaces in total hip arthroplasty. The Journal of arthroplasty 21, 47–52.

Reinisch, G., Judmann, K.P., Lhotka, C., Lintner, F., Zweymuller, K.A., 2003. Retrieval study of uncemented metal-metal hip prostheses revised for early loosening. Biomaterials 24, 1081.

Rieker, C.B., Schon, R., Kottig, P., 2004. Development and validation of a second-generation metal-on-metal bearing: Laboratory studies and analysis of retrievals. The Journal of arthroplasty 19, 5–11.

S. L. Smith,A. P. D. Elfick, A.U., 1999. An evaluation of the tribological performance of zirconia and CoCrMo femoral heads. J Mater Sci 34, 5159 – 5162.

Saikko, V., 1996. A three-axis hip joint simulator for wear and friction studies on total hip prostheses. Proceedings of the Institution of Mechanical Engineers Part H Journal of engineering in medicine 210, 175–185.

Saikko, V., 2005. A hip wear simulator with 100 test stations. Proceedings of the Institution of Mechanical Engineers Part H Journal of engineering in medicine 219, 309–318.

Saikko, V., Ahlroos, T., 1999. Type of motion and lubricant in wear simulation of polyethylene acetabular cup. Proceedings of the Institution of Mechanical Engineers Part H Journal of engineering in medicine 213, 301–310.

Saikko, V., Nevalainen, J., Revitzer, H., Ylinen, P., 1998. Metal release from total hip articulations in vitro: substantial from CoCr/CoCr, negligible from CoCr/PE and alumina/PE. Acta orthopaedica Scandinavica 69, 449–454.

Saikko, V., Paavolainen, P., Kleimola, M., Statis, P., 1992. A five-station hip joint simulator for wear rate studies. Proceedings of the Institution of Mechanical Engineers Part H Journal of engineering in medicine 206, 195–200.

Savarino, L., Granchi, D., Ciapetti, G., Cenni, E., Nardi Pantoli, A., Rotini, R., Veronesi, C.A., Baldini, N., Giunti, A., 2002. Ion release in patients with metal-on-metal hip bearings in total joint replacement: a comparison with metal-on-polyethylene bearings. Journal of biomedical materials research 63, 467–474.

Schmalzried, T.P., Szuszczewicz, E.S., Northfield, M.R., Akizuki, K.H., Frankel, R.E., Belcher, G., Amstutz, H.C., 1998. Quantitative assessment of walking activity after total hip or knee replacement. The Journal of bone and joint surgery. American volume 80, 54–59.

Scholes, S.C., Green, S.M., Unsworth, A., 2001. The wear of metal-on-metal total hip prostheses measured in a hip simulator. Proceedings of the Institution of Mechanical Engineers Part H Journal of engineering in medicine 215, 523–530.

Seeley, R.R., Stephens, T.D., Tate, P., 2000. Anatomy and Physiology, 5th Editio. ed. McGraw Hill.

Shepherd, E.F., McClung, C.D., Schmalzreid, T.P., Moreland, J.R., 2000. Improved Activity Assessment of Total Hip Replacement Patients, in: 46th Annual Meeting, Orthopaedic Research Society, March 12-15, 2000, Orlando, Florida. Orlando, Florida, p. 0223.

Sieber, H.P., Rieker, C.B., Kottig, P., 1999. Analysis of 118 second-generation metal-on-metal retrieved hip implants. The Journal of bone and joint surgery. British volume 81, 46–50.

Signorello, L.B., Ye, W., Fryzek, J.P., Lipworth, L., Fraumeni Jr., J.F., Blot, W.J., McLaughlin, J.K., Nyren, O., 2001. Nationwide study of cancer risk among hip replacement patients in Sweden. Journal of the National Cancer Institute 93, 1405–1410.

Silva, M., Heisel, C., Schmalzried, T.P., 2005. Metal-on-metal total hip replacement. Clinical Orthopaedics & Related Research 53–61.

Smith, S.L., Dowson, D., Goldsmith, A.A., 2001a. The effect of femoral head diameter upon lubrication and wear of metal-on-metal total hip replacements. Proceedings of the Institution of Mechanical Engineers Part H Journal of engineering in medicine 215, 161–170.

Smith, S.L., Dowson, D., Goldsmith, A.A.J., 2001b. The lubrication of metal-on-metal total hip joints: a slide down the Stribeck curve. Proceedings of the Institution of Mechanical Engineers, Part H: Journal of Engineering in Medicine 215, 483–493.

Smith, S.L., McNie, C.M., Duddy, S.M., Goldsmith, A.A., Bennett, D., Orr, J.F., Dowson, D., 2002. Demographic and occupational effects on the activity levels of normal subjects in the United Kingdom. Hip International 12, 28–36.

Smith, S.L., Unsworth, A., 2000. Simplified motion and loading compared to physiological motion and loading in a hip joint simulator. Proceedings of the Institution of Mechanical Engineers Part H Journal of engineering in medicine 214, 233–238.

Stansfield, B.W., Nicol, A.C., Paul, J.P., Kelly, I.G., Graichen, F., Bergmann, G., 2002. Hip Joint Forces, Calculated and Measured: An Evaluation of Musculoskeletal Modelling, in: Institution of Mechanical Engineers: Engineers and Surgeons: Joined at the Hip. London, p. C601/007.

Stansfield, B.W., Nicol, A.C., Paul, J.P., Kelly, I.G., Graichen, F., Bergmann, G., 2003. Direct comparison of calculated hip joint contact forces with those measured using instrumented implants. An evaluation of a three-dimensional mathematical model of the lower limb. Journal of Biomechanics 36, 929–936.

Stewart, T.D., Tipper, J.L., Insley, G., Streicher, R.M., Ingham, E., Fisher, J., 2003. Long-term wear of ceramic matrix composite materials for hip prostheses under severe swing phase microseparation. Journal of biomedical materials research. Part B, Applied biomaterials 66, 567–573.

Suzuki, K., Matsubara, M., Morita, S., Muneta, T., Shinomiya, K., 2003. Fracture of a ceramic acetabular insert after ceramic-on-ceramic THA--a case report. Acta orthopaedica Scandinavica 74, 101–103.

The Swedish National Hip Joint Arthroplasty Register, 2004. Annual Report.

Tipper, J.L., Firkins, P.J., Besong, A.A., Barbour, P.S.M., Nevelos, J.E., Stone, M.H., Ingham, E., Fisher, J., 2001. Characterisation of wear debris from UHMWPE on zirconia ceramic, metal-on-metal and alumina ceramic-on-ceramic hip prostheses generated in a physiological anatomical hip simulator. Wear 250, 120–128.

Tipper, J.L., Firkins, P.J., Ingham, E., Fisher, J., Stone, M.H., Farrar, R., 1999. Quantitative analysis of the wear and wear debris from low and high carbon content cobalt chrome alloys used in metal on metal total hip replacements. Journal of materials science. Materials in medicine 10, 353–362.

Tipper, J.L., Ingham, E., Jin, Z.M., Fisher, J., 2005. The science of metal-on-metal articulation. Current Orthopaedics 19, 280–287.

Wang, A., Essner, A., Schmidig, G., 2004. The effects of lubricant composition on in vitro wear testing of polymeric acetabular components. Journal of Biomedical Materials Research Part B: Applied Biomaterials 68, 45–52.

Williams, S., Jalali-Vahid, D., Brockett, C., Jin, Z., Stone, M.H., Ingham, E., Fisher, J., 2005. Effect of swing phase load on metal-on-metal hip lubrication, friction and wear. Journal of Biomechanics 39, 2274–81.

Williams, S., Leslie, I., Isaac, G., Jin, Z., Ingham, E., Fisher, J., 2008. Tribology and wear of metal-on-metal hip prostheses: influence of cup angle and head position. The Journal of bone and joint surgery. American volume 90 Suppl 3, 111–7.

Williams, S., Stewart, T.D., Ingham, E., Stone, M.H., Fisher, J., 2004. Metal-on-metal bearing wear with different swing phase loads. Journal of biomedical materials research. Part B, Applied biomaterials 70B, 233–239.

Wimmer, M.A., Artelt, D., Kunze, J., Morlock, M.M., Schneider, E., Nassutt, R., 2001. Friction and Wear Properties of Metal/Metal Hip Joints: Application of a Novel Testing and Analysis Method. Materials Science and Engineering Technology 32, 891–896.

Wimmer, M.A., Nassutt, R., Sprecher, C., Loos, J., Tager, G., Fischer, A., 2006. Investigation on stick phenomena in metal-on-metal hip joints after resting periods. Proceedings of the Institution of Mechanical Engineers Part H Journal of engineering in medicine 220, 219–227.

Wimmer, M.A., Sprecher, C., Hauert, R., Tager, G., Fischer, A., 2003. Tribochemical reaction on metal-on-metal hip joint bearings - A comparison between in-vitro and in-vivo results. Wear 255, 1007–1014.

Yan, Y., Neville, A., Dowson, D., 2006. Understanding the role of corrosion in the degradation of metal-on-metal implants. Proceedings of the Institution of Mechanical Engineers Part H Journal of engineering in medicine 220, 173–181.

Zahiri, C.A., Schmalzreid, T.P., Szuszczewicz, E.S., Amstutz, H.C., 1998. Assessing activity in joint replacement patients. The Journal of arthroplasty 13, 890–895.

Appendix 1

Hip simulator load cell readings for faulty station in CHapter 3

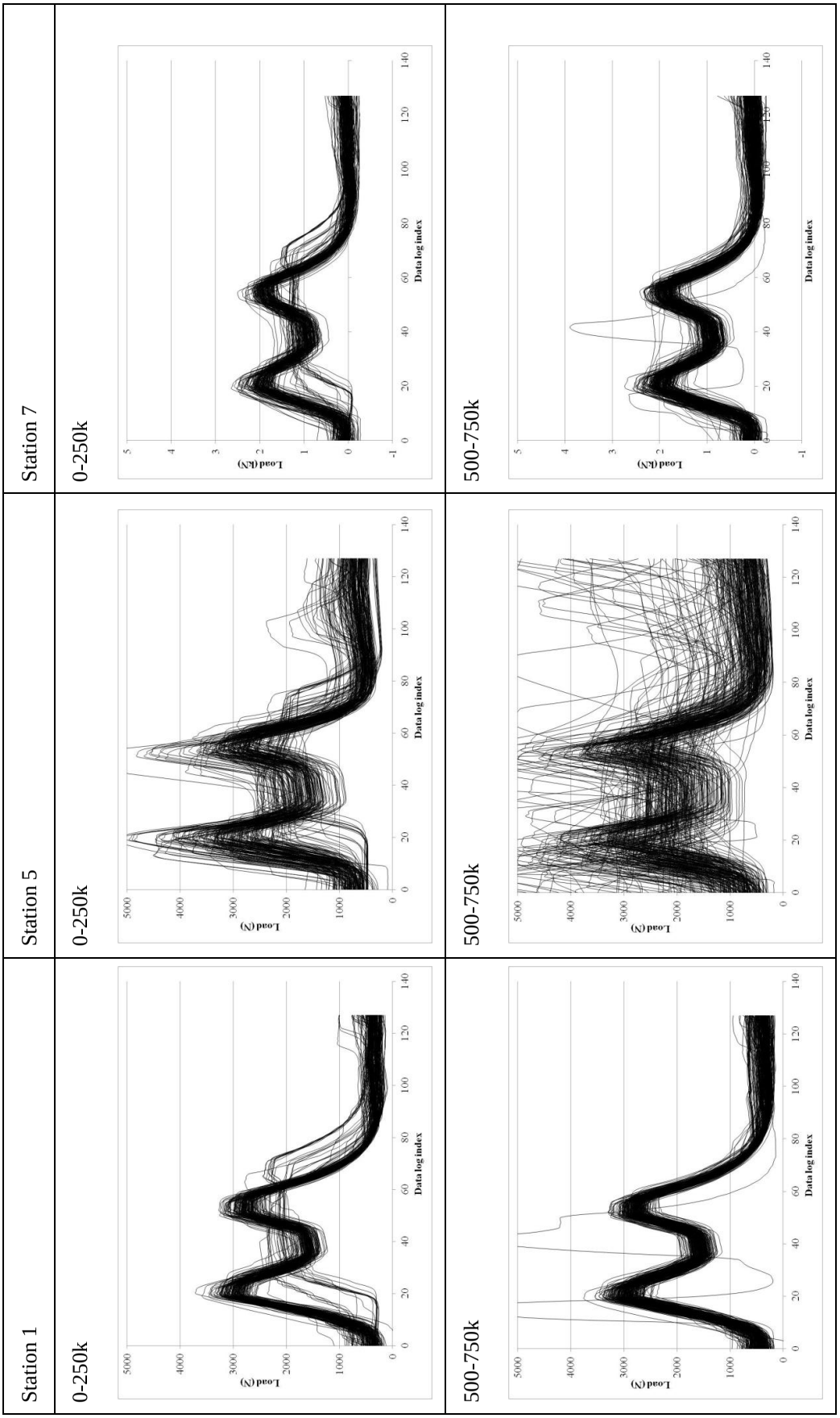

750k – 1mc	750k – 1mc	750k – 1mc
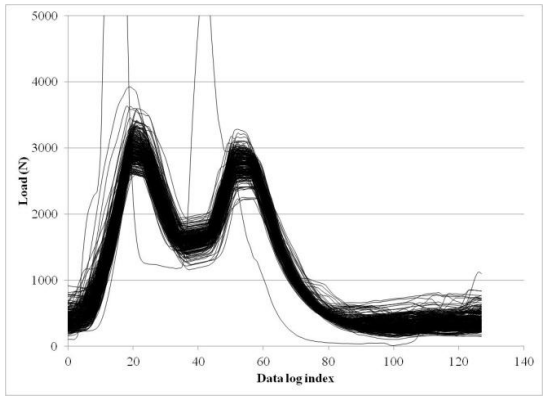	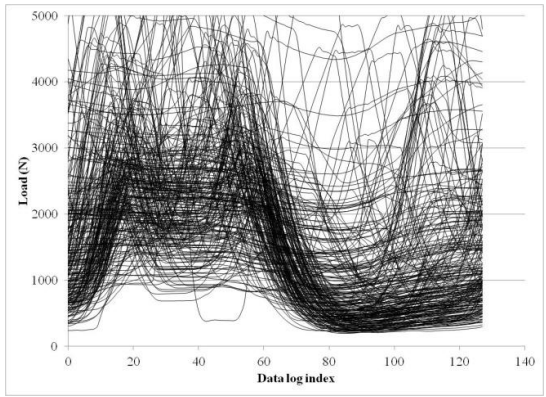	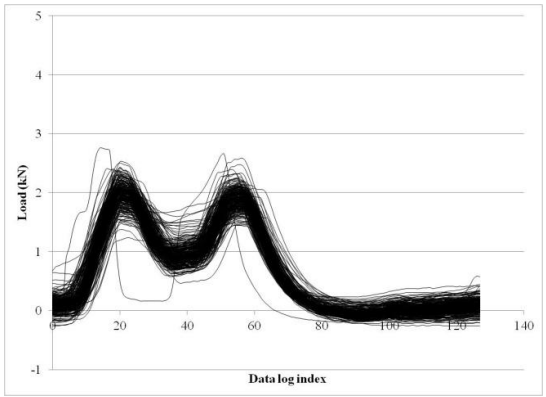
1.25-1.5mc	1.25-1.5mc	1.25-1.5mc
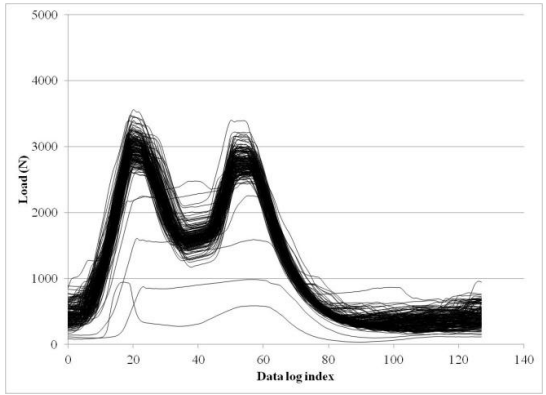	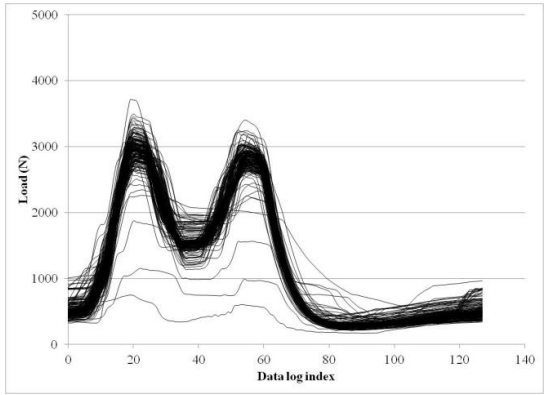	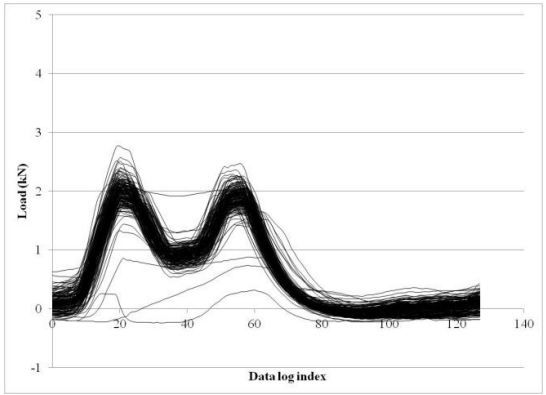

APPENDIX 2: PRESENTATIONS & PUBLICATIONS

Presentations

Megan Hadley; Zhongmin Jin; John Fisher; Cath Hardaker; Graham Isaac. *Functional and Geometrical Variables Affecting in vitro Wear of Hip Joints*. World Congress on Biomechanics, Singapore August 2010; Sym 2.08-02: Biomechanical and Biotribological Functions of Artificial Hip Joints.

Hadley, M.; Hadfield, F.; Hardaker, C.; Isaac, G.; Fisher, J.; Wye, J.; Barnett, J.; *Wear of metal-on-metal total hip replacements under severe in-vitro test conditions*. European Federation of National Associations of Orthopaedics and Traumatology, Copenhagen June 2011

M Hadley; C Hardaker; S Williams; Z Jin; G Isaac; J Fisher; *Development of a stop-dwell-start (SDS) protocol for in vitro wear testing of metal-on-metal total hip replacements.* Symposium on Metal-On-Metal Total Hip Replacement, May 8, 2012, Phoenix, AZ

Papers

M Hadley; C Hardaker; S Williams; Z Jin; G Isaac; J Fisher; *Development of a stop-dwell-start (SDS) protocol for in vitro wear testing of metal-on-metal total hip replacements.* STP1560 on Symposium on Metal-On-Metal Total Hip Replacement Devices *(in press)*